

# POLITECNICO DI TORINO



**Politecnico  
di Torino**

**College of Engineering**

**Department of Mechanical, Aerospace, Automotive and  
Production Engineering**

M.Sc. Thesis

**Steels for Car-Body Applications: State of Art and Future  
Trends**

Supervisor: *Prof. Paolo MATTEIS*

Candidate: *Ahmed Sameh Abdelrahim Hassane ELSAYED*

# Introduction

In the recent years, the Automotive field is focusing on developing materials that can provide high strength with reduced weight and can be shaped to complex shapes, in order to increase the passenger comfort, safety and reduce the weight of the vehicle, since the increased weight of the vehicle leads to consume more fuel which means more emissions, this point is so important since there are regulations that are setting targets, if these targets are not met it means that the car maker will pay a fine depends on the emissions of his fleet for example the allowable CO<sub>2</sub> emission for passenger cars is 95 g CO<sub>2</sub>/km in 2020 while in 2025 it shall be 80 g CO<sub>2</sub>/km and in 2030 it will be 65 g CO<sub>2</sub>/km in EU and the fine of each g CO<sub>2</sub>/km is 95 Euros.

Due to the previously mentioned reasons there were new materials that has been introduced also the car makers starting focusing on using a combinations of material in the vehicle structure by putting the right material in the right place since the price is playing a main role so they add the materials that has a high strength in the critical places from the point of view of the safety.

In this thesis a brief introduction of the steel phases and the main alloys that are used in the steel shall be covered then we will take an overview on the process route of the steel making we will discuss it in detail covering basic oxygen process, continuous casting, hot rolling, cold rolling and heat treatment. Steel performance chapter will cover some important measurements like tensile strength, r-value, , bending, hole expansion and formability limits.

Then a detailed review on the Automotive steel families shall be focused on, considering their microstructure, processing and application, then we will see a detailed analyses of the material evolution to see what is the trend of each segment, carmaker and year and knowing which material is used more and we will focus also on some critical areas from the safety point of view and see which materials where used.

# Contents

<b>1. Metallurgy</b>	<b>5</b>
1.2 ALLOYS	10
1.2.1-Carbon (C)	10
1.2.2- Manganese (Mn)	10
1.2.3- Silicon (Si)	11
1.2.4-Nickel (Ni)	11
1.2.5-chromium (Cr)	11
1.2.6-Molybdenum Steels (Mo)	12
1.2.7- Tungsten Steel (W)	12
1.2.8- Vanadium Steels (V)	12
1.2.9-Niobium (Nb)	12
<b>2. Process Route of steelmaking</b>	<b>13</b>
2.1 Basic-Oxygen process	15
2.2 Continuous casting	17
2.3 Hot Rolling	20
2.4 Cold rolling	21
2.5 Continuous heat treatment	22
2.5.1 Quenching (Strengthening Treatment)	22
<b>3. Low Carbon Steels Used for Car Body</b>	<b>25</b>
3.1 Interstitial-Free Steels (IF)	28
3.2 Bake Hardenable (BH) Steels:	29
3.3 High strength, Low-Alloy Low-Carbon Steels (HSLA)	30
3.4 Dual Phase (DP)	35
3.4.1 Effect of annealing parameters on DP steels	37
3.4.2 Processing of DP steels	39
3.5 Transformation-induced plasticity steels (TRIP)	40
3.5.1 Microstructure and properties of TRIP steels	40
3.5.2 Factors influencing TRIP effect	41
3.5.3 Processing of TRIP steels	41
3.5.4 Properties and applications	42
3.6 Twinning-induced plasticity steels (TWIP)	43
3.6.1 Properties and Applications	43

3.7 Quenching and partitioning treatment (Q&P) .....	44
3.7.1 Processing of steel through the Q&P route .....	44
3.7.2 Alloy design and composition for Q&P treatment.....	44
3.8 Hot formed steel or Press Hardening Steel (PHS) .....	46
3.8.1 Processing of PHS.....	46
3.8.2 Hot stamping line.....	47
3.8.3 Press Hardened Steel Material properties.....	48
<b>4. Steel Performance .....</b>	<b>51</b>
4.1 Tensile Test.....	51
4.2 R value .....	52
4.3 Hole expansion Stretch flanging.....	54
4.4 Bending.....	55
4.5 Formability Level Diagram .....	57
<b>5. OEMs needs and regulation.....</b>	<b>61</b>
5.1 History of steel usage in the vehicle’s body and significant events impacting steel application in vehicle design.....	61
5.2 Tradeoff material mass and application in vehicle.....	64
5.3 Safety regulations .....	64
5.4 Major Car Crash Test Providers.....	65
5.5 Fuel Economy.....	68
5.6 Concerns of CO <sub>2</sub> emissions.....	69
<b>6. Material Evolution .....</b>	<b>71</b>
6.1 Overview on the share of the market and different steels families that has been used in different segments.....	73
6.1.1 <i>The share of each segment of passenger vehicles in EMEA</i> .....	73
6.1.2 <i>Different steel families that are used in passenger vehicles in EMEA 2019</i> .....	75
6.1.3 Material Evolution in Europe and China based on “EuroCarBody from 2012 to 2020” and “8th China Lightweight Car Body Conference -20201129” .....	79
6.2 Detailed analysis considering.....	82
6.2.1 <i>Alfa Romeo (C&amp;D)</i> .....	82
6.2.2 <i>SKODA (C)</i> .....	85
6.2.3 <i>FORD (C)</i> .....	88
6.2.4 <i>HONDA (B)</i> .....	91
6.3 Electrical Cars.....	95

Conclusion .....	98
<b>References .....</b>	<b>101</b>

## List of Figures

Figure (1.1) Iron-Iron carbide phase diagram.....	8
Figure (2.1) Flow diagram showing the main steps of converting the raw materials into products.....	13
Figure (2.2) General operation of modern Blast Furnace.....	14
Figure (2.3) Steelmaking using the Basic-Oxygen process.....	16
Figure (2.4) Principle of continuous casting.....	18
Figure (2.5) Continuous casting machine.....	19
Figure (2.6) Rolling process.....	20
Figure (2.7) multi stage rolling.....	21
Figure (2.8) The effect of cold rolling on the $r_m$ value of Ti, Nb and Ti-Nb.....	22
Figure (2.9) The influence on the material properties considering the two scenarios that are caused by the cooling rate.....	23
Figure (2.10) the relation between the carbon content and temperature for starting and completing the martensite formation $M_s$ and $M_f$ .....	24
Figure (2.11) the relation between the carbon content and retained austenite.....	25
Figure (3.1) Automotive steel grades based on ductility and strength.....	26
Figure (3.2) Schematic representation of the bake hardening (BH) process and its effect on yield strength of steel.....	29
Figure (3.3) the hot rolling schedules used for different low carbon steel.....	31
Figure (3.4) The holding time on the left is 850 while on the right is 900 after hot rolling at 950C.....	32
Figure (3.5) Schematic representation of the effect of deformation between the $T_{nr}$ and the $T_{Ar3}$ on the austenite microstructure.....	32
Figure (3.6) the effect of rolling and coiling temperatures on the uniformity of the ferrite of the grain size in HSLA steels.....	33
Figure (3.7) example of some applications of HSLA steel.....	34
Figure (3.8) the weldability of different steels based on carbon content and carbon equivalent graph.....	35
Figure (3.9) SEM micrograph of (a) bainite-ferrite “BF” and (b) martensite-ferrite “MF” steel.....	36
Figure (3.10) SEM images of various grades: (a) DP600, (b) DP800, (c) DP1000.....	37
Figure (3.11) DP microstructure with cooling rate of: (a) 100° C/s and (b) 10° C/s.....	37
Figure (3.12) Scanning electron microscopy micrographs showing influence of heating rates on austenite formation under different conditions.....	38
Figure (3.13) Crack initiation in martensite in DP steels.....	39
Figure (3.14) micrograph showing the micro structure of TRIP.....	40
Figure (3.15) Illustration of TRIP effect during tensile test.....	41
Figure (3.16) Conventional processing route of TRIP steels.....	41
Figure (3.17) the typical microstructure of TWIP steel.....	43
Figure (3.18) Q&P processing route.....	44
Figure (3.19) Roles of alloying elements on the kinetics of several transformations during Q&P treatment.....	45
Figure (3.20) PHS.....	46
Figure (3.21) Schematic showing the (a) direct hot-stamping (b) indirect hot-stamping.....	46
Figure (3.22) Summary of hot forming.....	47
Figure (3.23) A typical hot stamping time-temperature profile.....	48
Figure (3.24) Base metal microstructure of 22MnB5 PHS (a) As-received condition; (b) Hot Formed condition.....	49
Figure (3.25) Continuous Cooling Transformation (CCT) curve of 22MnB5 steel and effects	

of additional alloying elements.....	50
Figure (3.26) Flow curves and microstructure evolution of 22MnB5.....	50
Figure (4.1) stress-strain curve .....	51
Figure (4.2) brittle and ductile.....	51
Figure (4.3) The effect of carbon content on the rm value of low carbon steel.....	53
Figure (4.4) HEC test after ISO 16630.....	54
Figure (4.5) HEC examples, left mild steel, middle HSLA steel, right DP steel.....	54
Figure (4.6) bending process VDA 238 schematic.....	55
Figure (4.7) photograph of test equipment.....	56
Figure (4.8) (a) doubly folded HSLA (b) DP steel VDA 238 bend test.....	57
Figure (4.9) Force-displacement diagram of VDA 238 bend test.....	57
Figure (4.10) Formability limit diagram (FLD).....	58
Figure (4.11) Specimen for uniaxial, plane, and biaxial strain path.....	58
Figure (4.12) represent FLD for different rolling directions.....	59
Figure (4.13) Comparison of forming limit curves: 40 and 90 $\mu\text{m}$ thickness.....	60
Figure (4.14) Overview of forming limit curves for different steel families.....	63
Figure (5.1) History of vehicle curb weight, CAFE mileage requirements and actual CAFE Performance for the U.S. fleet.....	63
Figure (5.2) USA's car production by cylinder type.....	64
Figure (5.3) steel families that are used in years 2009, 2012 and 2020 according to EuroCarBody Conference.....	66
Figure (5.4) front Impact test.....	66
Figure (5.5) Full Width rigid barrier.....	67
Figure (5.6) lateral Impact.....	67
Figure (5.7) side Pole.....	67
Figure (5.8) Far-side Impact.....	68
Figure (5.9) Whiplash.....	69
Figure (5.10) Fuel economy plan for year 2025.....	70
Figure (5.11) the regulations of different countries on the allowable Grams of CO <sub>2</sub> per Kilometer.....	74
Figure (6.1) the share of each segment from the market according to EMEA 2019.....	75
Figure (6.2) Steel families used in passenger vehicles in EU.....	76
Figure (6.3) Steel used in BIW (a) between 2018-2020 (b) between 2010-2020.....	78
Figure (6.4) material evolution between years 2009-2020 considering only B-segment.....	78
Figure (6.5) material evolution between years 2009-2020 considering only C-segment.....	79
Figure (6.6) material Evolution in (a) Europe (b) China.....	80
Figure (6.7) comparison between the year model and previous year for the same car brand.....	81
Figure (6.8) the trends of the steel families in Alfa Romeo for year model 2010 and 2016.....	83
Figure (6.9) BIW of Alfa Romeo Giulia 2016.....	83
Figure (6.9) BIW of Alfa Romeo Guiliotta 2010.....	84
Figure (6.10) steel families trend for Skoda between years 2012,2016 and 2019.....	85
Figure (6.11) Steel families trend for Ford between years 2011,2018 and 2020.....	88
Figure (6.12) Steel families trend for Honda between years 2013 and 2020.....	91
Figure (6.13) overall material evolution from 2009 to 2020.....	94
Figure (6.14) the average amount of used Steel families in the years between 2009 and 2020.....	94
Figure (6.15) Steel families used in electrical vehicles segments B and C.....	95
Figure (6.16) Steel families used in electrical vehicles segment J.....	96
Figure (6.17) Comparison between steel used in BEV and other passenger vehicles.....	97

## List of Tables

Table (2.4) the amount of different elements before and after the BOF and elements of the slag.....	17
Table (3.1) generations of AHSS.....	27
Table (3.2) UTS and YS of IF and IFHS.....	28
Table (3.3) YS of HSLA and plain carbon steel.....	30
Table (3.4) Typical application of HSLA steels.....	33
Table (3.5) comparison between BF steel and MF steel.....	36
Table (5.1) the passenger car and light truck average fuel Economy (CAFE) standards, 1978-1985.....	62
Table (5.2) the major car crash test providers.....	65
Table (6.1) steel grade is used in each family according to EuroCarBody.....	71
Table (6.2) the number of passenger vehicles in EMEA 2019.....	73
Table (6.3) quantities of steel families used in passenger vehicle in 2019.....	75
Table (6.4) steel used in BIW for B-segments between years 2010-2020 and 2018-2020.....	76
Table (6.5) steel used in BIW for C-segments between years 2010-2020 and 2018-2020.....	76
Table (6.6) the increment and reduction of different steel types used for a vehicle compared to the same car model but previous year.....	81
Table (6.7) comparison between Alfa Romeo Guilietta 2010 and Giulia 2016 in terms of steel used.....	82
Table (6.8) Steel used in focused parts of Alfa Romeo Guilietta 2010 and Giulia 2016.....	84
Table (6.9) comparison between Skoda rapid 2012 compared to Kodiaq 2016, 2018 and Octavia 4 2019 in terms of steel used.....	85
Table (6.10) Safety Results according to Euroncap for Skoda rapid 2012 compared to Kodiaq 2016, 2018 and Octavia 4 2019.....	87
Table (6.11) comparison between Ford focus 201a compared to focus 2018 and Mustag Mach-E 2020 in terms of steel used.....	88
Table (6.12) comparison between Honda Fit 2013 and E 2020 in terms of steel used.....	91



# 1. Metallurgy

Steels are widely used materials because of

- 1- The plenty of iron in the Earth's crust.
- 2- High melting temperature (1534 °C).
- 3- Range of mechanical properties, such as moderate (200–300 MPa) yield strength with excellent ductility, it reaches much more than 1400 MPa yield stress with fracture toughness up to 100 MPa m<sup>2</sup>
- 4- Associated microstructures produced by solid-state phase transformations by varying the cooling rate from the austenitic condition

in this chapter we will explain some important terms and describe the reasons and effects of alloying elements based on properties and characteristics of steel.

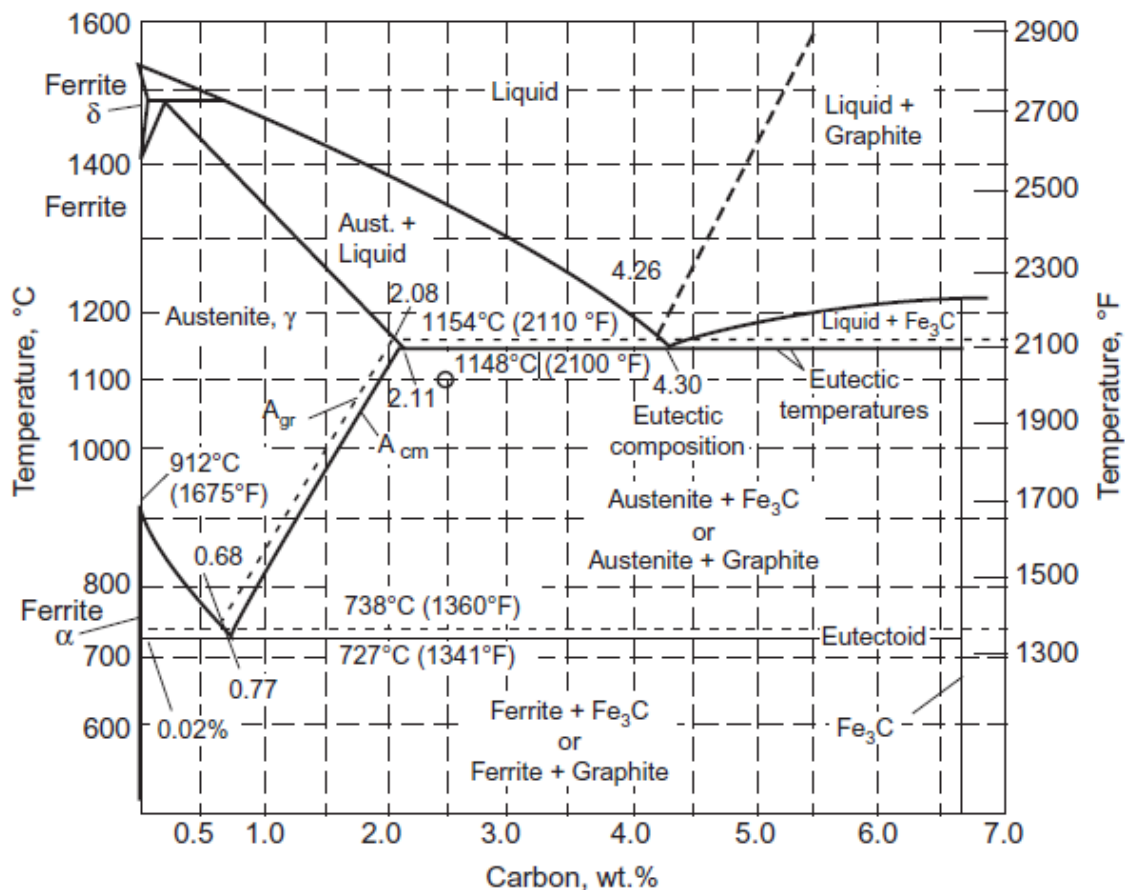


Figure 3.1 Iron-Iron carbide phase diagram [1]

Let's start by defining some important terms and distinguish the main differences among them.

The iron-carbon (Fe-C) diagram is a map that can be used to chart the proper sequence of operations for thermomechanical and thermal treatments of a given steel. However, because most steels contain other elements that modify the positions of the phase boundaries, it provides the scientific basis for the heat treatment of steel alloys at many different temperatures (which is represented at Y-axis (°C)) and with different carbon content (%) in iron up to 6.67% [3,4].

The iron possesses a body center cubic (bcc) lattice which is called  $\alpha$ -Fe or  $\alpha$ -iron starting from a low temperature up to 910 °C, starting from 910 °C up to 1400 °C the  $\alpha$ -iron crystals turn into  $\gamma$ -iron. Possessing face center cubic (fcc) lattice, above 1400 °C they again acquire a bcc lattice and usually called  $\delta$  crystals [1].

According to the Iron-carbon phase diagram the **steels** are classified as all the binary Fe- C alloys containing less than 2.11wt% "it could be 2.06 wt% depending on the source or it could be 2.14 wt% if it is thermodynamically calculated". [1]

If the carbon content is higher than the previous percent, then it is called **cast iron**.

**Plain-carbon steel** contains less than 0.8% carbon and contains low concentrations of manganese, silicon, phosphorus and sulphur, as well as minor amounts of other elements. [8]

Plain-carbon steels are used at ordinary temperatures and atmospheres that are not highly corrosive, also they have relatively low hardenability that limits the obtained strength, another fact that should be pointed to is in order to reduce the internal stresses almost all the hardened steels are tempered which shows a marked softening with increasing the tempering temperature such a behavior will lessen their applicability for parts that require hardness above room temperature.

Due to the previously mentioned limitations of plain-carbon steels, we needed to overcome it by the use of alloying elements.

An alloy steel may be defined as one whose characteristic properties are due to some element other than carbon. Although all **plain-carbon steels** contain amounts of manganese (up to about 0.90 percent) and silicon (up to about 0.30 percent), they are not considered alloy steels because the principal function of the manganese and silicon is to act as deoxidizers. They combine with oxygen and sulfur to reduce the harmful effect of those elements. [2]

The purposes of adding alloying elements to steel are many the most important are:

- 1- increase hardenability
- 2- improve strength at ordinary temperatures
- 3- improve mechanical properties at either high or low temperatures
- 4- improve toughness at any minimum hardness or strength
- 5- increase wear resistance
- 6- increase corrosion resistance
- 7- improve magnetic properties

It should be noted that the effects of a single alloying element on either practice or characteristics is modified by the influence of other elements. The interaction of alloying elements must be considered

We can discuss the effect of various alloying elements separately [1,2]

## **1.2 ALLOYS**

### ***1.2.1-Carbon (C)***

the type of the steel that can be made is determined by the amount of carbon (C). Carbon has a moderate tendency for macrosegregation during solidification, and it is often more significant than any other alloying elements. As the content of carbon (C) in steel increases the strength but weldability and ductility decreases. [1,20]

### ***1.2.2- Manganese (Mn)***

It is present in all the steels in amount of 0.30% or more and it is essentially a deoxidizer and desulfurizer, it has a less tendency for macrosegregation. [1]

Manganese also reduces the tendency of hot shortness (also called red shortness) which is happening because of sulfur [1,2]

Manganese favorably affects the surface quality regardless the amount of carbon in steel (except if the amount of carbon is extremely low), it decreases the weldability and forgeability. [2,20]

Steels that contain more than 0.60% of Mn cannot be rimmed, the presence of alloying element Mn in steels enhances the impurities such as P, Sn, Sb, and as segregating to grain boundaries and induces temper embrittlement. [1]

The steel is classed as an alloy if the percent of manganese content exceeds 0.8%, manganese contributes effectively to the strength and hardness but lesser than carbon and it contributes effectively in the higher carbon steel, the fine grained manganese steels have unusual strength

and toughness, for that reason they are often used for gears, spline shafts and axles. A special steels known as Hadfield manganese steel contains 12% manganese after a proper heat treatment it is characterized by high strength, ductility and excellent wear resistance. [2,19]

### *1.2.3- Silicon (Si)*

It is like manganese one of the principle and cheap deoxidizers used in steelmaking [20], the silicon content determines the type of steel for example the killed steel contain maximum 0.60% Si, while in the semi-killed steel the content of silicon is generally less than 0.10%

By adding the silicone Si to the steel the stress corrosion can be eliminated in Cr–Ni austenitic steels. In heat treated steels, Si is an important alloy element, and increases hardenability, wear resistance, elastic limit and yield strength, and scale resistance in heat-resistant steels.

If (Si) is combined with (Mn) and properly balanced produces steel that has a high hardenability, strength with good ductility and toughness this silicon- manganese steel (9260) is widely used for coil and leaf springs.[2]

### *1.2.4-Nickel (Ni)*

Nickel contributes to the critical temperature of the steel by lowering it and widening the temperature range for successful heat treatment.

Nickel increases the hardenability and when it is combined with the (Ni), (Cr), Molybdenum (Mo) raises the hardenability, toughness and fatigue resistance in steels. [19]

The 3.5% nickel steels (23xx series) with low-carbon are used for drive gears, connecting rods bolts and studs, the 5% nickel steel provides increased toughness are used for heavy applications such as truck gears and crankshafts

### *1.2.5-chromium (Cr)*

Chromium increases hardenability, corrosion and oxidation resistance of steels improves high-temperature strength and high-pressure hydrogenation properties, and enhances

abrasion resistance in high-carbon grades. Chromium carbides are hard and wear-resistant and increase the edge-holding quality.

The high chromium steel containing over 10% Cr are having a high resistance to corrosion

### *1.2.6-Molybdenum Steels (Mo)*

Molybdenum is a relatively expensive alloying element it is strongly affect the hardenability and strength of the steel [19], steels that are containing Molybdenum are less susceptible to temper brittleness than other alloy steels.

Molybdenum is often combined with nickel or chromium or with both of them

triple-alloy nickel-chromium-molybdenum steels (43xx and 47xx series) have the advantages of the nickel-chromium steels along with the high hardenability.

They are used in the aircraft industry for the structural parts of the wing assembly, and landing gear.

### *1.2.7- Tungsten Steel (W)*

the effect of the Tungsten on the steel is the same as molybdenum effect but with a larger quantity, approximately 2 to 3 % of W is equivalent to 1% of Mo.

Tungsten and molybdenum are the main alloying elements in high speed steel, but due to the fact that the tungsten is relatively expensive and a larger quantity is need in order to achieve an acceptable effect it is not used in general engineering steels.

### *1.2.8- Vanadium Steels (V)*

It is the most expensive of the alloying elements, it provides a very noticeable secondary hardening effect on tempering so it raises hot hardness and thus improves the cutting ability.

Also it increases the fatigue strength, wear resistance, edge holding quality and high temperature strength and improves notch sensitivities therefore it is used mainly as an additional alloying element in different types of steel.

### *1.2.9-Niobium (Nb)*

It is a very strong Carbide and nitride former, it is widely used in microalloying steels.

through a controlled cooling and rolling, a high strength and good toughness can be obtained. [20] For example, a medium carbon steel yield strength can be increased by 150 Mpa by using 0.03% Nb in austenite

The Niobium is used in the Cr-Ni austenitic steels for reducing corrosion. [1]

## 2. Process Route of steelmaking

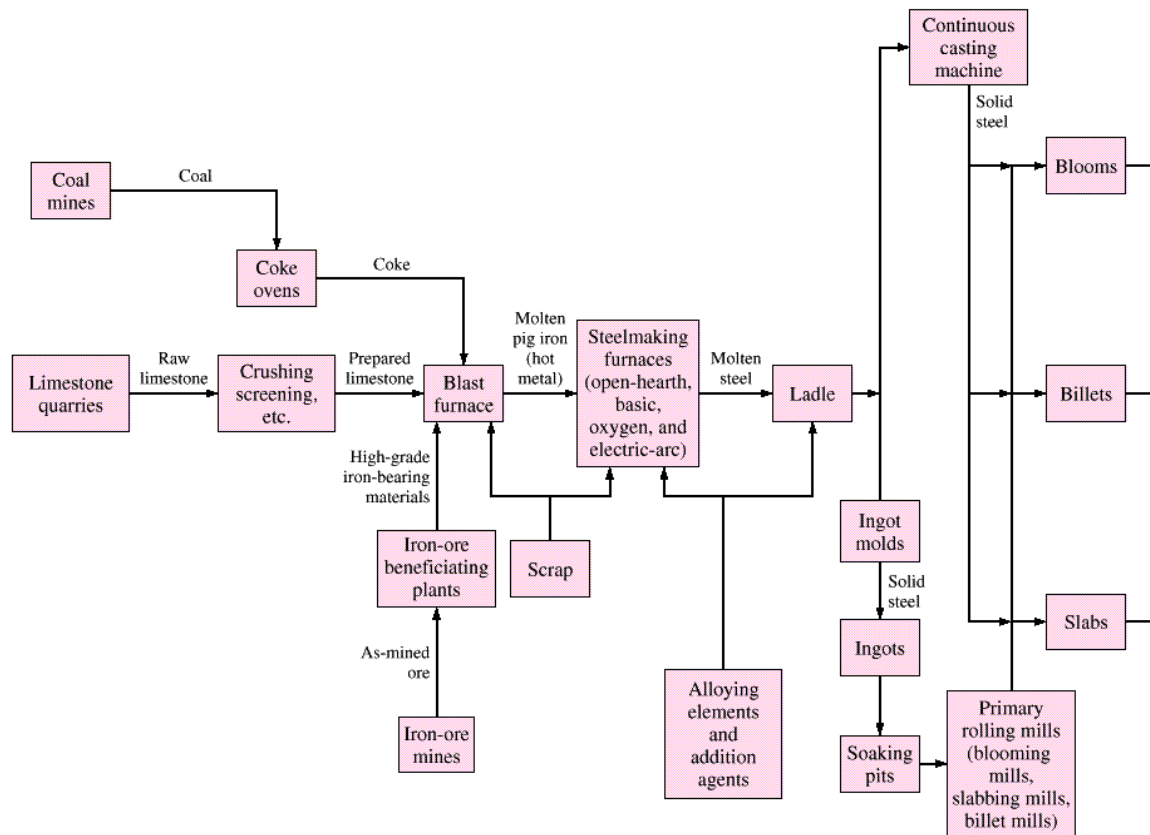


Figure 4.1 Flow diagram showing the main steps of converting the raw materials into products [3]

We will discuss in this section the production flow of steel and will take an overview on each stage separately,

Iron ore is commonly found in earth's crust which contains iron chemically bonded to oxygen, it is combined with coke and heated together for producing raw pig iron [3]



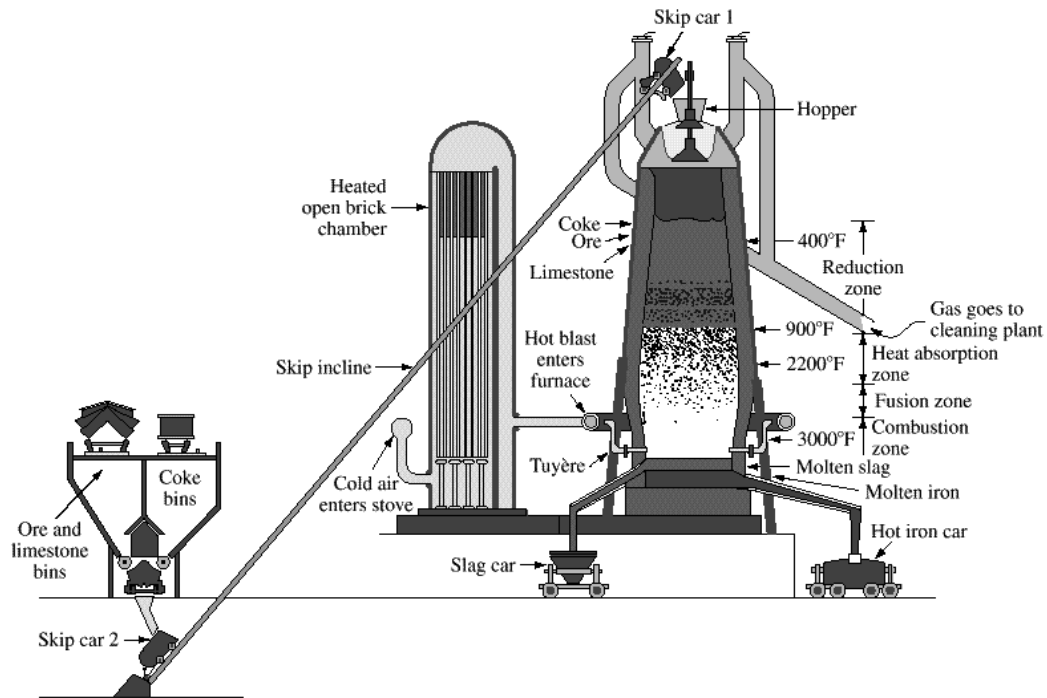


Figure 2.2 General operation of modern Blast Furnace [3]

Iron ore which previously produced is added to the blast furnace with Carbon which is supplied in form of coke and lime, then the hot air blast is injected continuously through the nozzle in the base of furnace which is called Tuyère, the high temperature causes chemical reduction and melting of Iron ore.

The limestone combines with the impurities to form a liquid called slag this process is called purification, calcium carbide will create calcium oxide which combines with  $\text{SiO}_2$  and  $\text{Al}_2\text{O}_3$  which is called the slag, it floats on the liquid iron, the liquid iron is drawn off from the bottom of the blast furnace and the slag is skimmed off and used for another industry like cement.



The metallic iron produced in the blast furnace contains about 4% of carbon, this 4% of carbon makes the iron so brittle and unsuitable for rolling or forging. and some substation amounts of impurities like Manganese, Sulphur, Silicon and Phosphor.

Starting from this point we will discuss the ways of converting the liquid pig iron into steel which can be done by

1- Oxygen steelmaking (BOP) "considered as the dominant method of producing steel from blast furnace"

## 2-Electric Furnace Steelmaking

We will focus more on the most commonly used method which is the Basic-Oxygen process [3,6]

### 2.1 Basic-Oxygen process

The scrap steel which is about 30% of the quantity is put into the vessel then the molten pig iron which has been pretreated is added. [3]

The lance blows high purity oxygen into the hot metal at approximately the twice speed of sound, this cause a rapid oxidization (burning or combustion) of carbon and creates carbon monoxide



Lime is added in a controlled amount during the blowing, it is combined with the oxidized impurities forming a slag, which is floating on the top of the steel path



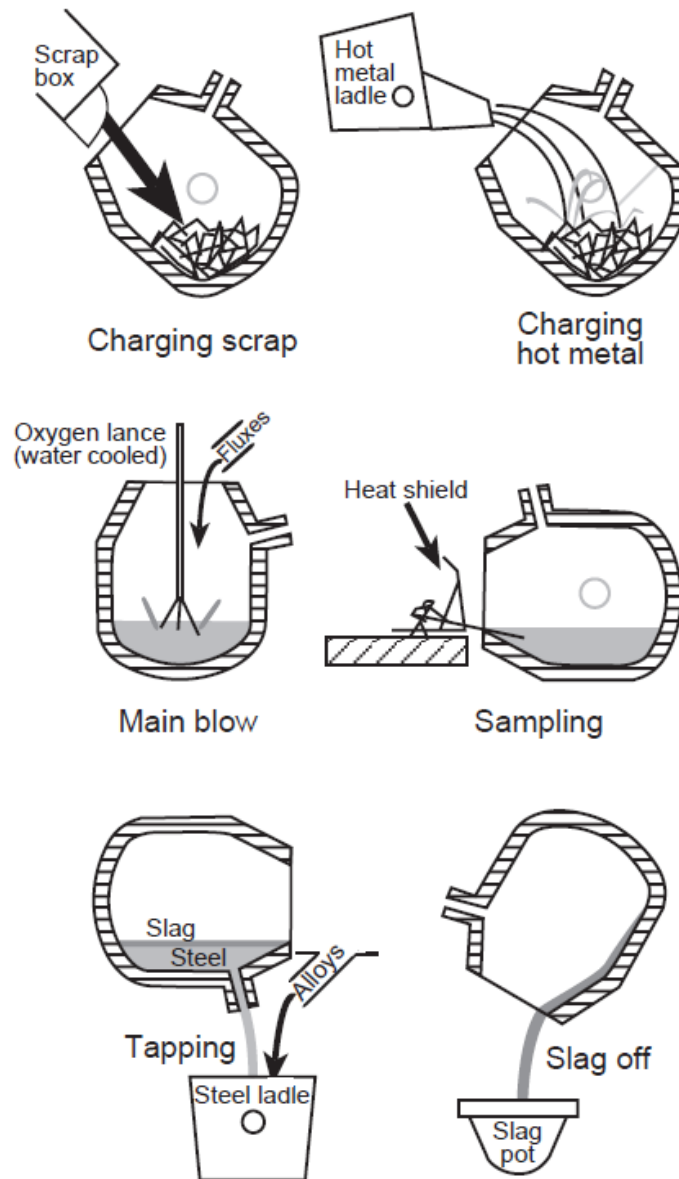


Figure (2.3) Steelmaking using the Basic-Oxygen process [6]

During tapping addition of alloys can be made for adjusting steel composition and meeting customer needs during this stage the carbon content is about 0.03% [3,6]. Reducing and controlling the amount of impurities specially Sulphur is an important goal for steelmaking process, as we have seen previously it was accomplished first inside the furnace by removing it from the liquid metal second when the flux was added for forming the chemical composition of the slag.

<b>Pig Iron BOF In</b>	<b>Steel BOF Out</b>	<b>Slag BOF</b>
<b>4.0% C</b>	<b>0.05-0.08% C</b>	<b>~40% CaO</b>
<b>0.8% Si</b>	<b>0.01% Si</b>	<b>~30% FeO</b>
<b>0.5% Mn</b>	<b>0.15% Mn</b>	<b>~12% SiO<sub>2</sub></b>
<b>0.060% S</b>	<b>0.035% S*</b>	<b>~10% MgO</b>
<b>0.035% P</b>	<b>0.010% P**</b>	<b>~3% MnO</b>
		<b>~2% Al<sub>2</sub>O<sub>3</sub></b>
		<b>~1% P<sub>2</sub>O<sub>5</sub></b>
	<b>40ppm N</b>	
	<b>Low/No H</b>	
	<b>Low Residuals</b>	
<b>1450°C</b>	<b>1700°C</b>	

\*: S-removal to BF slag and Ca<sub>2</sub>C pre-treatment,

\*\* : P-removal to BOF slag by high basicity slag and FeO

Table (2.1) the amount of different elements before and after the BOF and elements of the slag

We need to adjust the composition which is done in the secondary metallurgy, it is a very important step because at is the moment where we set the composition of the steel after that we can't change it anymore, so we add for example some **alloying** elements like Mn, Si Cr, Mo, Ni, Nb, Ti, V we also add Ca to influence the shape of the inclusion, we can also in the secondary metallurgy **remove** more of C and N by degassing, finally we do is Aluminum killing since the steel after BOF contains high level of oxygen which is removed by Aluminum (Al<sub>2</sub>O<sub>3</sub>) since it is extremely stable oxide, this process is important because if we left the oxygen in the steel the solubility of CO will decrease and bubbles are going to be formed and we will not be able to cast it because the material will be flowing over "foaming"

## 2.2 Continuous casting

Following the steelmaking casting is required to solidify the molten steel to make it ready for shaping or forming into suitable profile [4].

There are three main ways for casting sand casting, continuous casting and ingot casting.

We will focus only on the continuous casting because about of 96% of today's steel is cast continuously. [3]

The basic idea of continuous casting process for steel is teeming liquid steel vertically into a copper mould which is cooled by water and open at the bottom [7] as shown on the in the figure 2.4

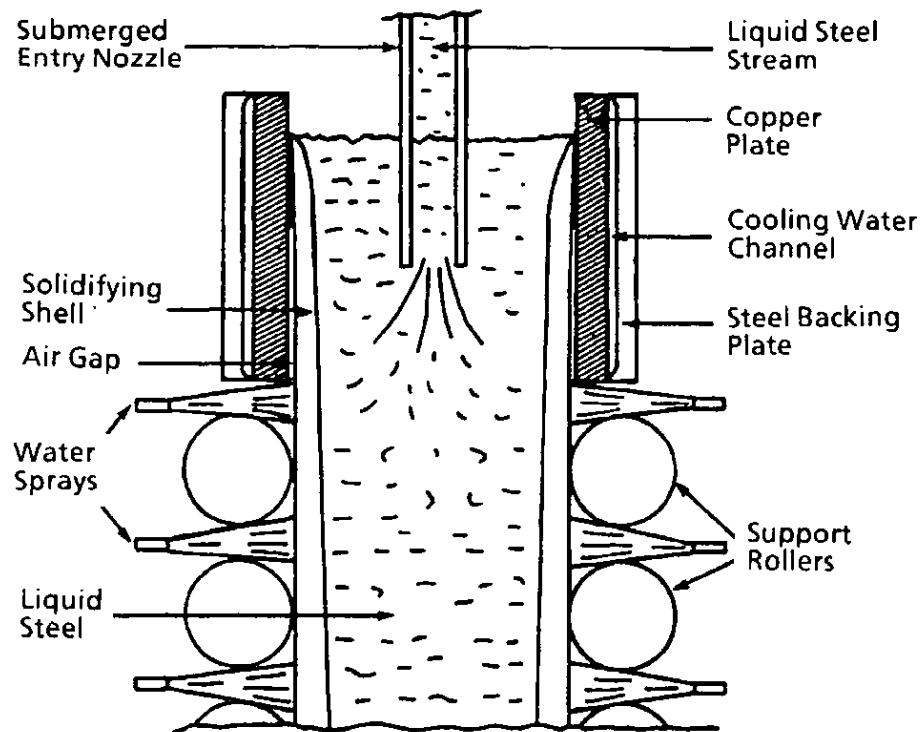


Figure (2.4) Principle of continuous casting [7]

The liquid steel is solidified immediately after passing through the water cooled copper, the solidified steel doesn't stick with the copper mould for two fundamental principles which are

- 1- the mould is reciprocated sinusoidally at a frequency
- 2- a lubricant has to be provided as an interface between the copper plate and the solidifying skin of steel.

As soon as the solidified steel skin is thick and able to contain the liquid steel which is inside "not solidified yet" it leaves the mould and cooled directly by water sprays then the solidified shell shall be withdrawn from the mould.

After understanding the main idea of continuous casting let's describe a schematic diagram of continuous casting machine.

The liquid steel is teemed from the steel making vessel to the ladle and the liquid steel follows a secondary process if needed then the ladle is moved to the continuous casting machine.

The liquid steel is poured through a refractory tube into the tundish the reason of pouring the steel through the refractory tube is in order to be protected from any oxidation from the atmosphere, note that the liquid steel is poured by the way of sliding gate valve mechanism.

The tundish acts simply as reservoir and it feeds the steel into the water cooled copper moulds, then as we mentioned previously when the steel skin is solidified it is drawn from the bottom of the mold through a curved arrangement of water sprays and support rolls.

After passing several meters the strand becomes completely solid depending on the cooling condition product thickness and casting speed, then it is cut to length by automatic gas burners

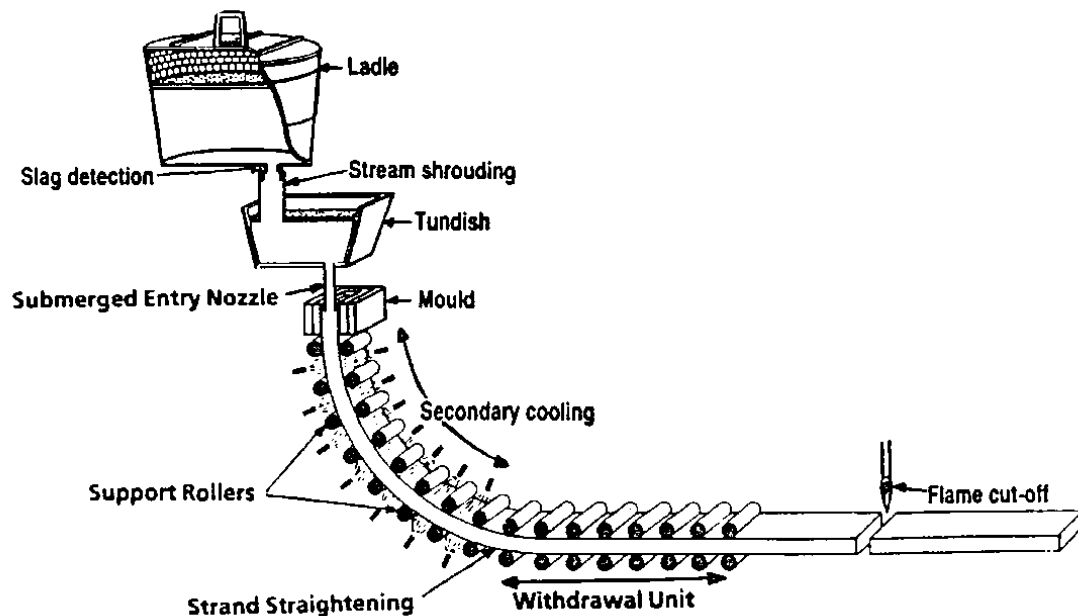


Figure (2.5) Continuous casting machine [7]

Depending on the size of the cut solid steels are called

- 1- **Billet** which is defined as small square section usually up to 150mm square and up to 150 mm diameter rounds.
- 2- **Bloom** is defined as a square or rectangular cross-sections greater than 150 mm square to as large as 800 mm x 400 mm usually with an aspect ratio less than 2. Also rounds with a diameter greater than 150 mm.
- 3- **Slab** anything larger than blooms and usually with an aspect ratio greater than 2. The largest slabs currently continuously cast are 2725 mm x 254 mm. [7]

Now the steel is ready for shaping into finished products, and this will take other to another topic which is steel rolling

## 2.3 Hot Rolling

When the steel is cold it has a high resistance for shaping, for that reason steel is rolled while it is hot at a certain temperature, in order to achieve this temperature, the steel is fed to a furnace and it travels through a several temperature zones until it reaches the required temperature for hot rolling.

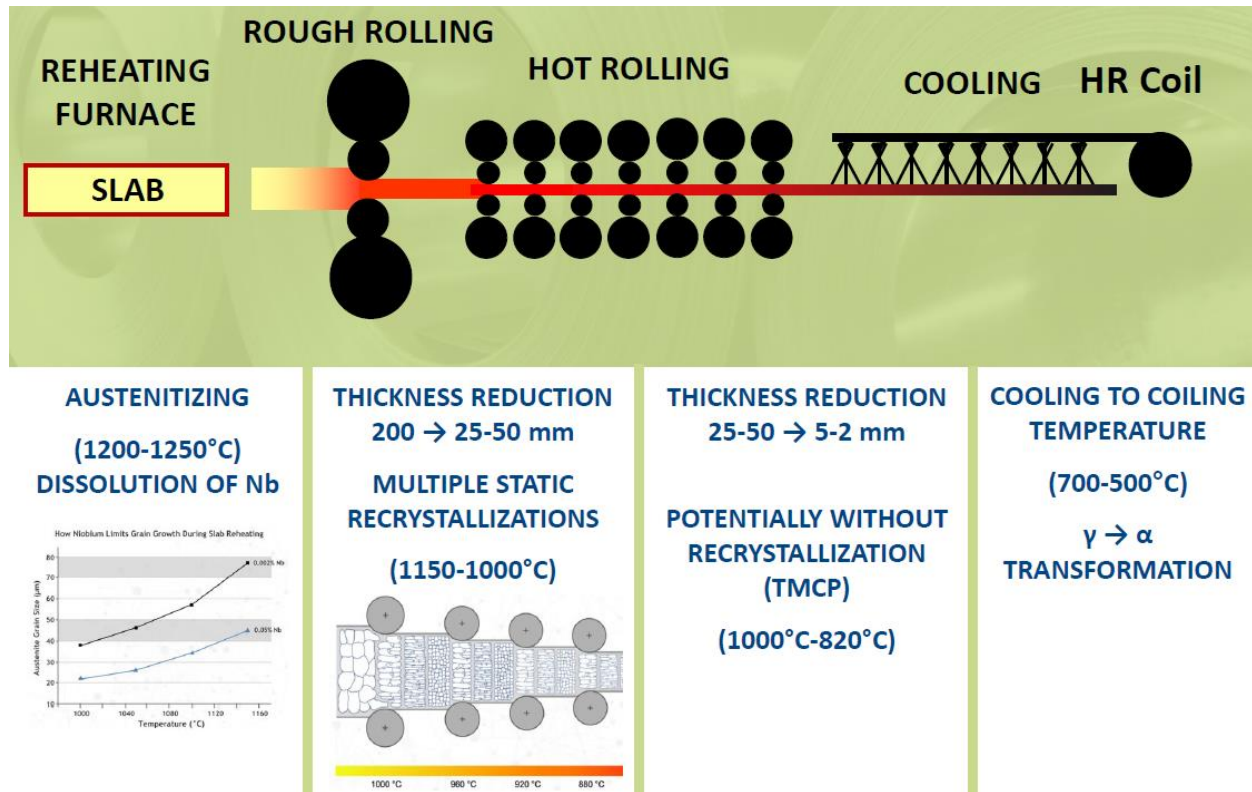


Figure (2.6) Rolling process [28]

the finishing temperature and the mill drafting are varying depending on the hot rolled product since these products are not having the same physical and metallurgical properties. [8]

in general, the optimum temperature for high Carbon steels reheated in oxidation atmosphere are usually in range of 1065.5-1121.1°C. For medium carbon steel the range is from 1093.3-1148.8°C While for low carbon steels that containing no alloying elements may be heated to 1287.7°C.

The process principle of rolling is simply the steel is squeezed between rolls until the final thickness and shape are achieved in order to do it millions of newtons which is equivalent to thousands of tons should be exerted by the rolls, the sequence of rolling operation involves reciprocation motion of the steel slab several strokes as shown in the following figure 2.7 [8]

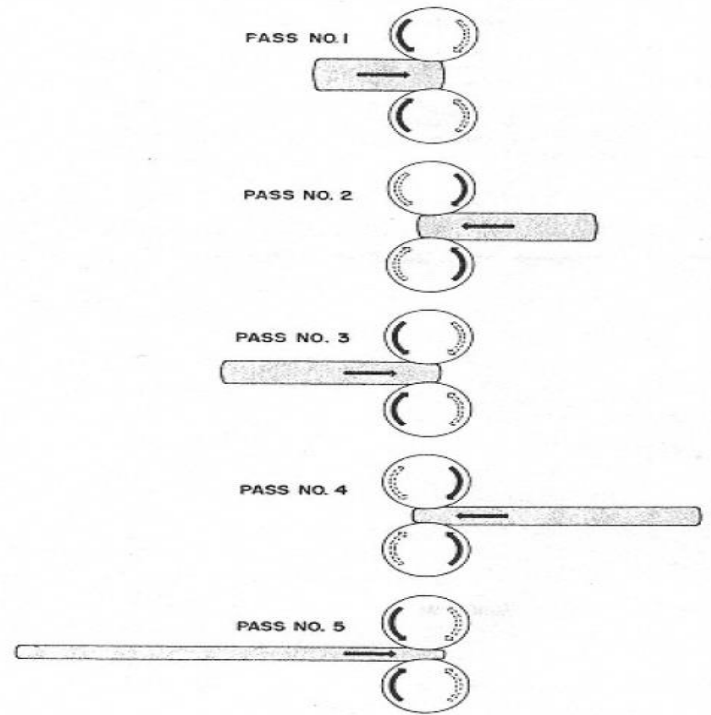


Figure (2.7) multi stage rolling. [8]

## 2.4 Cold rolling

Once after the hot rolled steel is cooled into about room temperature it is re-rolled again for achieving better surface quality and more exact dimensions, the steel sheets are undergoing compression between rollers same as hot rolled process, due to the friction between the steel sheets and the rollers the temperature might raise so it is continuously cooled by oil which make the surface often oily and smooth.

As the metal's is shaped the resistance against deformation, tension breaking, metal hardness, yield and ultimate tensile strengths are much higher compared to the only hot rolled metal while the ductility is decreased. [9]

Cold rolling is an important factor that affects the drawability of the steel It has been observed that the  $r_m$  value at least increases by 90% by increasing the cold rolling reduction as shown in the following figure 2.8 [10]

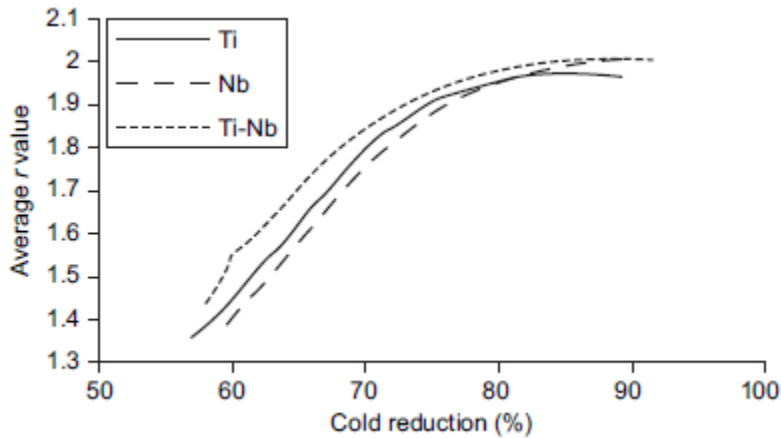


Figure (2.8) The effect of cold rolling on the  $r_m$  value of Ti, Nb and Ti-Nb [10]

We can see in the previous figure that the average or  $r_m$  value is much higher when titanium (Ti) and Niobium (Nb) are combined together as the percentage of cold rolling reduction is increased

## 2.5 Continuous heat treatment

### 2.5.1 Quenching (Strengthening Treatment)

By a controlled heat treatment, the mechanical properties of the steel can be changed for example the hardness of unalloyed carbon steel can be increased up to 500% just by changing the cooling rate from austenitizing temperature from extremely slow cooling to extremely fast cooling. [1]

this extremely fast cooling determines the desired mechanical properties but it may cause formation of transformational stresses and thermal stresses that are changing the size and the shape which leads to quenching cracks

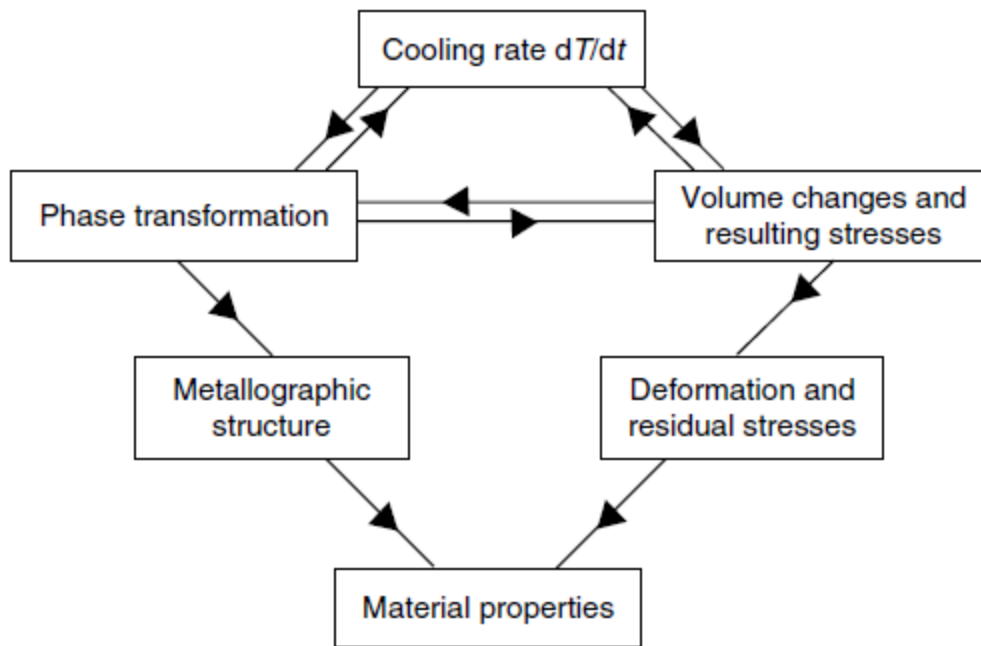


Figure (2.9) The influence on the material properties considering the two scenarios that are caused by the cooling rate.

So now we can understand that the main objective of the quenching process is to achieve the desired hardness, strength and microstructure while minimizing the distortion and stresses, the carbon concentration should be limited to 0.7% [1] otherwise cracks can be formed. the most common quenchants are liquids like water and water that contains salt, molten salt or metal and hardening oils, it could be also inert gases. [18]

A certain amount of austenite remains during quenching even if the content of carbon is so low for that reason it is impossible to reach the maximum hardness of the workpiece the steel must undergo subzero treatment since the austenite is stable in room temperature and it passes to martensite at a lower temperature

There are two quenching technique that are used for liquid the first one is **Immersion quenching** where the workpiece is submerged into the quenchant, this technique is the mostly used, the workpiece maybe quenched directly from the austenitizing temperature to the room temperature or it can be cooled to a temperature above the  $M_s$  (martensite starts) temperature and then held for a period of time then it is cooled at a slower cooling rate in a second medium.



Another technique is **spray quenching** where the liquid is sprayed onto specific areas on the workpiece where higher cooling rates is desired.

### INFLUENCE OF CARBON concentration

The high amount of carbon increases the hardness of the steel before quenching, the reason is that by increasing the dislocation density and distortion of the body centered martensite lattice due to the inserted carbon atom.

The temperature of completing the martensite formation  $M_f$  is below the room temperature as we can see in the following figure 2.10, the retained austenite is increasing in the martensite structure with increasing the content of the dissolved carbon as shown in figure 2.11 due to this volume expansion of this transformation there are changes in shape and size that results a cracks in the workpiece.

Rising the concentration of carbon tends to decrease the toughness of the martensite with high local stresses for that reason the carbon content shown be below 0.7% [1]

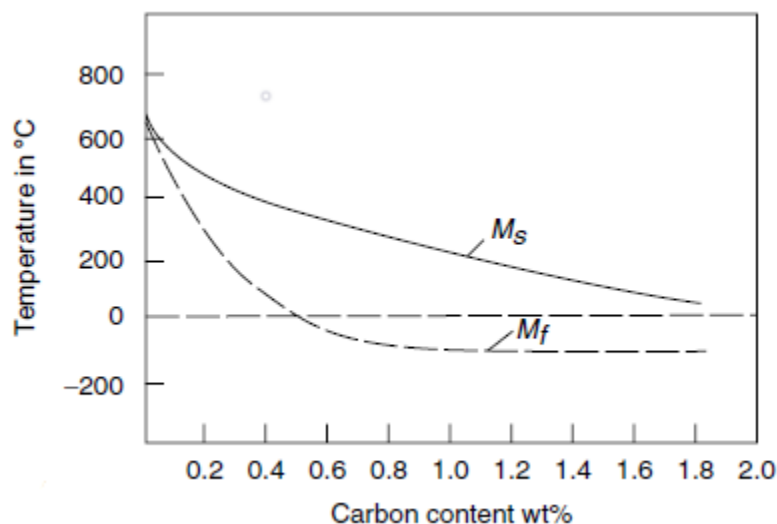


Figure (2.10) the relation between the carbon content and temperature for starting and completing the martensite formation  $M_s$  and  $M_f$ . [1]

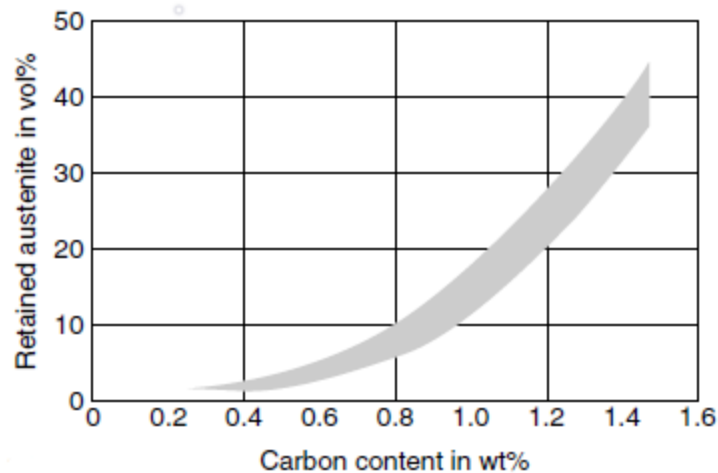


Figure (2.11) the relation between the carbon content and retained austenite. [1]

### 3. Low Carbon Steels Used for Car Body

Steels that contain less than 0.25% of carbon is called low carbon steel [4,11] Automotive sheet application is one from the major applications of low carbon steels, the need of the low carbon steel were driven by manufacturing needs since it has good formability and weldability also performance needs since it combines the strength and fracture resistance.

In the past in order to increase the load carrying capacity by the low carbon steels the design of the structure involves increasing its section size, recently due to the need to reduce the fuel consumption, the economic factors and safety concerns approaches have been followed for vehicles for developing low carbon steel's microstructures for higher strength in order to reduce the weight and section size.

As a result, there are continuous changes in the composition of the low carbon steels that tends to having a higher strengths and improving the weldability, formability and toughness or fracture resistance

On the following graph we can see different types of low carbon steels that has been developed starting from the 21<sup>th</sup> century

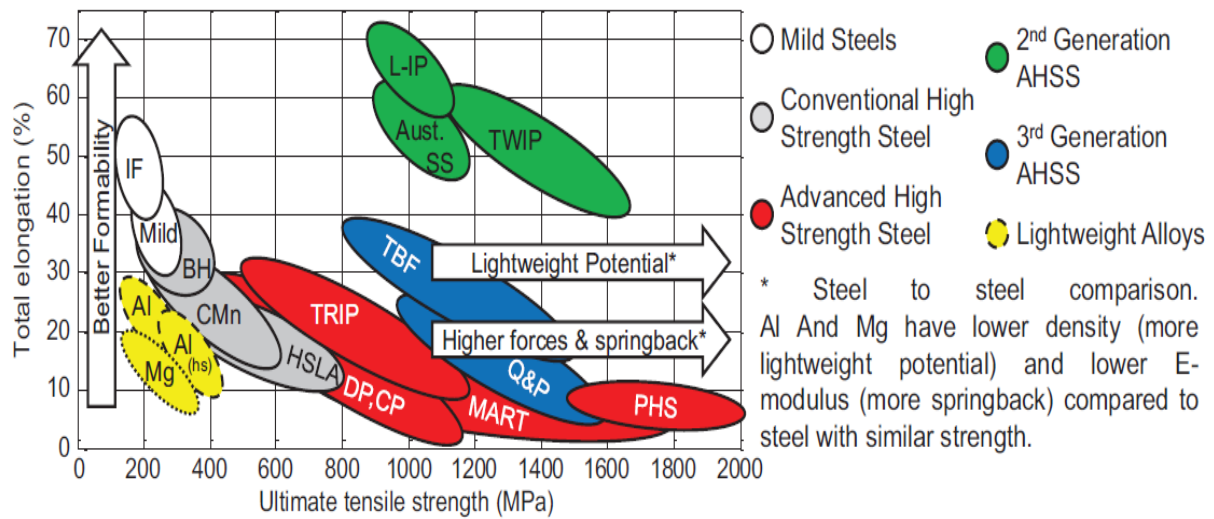


Figure 3.1 Automotive steel grades based on ductility and strength [10]

BH: bake hardening, CP: complex phase, DP: dual phase, HSLA: high strength low alloy, CMn: carbon manganese, IF: interstitial free, IF-HS: interstitial free high strength, TRIP: transformation-induced plasticity, MART: Martensitic, TBF: TRIP bainitic ferrite, Q&P: Quenching and Partitioning steel, PHS: Press Hardening steel.

AHSS category	Characteristics	limitations	Steels type
First generation	<ul style="list-style-type: none"> <li>• Ferrite based with multiphase microstructure.</li> <li>• Higher strength than HSS.</li> <li>• Product of TS-EL &lt;25000 MPa%.</li> </ul>	<ul style="list-style-type: none"> <li>• Limited formability and ductility.</li> </ul>	<ul style="list-style-type: none"> <li>• Dual-phase (DP)</li> <li>• (CP)</li> <li>• TRIP</li> <li>• MART</li> </ul>
Second generation	<ul style="list-style-type: none"> <li>• AHSS with austenite stabilized in the microstructure.</li> <li>• Containing high Mn and other alloy elements.</li> <li>• Has excellent combination of strength and formability.</li> <li>• Product of TS-EL &gt;50000 MPa%.</li> </ul>	<ul style="list-style-type: none"> <li>• Due to high alloy additions the cost is high.</li> <li>• Poor weldability and tendency of delayed cracking.</li> </ul>	<ul style="list-style-type: none"> <li>• TWIP</li> </ul>
Third generation	<ul style="list-style-type: none"> <li>• Extension of the first generation by different processing routes at lower cost and grain refinement.</li> <li>• Acts in between of first and second generation since the product of TS-EL &gt;25000 MPa%.</li> </ul>	<ul style="list-style-type: none"> <li>• Special processing routes are required including controlled cooling at high rates.</li> </ul>	<ul style="list-style-type: none"> <li>• Q&amp;P</li> </ul>

Table 3.1 Generations of AHSS. [22,15,17]

Let's show now the details of each type of these steels

### 3.1 Interstitial-Free Steels (IF)

it is also referred to as ultra-low-carbon (ULC) or extra-low-carbon (ELC) this type of steels have a very low carbon and nitrogen contents, also it has a very high ductility and formability at low strengths as shown in the previous figure 3.1.

Products of IF typically contain 20 to 50 ppm of carbon and from 10 to 50 ppm of nitrogen. [4,10], further by adding Titanium and/or Niobium for removing the carbon and nitrogen from the solid solution and the matrix becomes nearly completely free of interstitials.

A minimum amount of titanium (Ti) and niobium(Nb) is required in order to stabilize the total carbon and nitrogen in IF steels, the percentage of solute carbon and nitrogen is kept below 0.003% in IF steels, normally titanium and niobium amounts are above the stoichiometric and they are considered as a main parameter that determines the behavior of IF steels.

By adding a small amount of sulfur(S) it reacts with (Ti) and (C) forming carbosulfide precipitates at relatively high temperature. Formation of these precipitates over other carbon containing precipitates (i.e., TiC) is always more beneficial, as these are bigger in size and therefore do not adversely influence recrystallization and the subsequent grain growth process. [10]

The most common alloying elements that are added to IF steels are Manganese (Mn) and phosphorus (P) that are increasing the mechanical strength and resulting grade that is called IFHS steel, by adding 0.1% (P) that leads to an increment in strength of more than 100 MPa, while by adding Si, Cr and Cu with the same quantity which is 0.1% that leads to increase the strength of 4-8 MPa, although the effect of (Mn) is quite similar to Si, Cr, Cu but Mn is preferred among them because it is inexpensive and it has a less harmful effect on overall properties of steels.

When increasing the P content there is a high risk of cold work embrittlement, by adding a small amount of boron we can overcome the problem, boron segregates to grain boundaries and forces P to remain in solid solution.

In the following table we can see the Yield stress (YS) and the ultimate tensile strength (UTS) of the interstitial free steels (IF) and the high strength interstitial free steels (IFHS).

	Yield stress (YS)	ultimate tensile strength (UTS)
interstitial free steels (IF)	140-150 MPa	280-290 MPa

high strength interstitial free steels (IFHS)	220-320 MPa	390-440 MPa
---	-------------	-------------

Table 3.2

The higher strength is achieved by adding a solid solution strengthening element such as Mn, Si and P to the interstitial free steels (IF), these elements increase the strength but on the other hand it reduces the formability and deep drawability.

### 3.2 Bake Hardenable (BH) Steels:

It is a special grade of low carbon steels, the static strain aging property of free carbon is exploited in a controlled way, a unique feature of this steels in chemistry and processing design is to keep the carbon in the solution during steelmaking this amount of carbon not going to strongly affect the formability of the steel and then allowing this carbon to come out of the solution in the paint.

This process increases the steel by strength by 30-90 MPa, they are exclusively used in the production of automotive outer panel thanks to their high dent resistance, an increase in yield stress of about 40 MPa would compensate in reduction of gage about 0.1 mm for the same dent resistance.

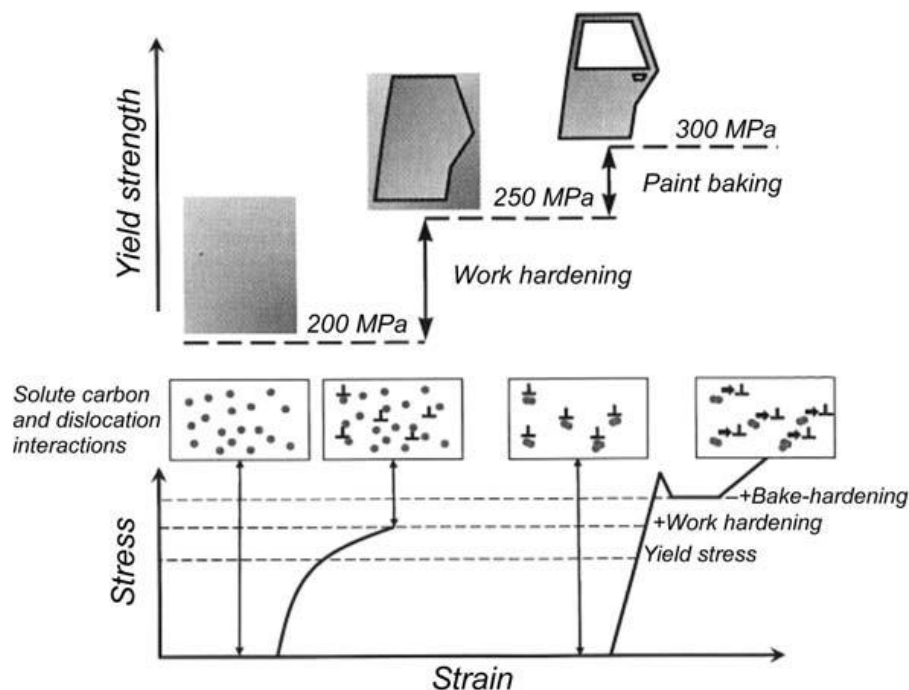


Figure 3.2 Schematic representation of the bake hardening (BH) process and its effect on yield strength of steel [10]

Two mechanisms are responsible for having the BH effect:

- 1- Dislocation pinning: during the press forming process dislocation is generated which will lead to form of Cottrell atmosphere due to the presence of carbon atoms at the vicinity of dislocation cores.
- 2- Precipitation hardening which is a heat treatment technique at low temperature, at later stages of aging process some are formed and contributes to the Yield strength

### 3.3 High strength, Low-Alloy Low-Carbon Steels (HSLA)

They have better mechanical properties, higher strength and/or greater corrosion resistance than plain carbon with nominal ferrite-pearlite microstructure [4,11]

HSLA steels are offering a good fatigue, rigidity, torsional and impact strength, which means they are offering weight reduction for reinforcement and structural components [10]

The HSLA steels contains a small amount of microalloying elements such as niobium, vanadium and titanium that are combined together with controlled rolling in order to produce a good weldability and toughness [4], for example HSLA-V steels with ultrafine grains offers an excellent balance of strength and ductility [10], The carbon content may vary from 0.05 to 0.25%C for different mechanical requirements and thicknesses [11].

In the following table we can see the Yield stress (YS) of the alloyed high strength low alloys steels and the plain carbon steels.

	Yield stress (YS)
Plain carbon steel	170-250 MPa
HSLA-microalloyed	260-690 MPa

Table 3.3

Because of the solubility of microalloying elements varies in austenite, each of them has a particular role during the thermomechanical processing (TMP) of HSLA steels. TiN is used to control the grain coarsening of austenite during reheating, Nb(C and/or N) are used for controlling the non-recrystallization temperature ( $T_{nr}$ ) and the transformation temperature

( $T_{Ar3}$ ) and  $V(C \text{ and } N)$  are used for precipitation strengthening during the transformation from austenite to ferrite under controlled cooling condition

On the following schematic 3.3 we can see the hot rolling schedules used for different low carbon steel like (a) normal processing (b) controlled rolling of C-Mn steels (c) controlled rolling of Nb-containing steels (d) controlled rolling of Nb-containing steels with finishing temperature  $Ac_3$ .

The critical temperatures are  $Ac_1$  and  $Ac_3$ ,  $T_R$  is the temperature where the austenite does not recrystallize. [4]

As shown in the schematic microaddition of Nb effectively raise the  $T_R$  and it is extensively used in HSLA steels

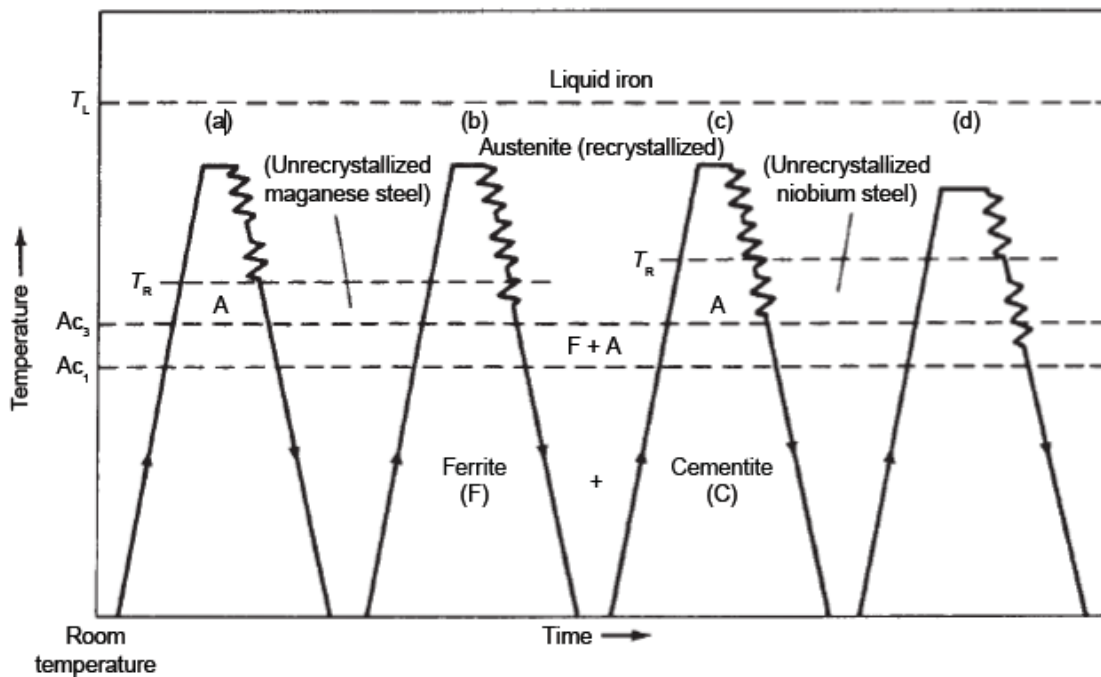


Figure 3.3 hot rolling schedules used for different low carbon steel (a) normal processing (b) controlled rolling of C-Mn steels (c) controlled rolling of Nb-containing steels (d) controlled rolling of Nb-containing steels with finishing temperature  $Ac_3$ . [4]

For better understanding the strong effect of adding a small amount of Nb we can compare between experimental studies that shows its effect on austenite recrystallization.

As indicated in figure 3.4 a specimens of 0.11%C and 1.3%Mn" curve number 1" were hot rolled at temperature of 950 C and the deformed austenite was then held at different temperatures for different times and it was figured out that the steel was recrystallized evenly at low austenitizing temperatures

By repeating the experiment while using 0.10%C and Nb contents between 0.031% and 0.21% "curves number 2,3,4,5" it starts to recrystallize after a bout of 10,000 seconds (167 min) of holding time. [4]



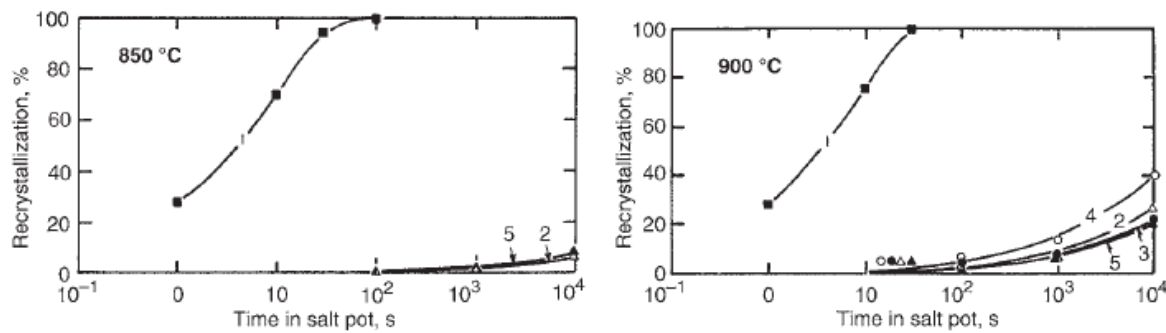


Figure 3.4 The holding time on the left is 850 while on the right is 900 after hot rolling at 950C [4]

The non-recrystallization temperature is one from the most important tools for controlling the austenite in terms of (1) microstructure uniformity in the transfer bar, before entering the finishing mill. (2) deformation between the  $T_{nr}$  and  $A_{r3}$  that produces a large number of intercrystalline defects as shown in the following schematics 3.5 [10]

HSLA-Nb is relatively used for its formability instead of having a very fast recrystallization in the hot roll process between the two rolls by adding Nb we will have a recrystallization that is slower.

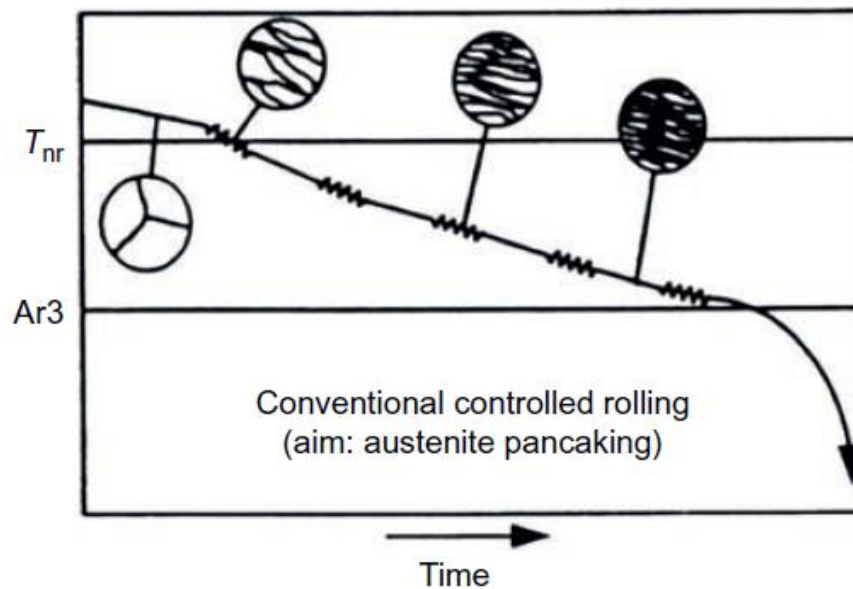


Figure 3.5 Schematic representation of the effect of deformation between the  $T_{nr}$  and the  $T_{Ar3}$  on the austenite microstructure [10]

It is important to say that the proper selection of finishing rolling temperature and coiling temperature will affect the uniformity of the ferrite as shown in figure 3.6 the information in

this figure is clearly says that finer ferrite microstructure in HSLA steels occurs when the finishing temperature is coupled with the lower coiling temperature.

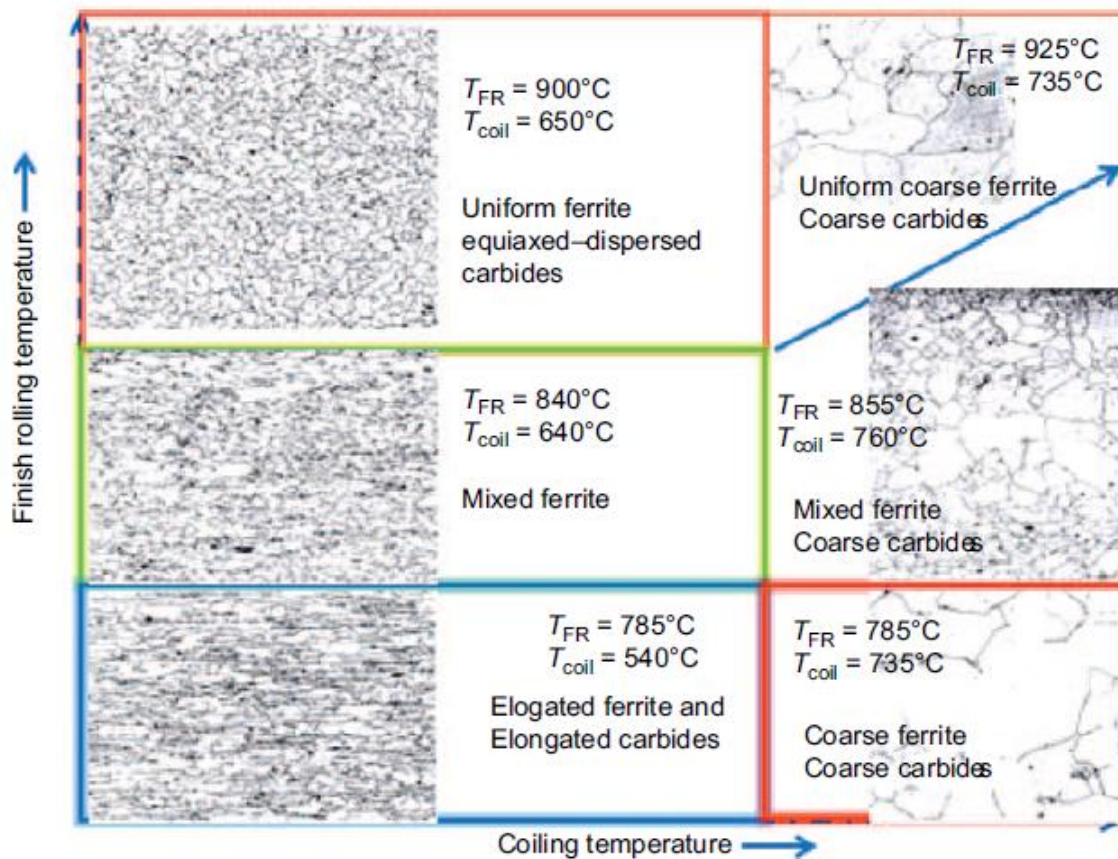


Figure 3.6 the effect of rolling and coiling temperatures on the uniformity of the ferrite of the grain size in HSLA steels

Typical application of HSLA steels are shown in the following table 3.4

Grade	Product type	functional properties	Main applications
HSLA 260-420	Hot rolled	Cold forming	Chassis, Suspension parts, wheels rim and disks
HSLA 550	Hot rolled	Cold forming	
HSLA 750	Hot rolled	Cold forming	
HSLA 320	Cold rolling for hot	Cold forming	Automotive parts that require certain

HSLA 420	dip galvanizing		level of stretch-forming and deep drawing characteristics
HSLA 590			

As shown in the previous table 3.4 the hot rolled HSLA steels are chosen for some major required properties that are strength, fatigue flexural resistance and moment of inertia While in the cooled rolled HSLA steels are reinforcement center body pillar and pillar body lock inner that are shown in the following figure 3.7 [10]



Reinforcement center body pillar (1.50 mm—HSLA Gr350)



Pillar body lock inner (1.30 mm—HSLA Gr350)

Figure 3.7 example of some applications of HSLA steels

One of the things that happens is that we go for structure hardening using carbon as the main alloying elements there are some secondary factors that comes to the play one of them is the weldability, which is related to the so called carbon equivalent value which is basically an empirical quantity ( $C.E. = C + Mn/6 + (Ni + Cu)/15 + (Cr + Mo + V)/5$ ). that gives us an idea about how easily we can turn the steel into martensite, and the other thing is the property of the martensite itself which expressed on y-axis that is expressed by the carbon content

So when we look at the weldability of the steel, we must make sure that we didn't do too much martensite when we are welding because we heat up the material very quickly and cool it very quickly so the material will be hard and brittle if they contain a lot of carbon, so as we can see

in the following diagram 3.8 HSLA steels are in the readily weldable region, we don't have to worry about it in terms of weldability and for that reason it is widely used

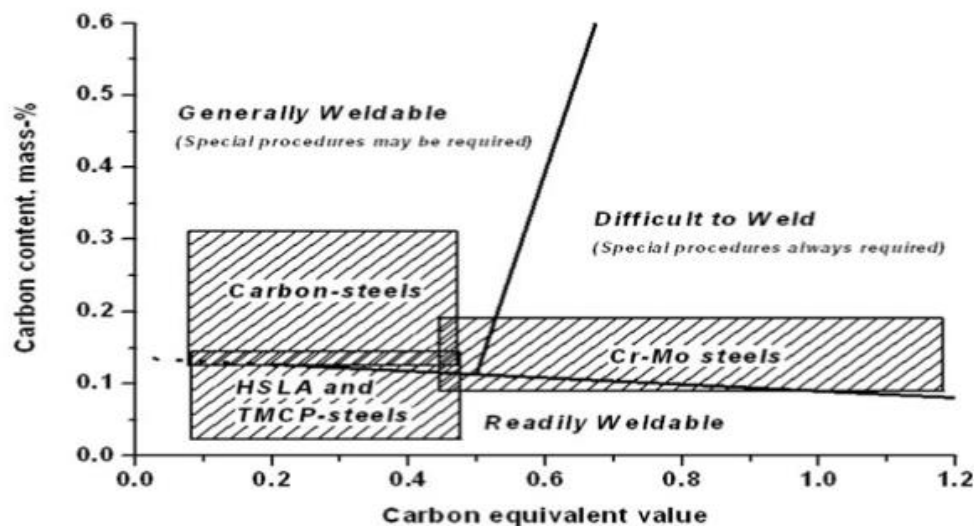


Figure 3.8 the weldability of different steels based on carbon content and carbon equivalent graph

### 3.4 Dual Phase (DP)

[10,12,17,14] The main feature of DP steels is the balance between the strength and ductility (formability), they range in a tensile strength from 450 to 1200 Mpa [10],

DP contains carbon in range of (0.05-0.20%), silicon (0.30-0.60%), Manganese of (1.2-1.6%) and some micro-additions up to 0.1% of Ti, V and Nb

instead of having a ferritic microstructure we will have a multiphase microstructure it consists of ferritic mixture containing hard martensitic second phase or bainite. [12]

the properties like strength and percent elongation are controlled by the amount of bainite/martensite and their distribution in the ferrite matrix. Other property like the ductility and the toughness are linked to DP steels that has ferrite embedded bainite but on the other hand it has less tensile and yield strength value when it is compared to ferrite-martensite steels.

In the following figure 3.9 we can see on the left (a) bainite-ferrite steel "BF" while on the right (b) martensite-ferrite steel "MF" both of them are containing equal ferrite (34%) beside with harder bainite or martensite.

In the following table 3.5 we can see with numbers the effect of MF and BF on UTS, percentage of elongation and Charpy impact energy

	UTS	percentage of elongation	Charpy impact energy
bainite-ferrite steel "BF"	1424 Mpa	13.77 %	36.50 J
martensite-ferrite steel "MF"	2190 Mpa	8.12 %	10 J

Table 3.5

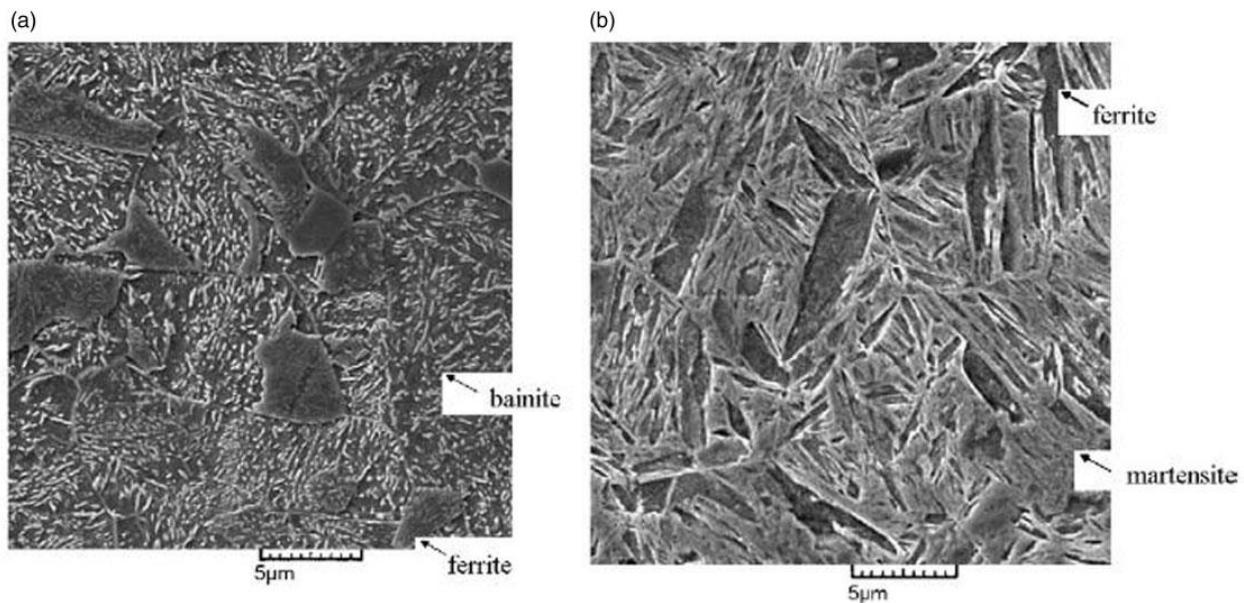


Figure 3.9 SEM micrograph of (a) bainite-ferrite "BF" and (b) martensite-ferrite "MF" steel. [17]

In order to achieve different strength-ductility combination we have to alternate the fraction of phases, distribution of phases, carbon content in harder phases and grain size of the DP microstructure.

Martensite volume fraction (MVF) for DP600, DP800 and DP1000 steels is 18%, 32% and 50% respectively while their limiting drawing ratio (LDR) is 2.19, 2.15 and 2.07 respectively.

Figure 3.10 represents the scanning electron of micrograph of DP600, DP800 and DP1000 steels showing different properties of various DP grades so we can see that DP600 and DP800 steel's martensite's steel is an islands shaped while for DP 1000 it is mesh type so as result we can say that by increasing the Martensite volume fraction (MVF) and mesh type structure the strength increase while the LDR decrease.

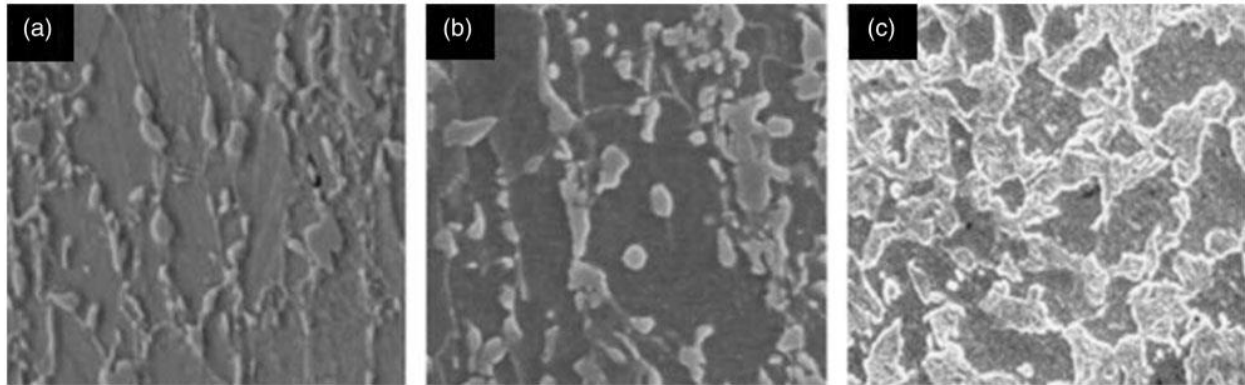


Figure 3.10 SEM images of various grades: (a) DP600, (b) DP800, (c) DP1000. [17]

#### 3.4.1 Effect of heat treatment parameters on DP steels

at different cooling rates after austenization temperature we will have different microstructure which tends to have different properties, in the following figure 3.11 we have 2 cooling rates on the left we have DP microstructure with a cooling rate of  $100^{\circ}\text{C/s}$  while on the right the cooling rate is  $10^{\circ}\text{C/s}$ , the faster cooling rate resulted ferritic-bainitic/martensitic micro structure while the slower cooling rate resulted ferritic-pearlite structure.

The faster cooling rates are required in order to avoid the pearlite and other carbide formations since they are decreasing the strength of the DP steel.

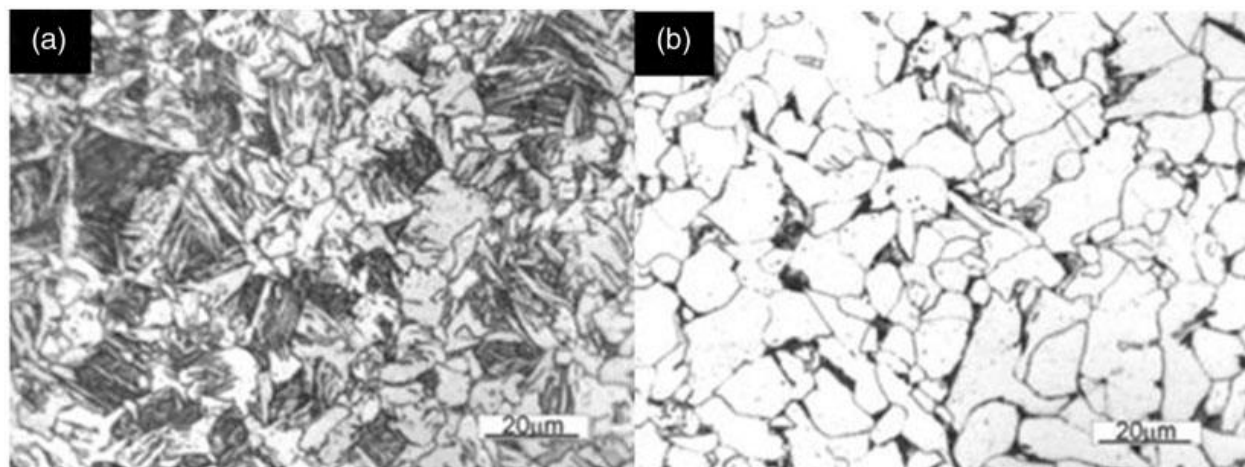


Figure 3.11 DP microstructure with cooling rate of: (a)  $100^{\circ}\text{C/s}$  and (b)  $10^{\circ}\text{C/s}$ . [17]

Now let's see the influence of heating rate on recrystallization of the formation of ferrite and austenite in DP steel, considering a steel composition of (0.1% C, 0.4% Si, 1.6% Mn, 0.017% Cr, 0.013% P, 0.006% S, Fe: balance) and heating it to inter-critical temperature ( $730^{\circ}\text{C}$ ,  $770^{\circ}\text{C}$ ,  $790^{\circ}\text{C}$ ).



°C, 830 °C) at different rates of heating (5 °C /s, 50 °C /s, and 500 °C /s) and then quenched back to room temperature without soaking at the austenization temperature.

By scanning the electron micrograph of sample at different heating rates as shown in figure 3.12 where the white arrows are showing carbide desparation and the black arrows are showing the austenite nucleation

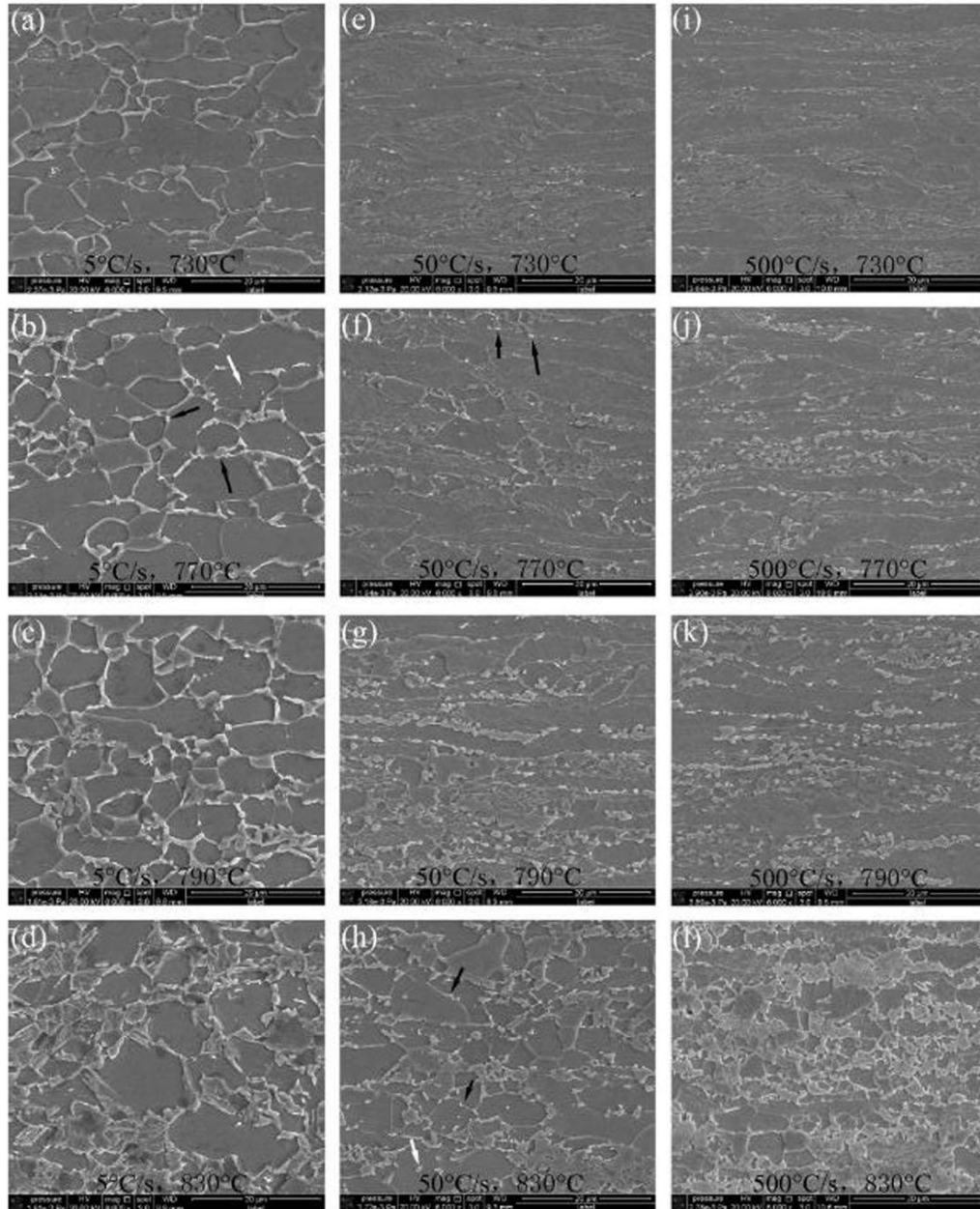


Figure 3.12. Scanning electron microscopy micrographs showing influence of heating rates on austenite formation under different conditions. [17]

We can see that the shape of the martensite has changed to chain shape structure from network with increasing the heat rate at low annealing temperature, so we can conclude that at high heating rates with high temperature is refinement the grains and improves the strength.

The increment of inter-critical annealing temperature (ICAT) improves the hardness and strength this increase attributed to increase in austenite fraction thus increase in martensite fraction on subsection cooling, on the other hand the ductility is reduced since the fraction of ferrite phase is reduced.

### 3.4.2 Processing of DP steels

For fabrication of the DP steels there are few commonly used processing routes one of them (let's call it route A) involves rapid cooling from the inter-critical temperature to room temperature resulting a microstructure that contains ferrite and martensite.

The higher the inter-critical temperature for the same soaking time the larger the amount of martensite which means higher tensile strength and lower percentage of elongation.

Cracks are linked to the amount of martensite fraction in DP steel since it promotes it which tends to a poor ductility as shown in Figure 3.13 for that reason martensite fraction is kept in range of 10% -40%.

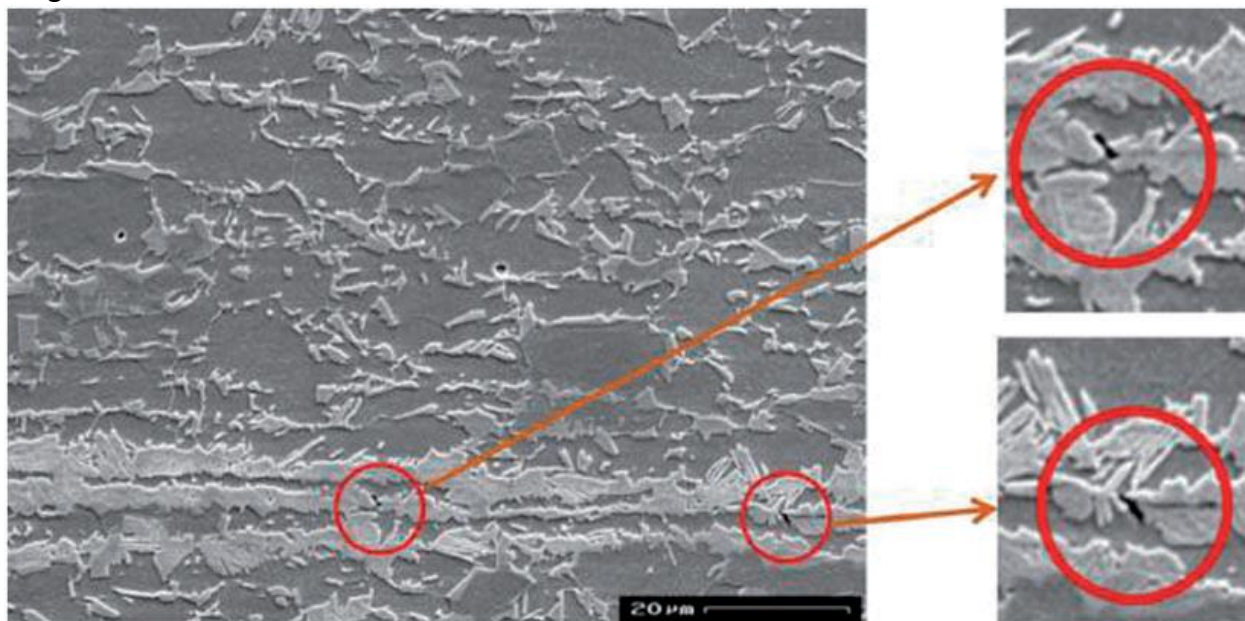


Figure 3.13 Crack initiation in martensite in DP steels. [17]

Another method (Route B) involves slow cooling from fully austenitic region to desired ferrite transformation temperature then it is followed by quenching to room temperature for transforming the rest of austenite to martensite.

The properties that are obtained from this method is lesser tensile strength and higher ductility compared to the first method (Route A) that's due to in Route B the austenite grain size is larger than in Route A.



### 3.5 Transformation-induced plasticity steels (TRIP)

[17,23] it is a first generation AHSS, it has a multiphase microstructure of ferrite, retained austenite, bainite and possibly martensite.

#### 3.5.1 Microstructure and properties of TRIP steels

In this steel the austenite stabilizers are present mainly C, Mn, and/or Ni. Also N is recommended in this steels without Al.

Because of weldability concerns the carbon content is in range of 0.20%-0.25%.

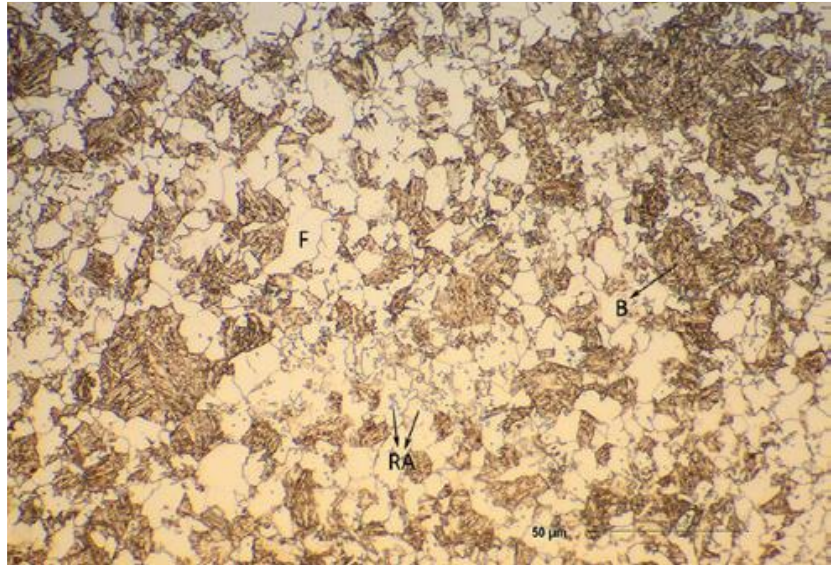


Figure 3.14. micrograph showing the micro structure of TRIP steel. F, ferrite B, bainite, RA retained austenite. [23]

TRIP steels contains multi-phase micro structure that composed of ferrite, bainite, retained austenite and martensite with these ranges (50%-55%), (30%-35%), (7%-15%) and (1%-5%) respectively.

We have the TRIP effect which is the conversion of the retained austenite to martensite such a transformation makes excellent ductility and strength in TRIP steels.

As we can see in figure 3.15 the TRIP effect during tensile test of a specimen, it showed an excellent strength and percentage elongation and also it offers a high impact resistance.

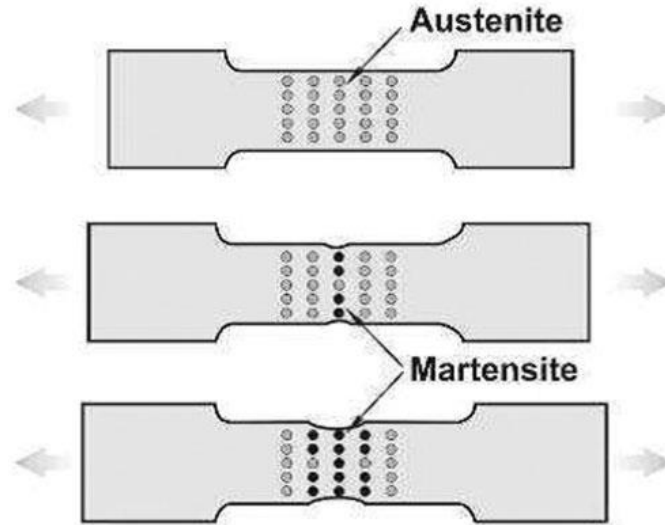


Figure 3.15. Illustration of TRIP effect during tensile test. [17]

### 3.5.2 Factors influencing TRIP effect

Factors that are influencing the TRIP effect are:

- The volume fraction of the retained austenite and its resistance to convert to martensite during transformation.
- The retained austenite carbon content.
- The austenite's grain size.
- The alloying element present in the steel.

### 5.3 Processing of TRIP steels

There are two processing routes for TRIP steel: hot and cold rolling.

The hot rolling starts, it is mainly processed by heating the steel to full austenitic region then the sheet goes to run out table and controlled cooling is applied and during the cooling ferrite forms.

The sheet is coiled in the bainitic region and the austenite is transferred to the bainite with subsequent soaking in bainite region and finally it is quenched to the room temperature as shown in Figure 3.16

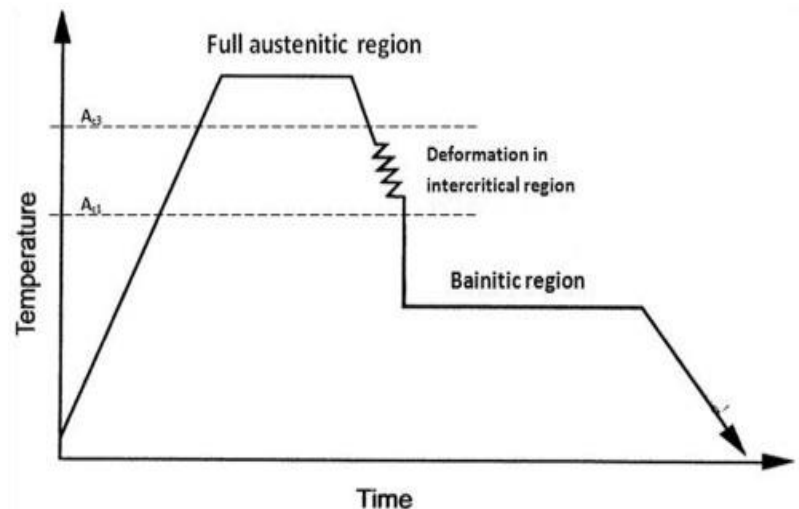


Figure 3.16. Conventional processing route of TRIP steels.[17]

In the inter-critical temperature region increases the rate of transformation from austenite to ferrite  $\alpha$ , the remaining austenite  $\gamma$  is enriched with C content which tends to stabilization of austenite  $\gamma$  at room temperature.

We have more stability in  $\gamma$  during TRIP effect when we have more C in  $\gamma$ , it should be noted that it takes more time to transform into martensite which increases the stability of the TRIP steels.

In contrast the cold rolled TRIP steel is transformed in two stage the first one is intercritical annealing, the second is isothermal bainitic transformation.

In the first stage the steel is heated into intercritical temperature of the region where 2 phases microstructure of ferrite and austenite are formed, the as a second stage the steel is rapidly cooled to avoid formation of pearlite and quenched to lower temperature where occurs the partial transformation of austenite to bainite, the remaining austenite is enriched with C resulting that the remaining austenite being stable at room temperature.

The transformation from austenite to martensite in the final microstructure increases the combination of strength- ductility combination. Due to that fact that we need special arrangements to deform the material at high temperature the processing route for TRIP steels are very time consuming.

#### *5.4 Properties and applications*

TRIP steels have microstructure of ferrite with retained austenite (5-20 vol.%) and hard phases of bainite or martensite.

When the TRIP steel is deformed

- The second phase the hard martensite is dispersed in the soft ferrite creates high strain hardening rate.
- The strain hardening rate is increased at higher strain levels due to the transformation of retained austenite to martensite.

So the strain hardening rates of TRIP steels are much higher than other conventional steels, as a result of combining the high strain hardening rate, mechanical strength and strong bake hardening effect provides an excellent energy absorption ability so it is a good choice for crash performance if it is compared to DP and low carbon steel.

TRIP steel is suitable for reinforcements parts of complex shapes such as B-pillar, cross members, longitudinal beams, sills and bumper reinforcements

### 3.6 Twinning-induced plasticity steels (TWIP)

[17.23] TWIP steels belongs to the second generation of AHSS, it has a superior combination of tensile strength and the elongation, the micro structure of the TWIP steels consists of austenite and contains a composition of C, Mn, or Ni, Si and Al in range of (15-35%), (1%) and (1-3%) respectively, Ni or Mn are used in order to obtain retained austenite even at room temperature, C assist in stabilization of austenite and strengthen it, Si also increasing the strength.

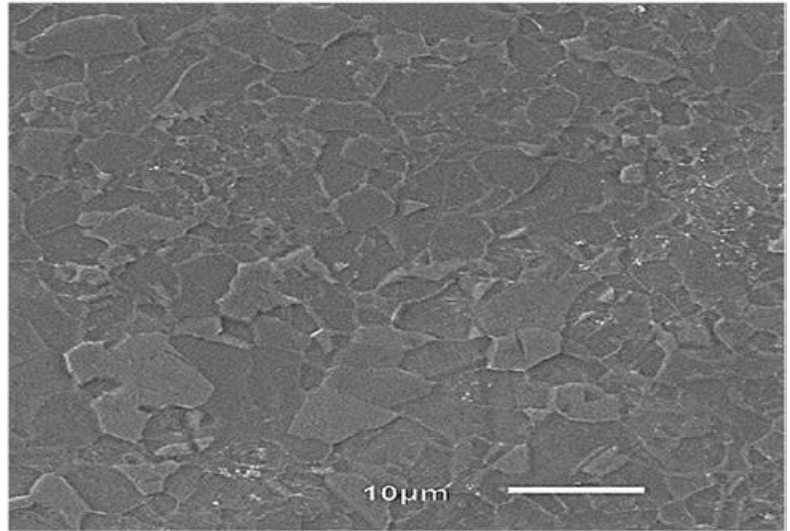


Figure 3.17. the typical microstructure of TWIP steel.[23]

Al also increases the stacking fault energy (SFE) of the austenite and also strengthen it.

The TWIP steels are produced by the same manufacturing methods as other grades of steels, also different processes can be applied to TWIP steel such as rolling, continuous casting and pressing.

There are some technical difficulties of the production of the TWIP steels such as

- Thee high manganese partial pressure during melting and casting.
- Due to the tendency of formation of strong oxide scale cracks appears during the hot rolling
- Due to their high strength they require a strong rolling equipment.

#### *6.1 Properties and Applications*

The mechanism of strain hardening for TWIP steels involves both dislocation glide and deformation twinning, twins are continuously formed during straining, which leads to subdivide the grains twin boundaries, so it acts as a barrier to dislocation movement, which leads to high strain hardened and results a good combination of strength and ductility which makes the TWIP steel suitable for manufacturing structural frame and safety parts such as B-pillar.

### 3.7 Quenching and partitioning treatment (Q&P)

[13,17,16,21] Quenching and partitioning heat treatment is third generation of AHSS it is more effective obtaining the TRIP effect which was defined previously as conversion of retained austenite to martensite. So it obtains a superior combination of strength and ductility without excessive use of Mn, Ni as austenite stabilizers. The Q&P steel microstructure comprises of (5-12%) metastable retained austenite, (20-40%) ferrite, (50-80%) martensite and about 4% alloys.

#### 3.7.1 Processing of steel through the Q&P route

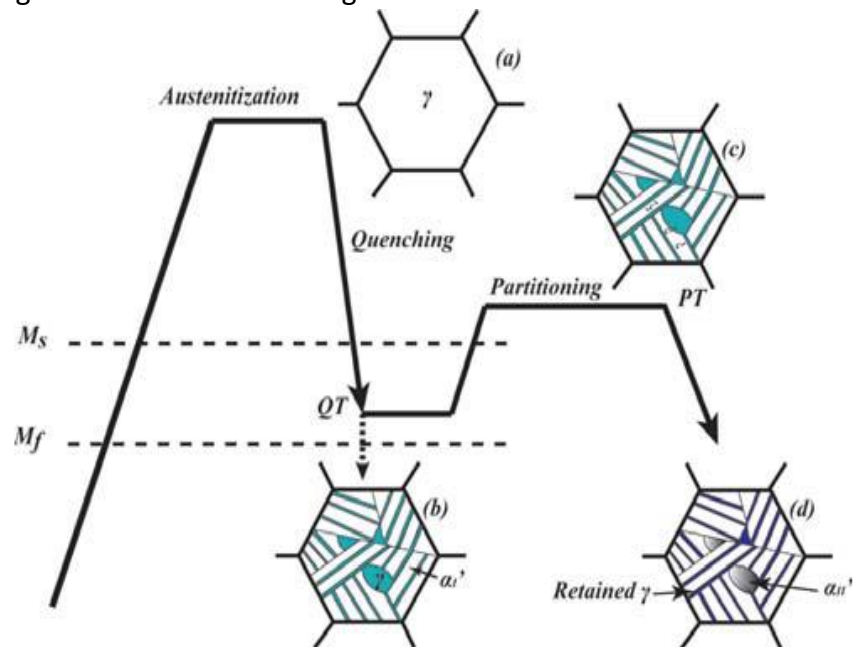
This steel is produced through a multistage heat treatment route, the first step is heating the steel to austenite temperature and the quenching it to martensite temperature ( $M_s$ ) which is usually between 200-350 °C so we will have a microstructure of martensite and austenite then in the second stage in order to provide the increased carbon content in austenite, during partitioning after quenching at temperature ( $T_q$ ) which is below the temperature of start martensite ( $M_s$ ) and above the temperature of martensite finish ( $M_f$ ), the controlled fraction of martensite is formed then in order to complete the carbon diffusion from the supersaturated martensite with carbon to the neighboring austenite, the microstructure is treated at a higher or the same temperature which is called partitioning temperature ( $T_p$ ) which is between 300-500 °C. Then finally it is quenched to the room temperature.

At the end we will have austenite that enriched with carbon is metastable at room temperature, while the rest is transformed to martensite as shown in the following schematic 3.19 the process of Q&P.

Tensile strength level of Q&P steels are usually between 1000-1500 MPa and total elongation is 20%. Due to this high strength level it is used in safety components in the vehicle.

#### 3.7.2 Alloy design and composition for Q&P treatment

The chemical composition is general Carbon less than 0.5%, 1.5% of Mn and Si and some microalloying elements like 0.2% Mo and 0.02% Nb.



Let's focus on each one separately

- 1- C is the most effective element to strengthen the martensite matrix and it increases the stability austenite, the austenite cannot be stabilized by a low content of carbon on the other hand the high content produce twin martensite which tends to lower the toughness and elongation and poor weldability.
- 2- Mn is so important since it controls the transformation behavior and stabilize the retained austenite.
- 3- Si doesn't allow the formation of cementite during participating, it is added to protect C from the formation of cementite, it increases the strength of the steel by solid solution hardening, by increasing the Si content we will have a poor surface coatability of cold rolled steel and poor surface quality of hot rolled steel.
- 4- Nb it has a direct effect on preservation of austenite at room temperature.

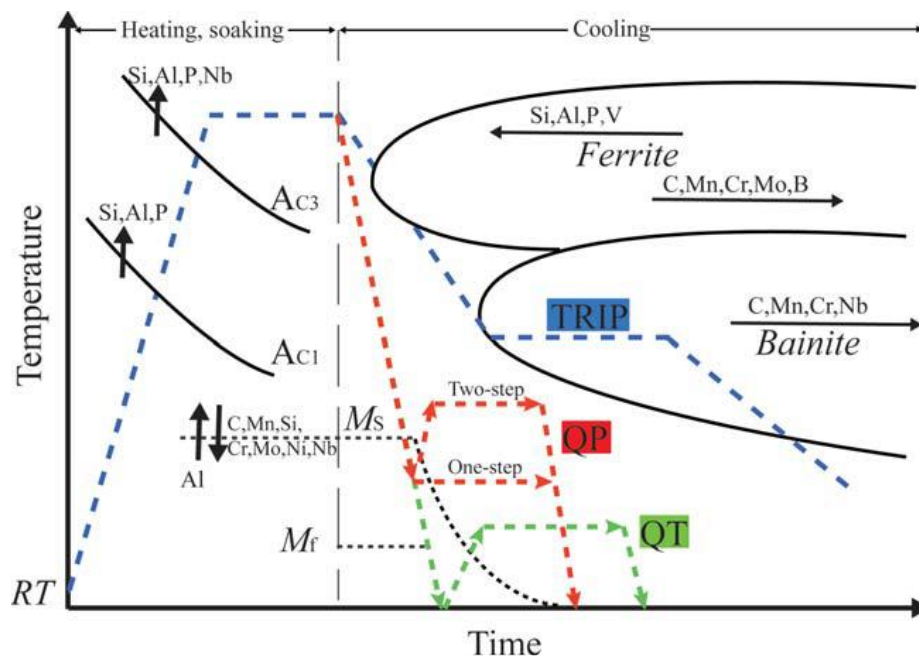


Fig.3.19 Roles of alloying elements on the kinetics of several transformations during Q&P treatment comparing with QT and TRIP treatments

### 3.8 Hot formed steel or Press Hardening Steel (PHS)

[10,32,22] It is a special process for forming typically 22MnB5 into complex shapes, manganese boron-alloy steel in as received (AR) condition has UTS 600 MPa and after austenitisation and quenching process with cooling rate of 27 °C/s the UTS reaches up to 1500 MPa.

#### 3.8.1 Processing of PHS

There are 2 methods for making the press hardening steel or hot formed steel, as shown in figure 3.21 (a), the most commonly used is called **direct process** where the Blank is heated up to austenitisation temperature ( $T > A_{C3}$  or 850-900 °C) and then it is held for about 4-10 minutes, after that the blank is transferred to hot stamping press where it is quenched and formed using cooled water die for about 6-10 seconds. In order to avoid the formation of bainite or ferrite forms in the microstructure the blank must be transferred quickly to the press from the furnace.

For the **indirect** as shown in the figure 3.21 (b) it starts with the cold formed and trimmed part then it is heated in the furnace and then it is quenched in the die.

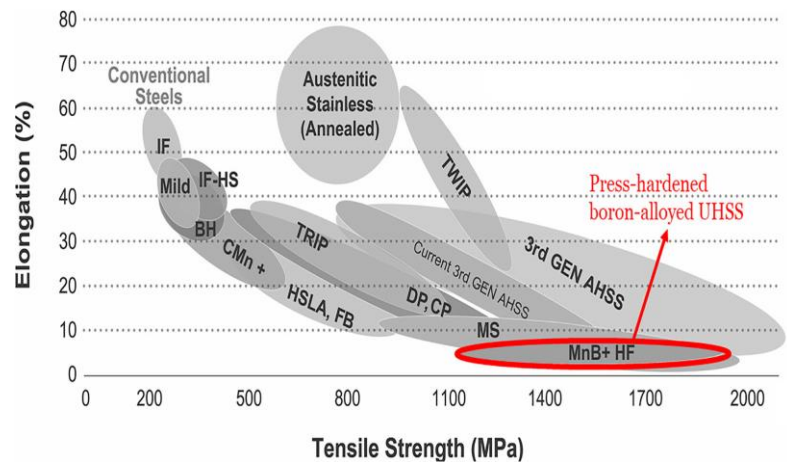


Figure 3.20[32]

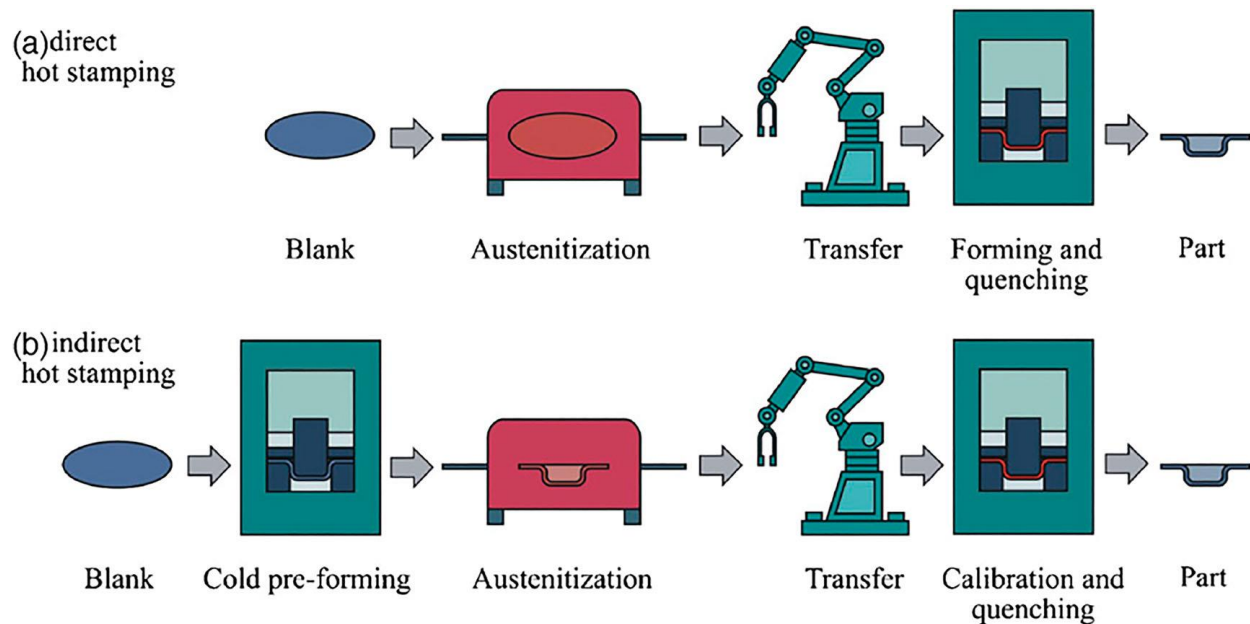


Figure 3.21 Schematic showing the (a) direct hot-stamping (b) indirect hot-stamping [32]



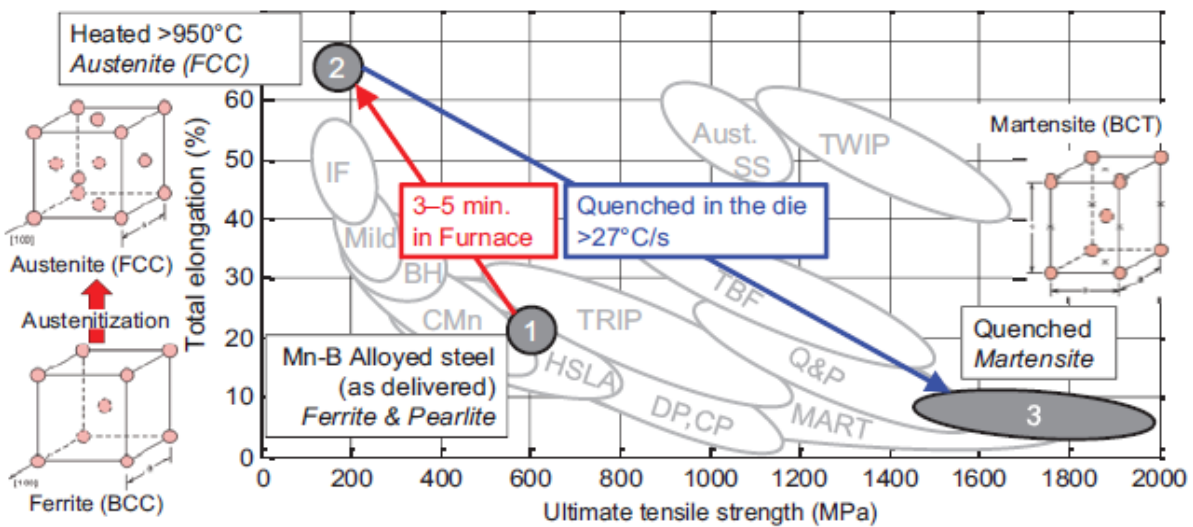


Figure -3.22 Summary of hot forming. [10]

In order to understand more the process, we can see in Figure 3.22 the summary of the hot forming process where point 1 represents the properties of manganese boron-alloy steel in as received (AR) condition then it is heated in the furnace until it reaches the austenitisation temperature which is represented by point 2 at the end it is quenched in the die with a cooling rate of 27 °C/s.

### 3.8.2 Hot stamping line

the line consists of (1) furnace (2) material handling system (3) press machine (4) die set (5) exit line (6) piercing/trimming systems.

**Roller hearth furnaces** are typically used, they are gas and/or electric heated, double decker furnace are used for saving space and used in mass production, conduction heating is also used by Lexus/Toyota to heat blanks for hot stamping.

In order to ensure the shortest transfer time **linear feeders or robots** are used, to reduce the heat losses by radiation.

The **hydraulic presses** are used in the hot stamping, the high speed is required to ensure that the blank is in austenite phase while the press load should be low so there are several designs to ensure that we are having at the beginning high speed low force and at the bottom high force low speed:

- 1- Hydraulic press with accumulator drive
- 2- Multi-cylinder hydraulic press
- 3- Hydraulic press with a flywheel
- 4- Servo mechanical presses



There are 2 functions for the **die sets** the first is to form the part the second is to extract the heat from the blank, the die should extract 17.5 KW/Kg to achieve the critical cooling rate (27 °C/s for 22MnB5).

Finally, for **trimming and piercing** the die cutting is not commonly used since die stresses are extremely high so laser cutting is the industry standard.

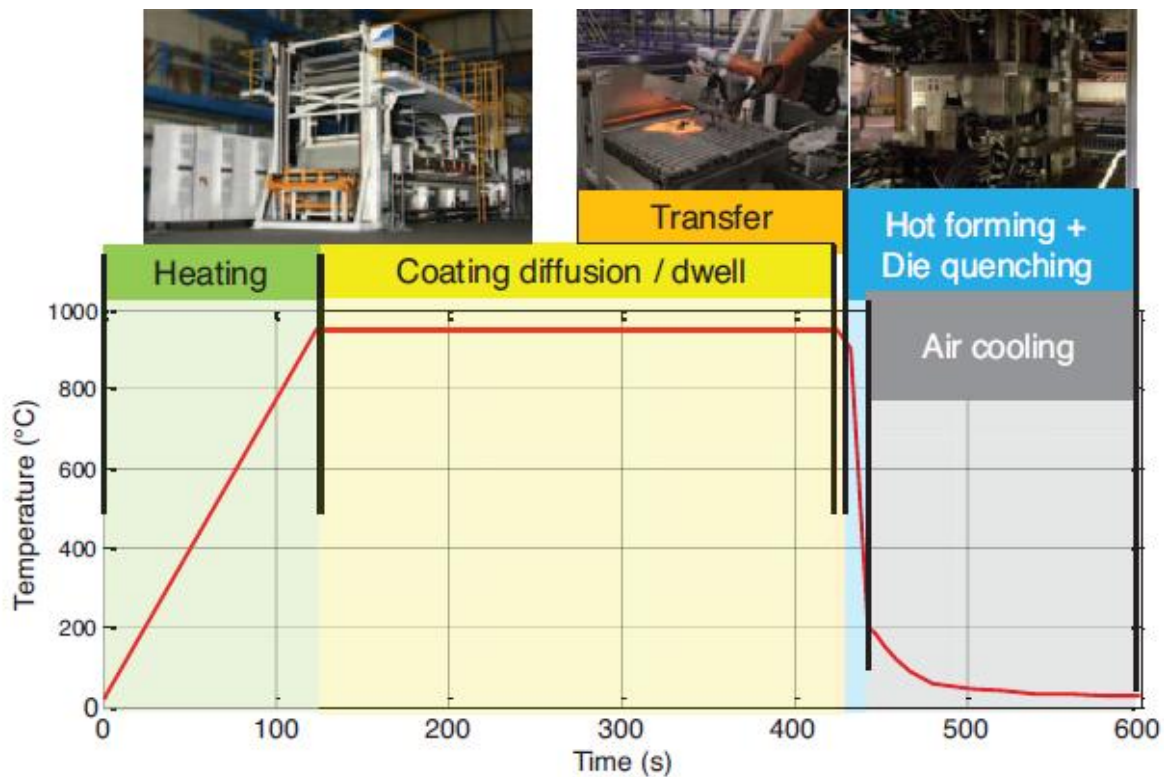


Figure 3.23 A typical hot stamping time-temperature profile. [10]

### 3.8.3 Press Hardened Steel Material properties

The boron acts as strong hardening agent with excellent hardenability while the steel is having a good formability.

The only types of PHS that are producing a fully martensitic structure are the following grades:

- 22MnB5
- 37MnB4
- 37MnB4

The most used grade in the automotive hot stamping is 22MnB5 due to the fact that after the hot forming it reaches UTS 1500 MPa and yield strength of 1100 MPa.

The microstructure of the boron alloyed steel in as the received condition consists of ferrite, pearlite and small amount of martensite in the grain boundaries of the ferrite. As shown in

figure 3.24 (a), the microstructure of the material after the hot formed condition as we can see in the in figure 3.24 (b) it can be observed that the lath of martensite are parallel to each other and some of the are containing distributed carbides.

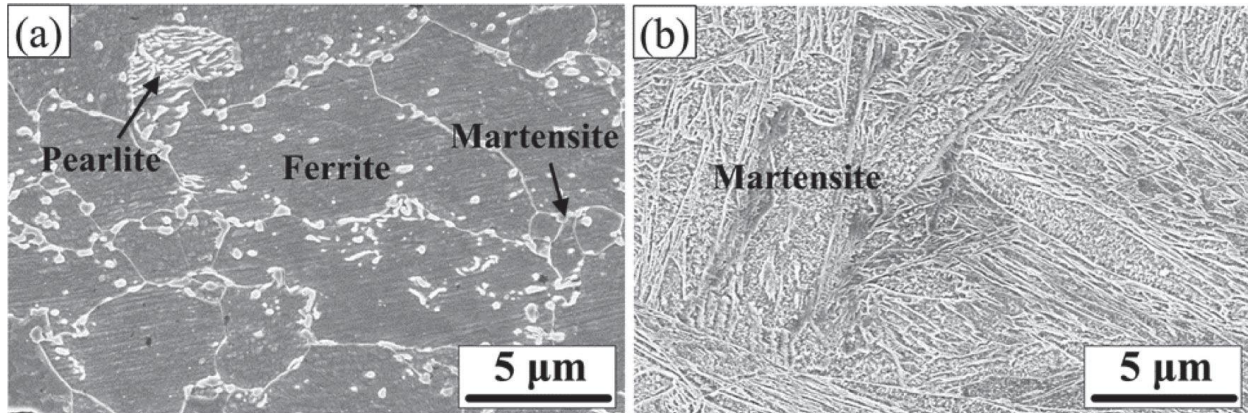


Figure 3.24 Base metal microstructure of 22MnB5 PHS (a) As-received condition; (b) Hot Formed condition. [32]

A small quantity of boron is added in order to increase the hardenability typically it is ranging from 10-30 ppm, it increases the hardenability because it segregates to the austenite grain boundaries. Mn has an important effect since it plays as a hardening agent that helps to retard austenite decomposition reactions.

The boron and manganese are decreasing the cooling rate that is necessary to avoid ferrite formation during cooling and increasing the possibility of having a fully martensitic microstructure by pushing the CCT diagram that is shown in figure 3.25 to the right.

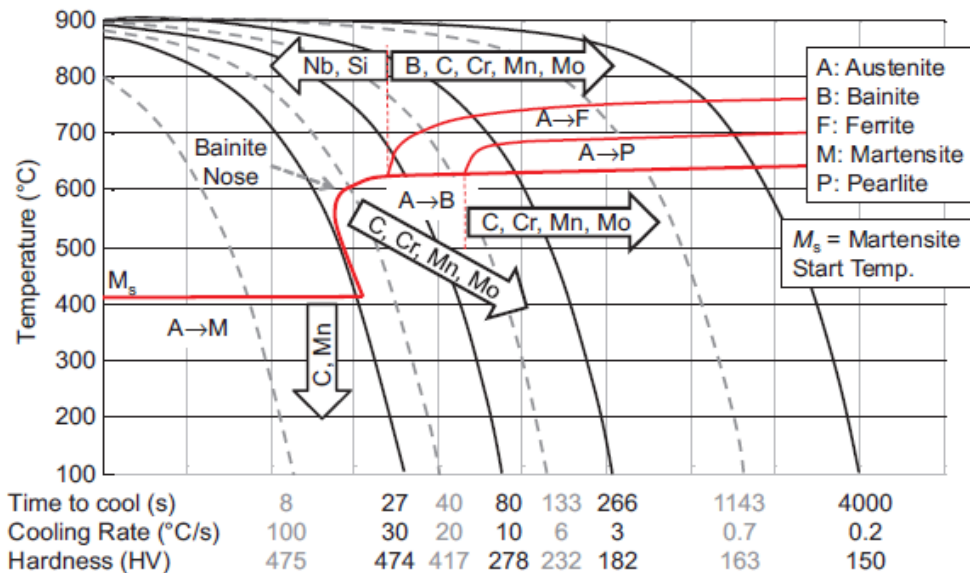


Figure 3.25 Continuous Cooling Transformation (CCT) curve of 22MnB5 steel and effects of additional alloying elements. [10]

In the following Figure 3.26 we can see the transformation of 22MnB5 from ferrite (bcc) structure to austenite (fcc) structure during the heating stage and the lastly to martensite (bct) during the rapid quenching and we can see also the stress strain curve of 22MnB5 before and after the hot stamping.

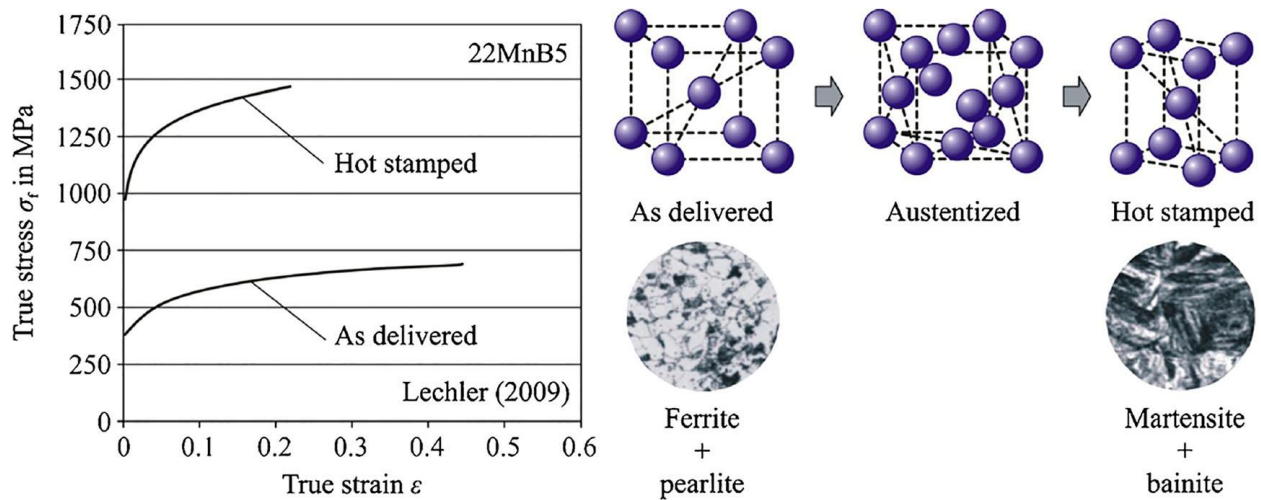


Figure 3.26. Flow curves and microstructure evolution of 22MnB5 [32]

## 4. Steel Performance

Steel is having excellent performance in terms of stiffness, strength, formability, fatigue and mechanical properties are considered as one of the most important properties of the metal since it includes a combination of high strength with the ability to bend without breaking, in order to characterize these mechanical properties of the steel some tests have to be done.

### 4.1 Tensile Test

[5] This test is used to evaluate the **strength** of the steel. a cylindrical rod is pulled apart in a machine with a known force  $F$  from the top of the rod while the end of the rod is attached to the machine so the force is applied parallel to the axis of the rod as shown in the figure

The rod gets longer as the force increase, the increment in length is represented by  $\Delta l$  while  $l$  refers to the original length of the rod.

The Tensile force is when the applied force is along the axis of the rod. The stress is plotted on Y-axis while the strain is plotted on X-axis.

There are two regions in the stress-strain

diagram the first one is called the elastic region and it is defined as when we apply a stress that elongates the rod and then release it the rod returns to its original length while the second is region is called plastic region which is defined as when the stress exceeds a critical value that is called the yield stress and then release the stress we will see that the rod is permanently elongated. The maximum stress value is called ultimate tensile strength (UTS) or tensile strength (TS) after this value in the plastic region the stress drops a little before breaking the rod.

The stress strain curve measures also the **ductility** of the metal, which is defined as the amount that the metal elongated after the stress increase beyond the yield stress and before the sample breaks.

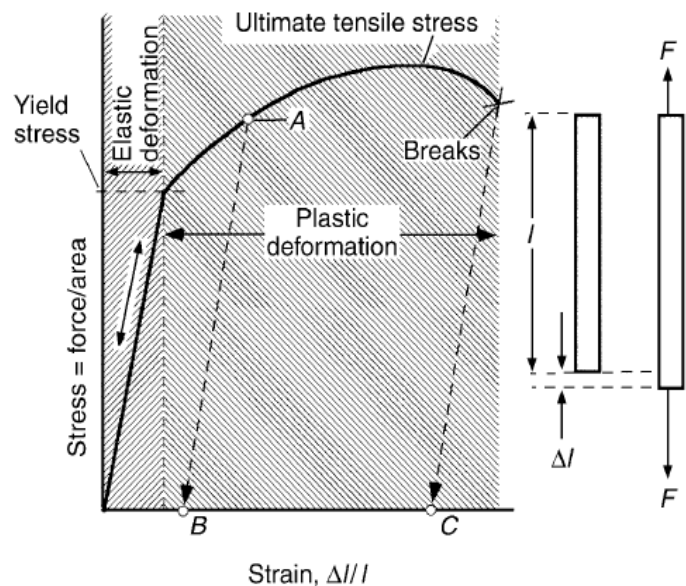


Figure 4.1 stress-strain curve

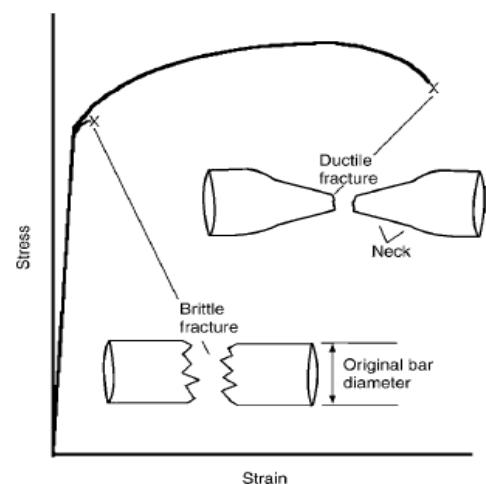


Figure 4.2 brittle and ductile

The following figure represents the possible stress strain diagrams for the brittle and ductile metal, as we can see in the brittle case the diameter of the bar of the brittle failure remains close its original value while in the ductile material this diameter reduction is present and called necking which develops just before the failure.

Two general characteristics of the steel can be mentioned is that (1) the YS and TS are increasing with increases the percentage of carbon (2) the ductility drops with increasing the percentage of carbon.

## 4.2 R value

we need to introduce an important parameter which is the Lankford parameter which is also known as plastic strain ration and denoted by letter “r” it is used extensively as an indicator of the drawability of sheet metals.

“r” is defined as the ratio of true in-plane strain to true through thickness strain

$$r = \frac{\text{true in-plane strain}}{\text{true through thickness strain}} = \frac{\epsilon_w}{\epsilon_t}$$

where  $\epsilon_w$  and  $\epsilon_t$  are the true strain in width and in thickness, the r values are determined for metal sheets for 3 directions of loading in-plane ( $0^\circ$ ,  $45^\circ$  and  $90^\circ$ ) to the rolling directions, they are denoted by  $r_0$ ,  $r_{45}$  and  $r_{90}$ , the normal or average value of r is noted as  $r_m$  it is measured as follows

$$r = \frac{1}{4}(r_0 + 2r_{45} + r_{90})$$

Increasing the solute carbon in the IF steels tends to reduce the  $r_m$  value it has been observed that the  $r_m$  is steadily decreases with increasing carbon/sulfur ratio as seen in the following figure

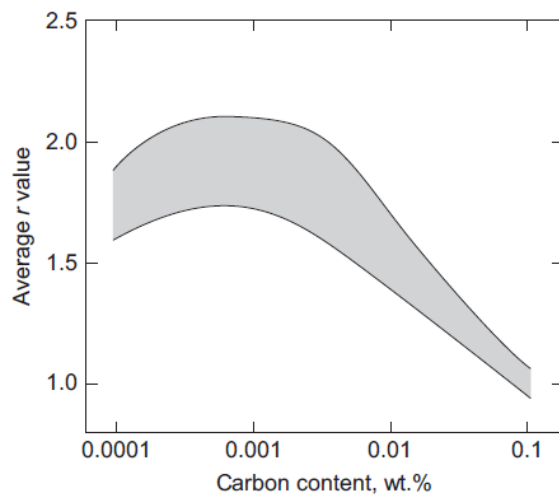


Figure 4.3 The effect of carbon content on the rm value of low carbon steel [4,10]

### 4.3 Hole expansion Stretch flanging

[33,34,36] For stretch flanging the Hole Expansion capacity is measured according to ISO 16630, the test sequence is schematically shown in the following figure 4.4

Where the initial hole diameter is a standardized and it is 10 mm and the material thickness is 6 mm.

We have a hole Expansion Capacity (HEC) and it is  $= \frac{D-D_0}{D_0}$

Where  $D_0$  is the initial diameter of the hole and  $D$  is the diameter of the hole expanded so far as a through thickness crack is just observed.

HEC is a key indicator to evaluate the stretch flanging performance of the steel sheet.

We can see in Figure 4.5 some examples of material performance in HEC in the left we have mild steel and in the middle HSLA steel and on the right Dual-Phase (DP) steel.

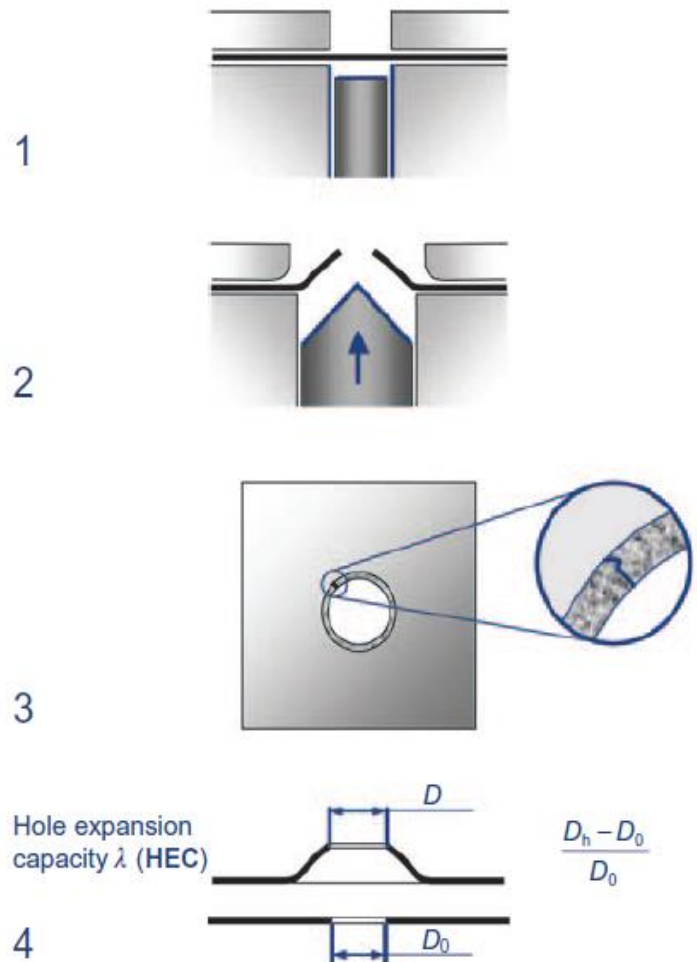


Figure 4.4 HEC test after ISO 16630.[35]

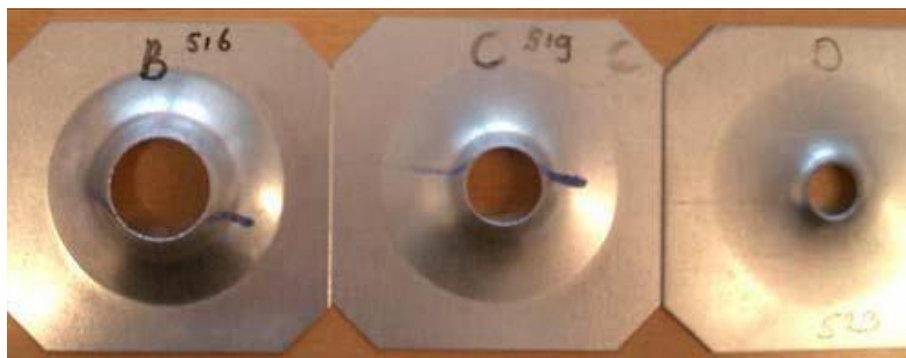


Figure 4.5 HEC examples, from the left mild steel, middle HSLA steel, right DP steel [10]



## 4.4 Bending

[10] It is mainly characterized by a gradient strain over the thickness. According to Kirchhoff assumption we can estimate the strain in the bending. The assumption states that flat planes perpendicular to the mid-plane of the sheet remain flat and perpendicular during forming. According to that the sheet is folded onto it self and it has an out strain of 100%.

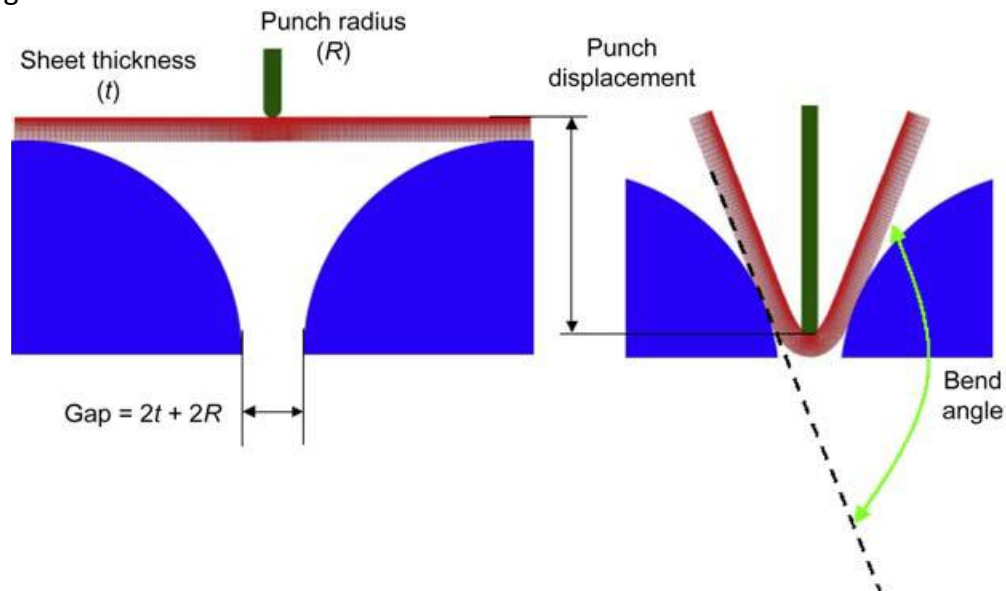


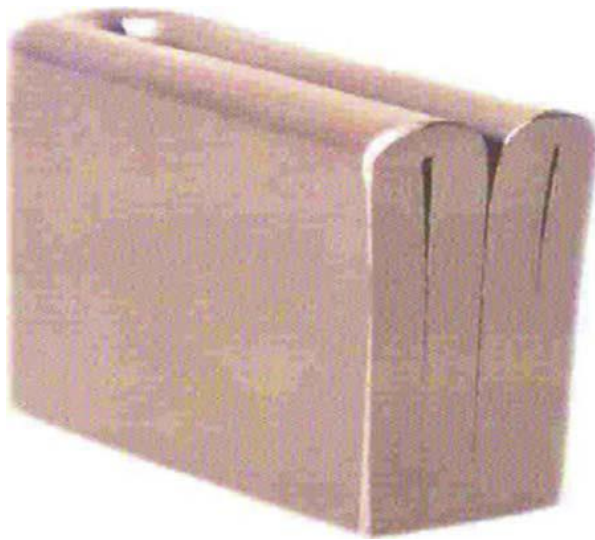
Figure 4.6 bending process VDA 238 schematic



Figure 4.7 photograph of test equipment



It should be noted that the higher the strength of the material the more difficult to be folded without problems as we can see in the following figure the HSLA is doubly folded and we cannot see any cracks compared to the picture of the folded DP steel we can see the cracks.



(a)



(b)

Figure 4.8 (a) doubly folded HSLA (b) DP steel VDA 238 bend test.[10]

The German automotive industry developed a standard test for bending which called VDA 238-100 and it became the standard for entire European car makers, a sharp bending knife that has a radius of 0.3 mm is used as in figures 4.6, 4.7

A force-displacement diagram is recorded during the test to measure the performance of the material DP600 as shown in figure 4.9, the VDA standard stated that the point of load drop should be identified however by considering only the geometrical effect there is no any fracture occurred as represented by the red line (FEM) while the blue lines that are the experimental curves based on the test results show us the bendability level.

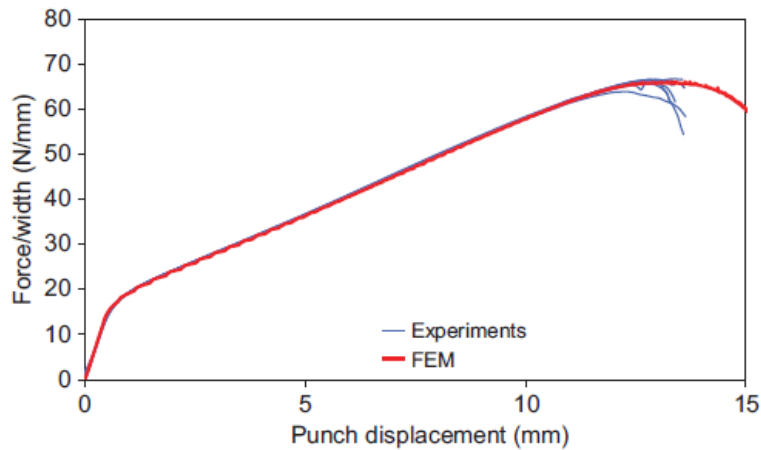


Figure 4.9 Force-displacement diagram of VDA 238 bend test

## 4.5 Formability Limit Diagram

[37,10] Formability limit diagram is a curve used to predict the forming behavior of sheet metal. The graph describes the material failure tests by evaluating the major strain and minor strain since strains are plotted on stamped parts and predict how close the part is to splitting. According to the sheet thickness, thin sheets may suffer defects and require high precision.

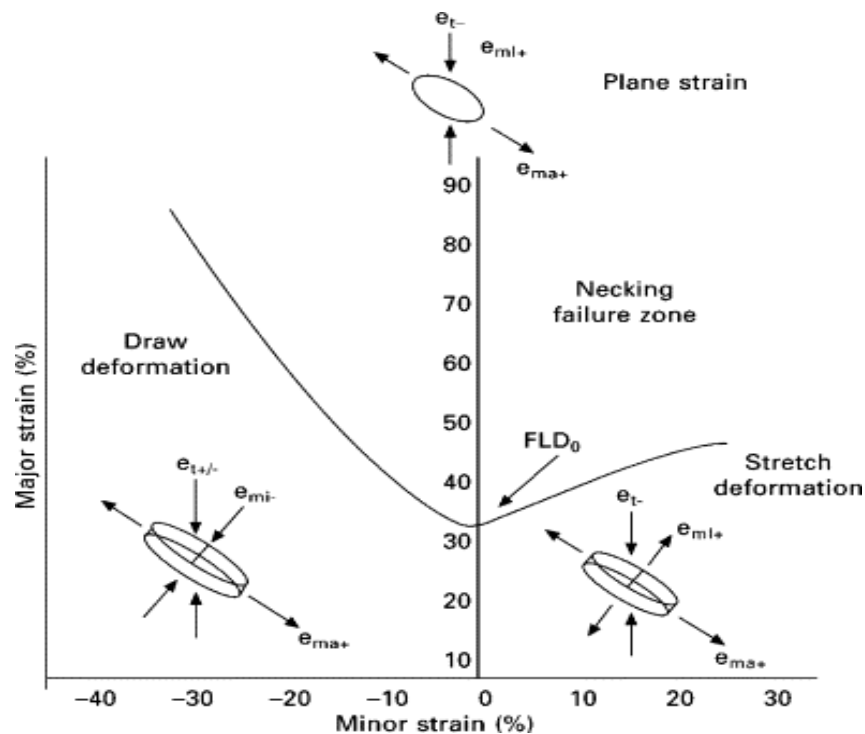


Figure 4.10 Formability limit diagram (FLD)

Three strain points are required in order to generate the formation limit diagram, these points are uniaxial strain, plane strain, and biaxial strain their dimensions are shown in the following figure 4.11

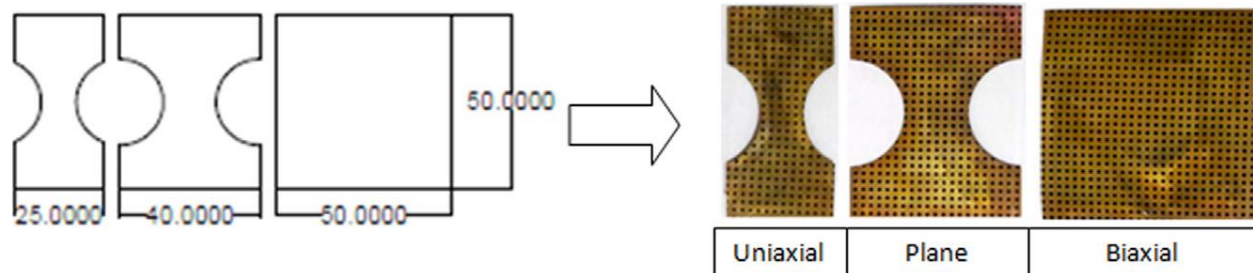


Figure 4.11 Specimen for uniaxial, plane, and biaxial strain path. [37]

#### 4.5.1 Effect of rolling direction on forming limit curve

[38] Mild steel has been used for the following example, as shown in figure 4.12 the effect of rolling direction on formability of the two thicknesses. For 40  $\mu\text{m}$  thickness the forming limit curve for 0 degree is more safety zone as compared with 45 and 90 rotation degrees. The 90-degree rolling direction specimen has the lowest safety zone. For the 0 and 90 degrees the uniaxial strain and biaxial strain points have almost the same value. Plane strain point shows more variation with different rolling directions.

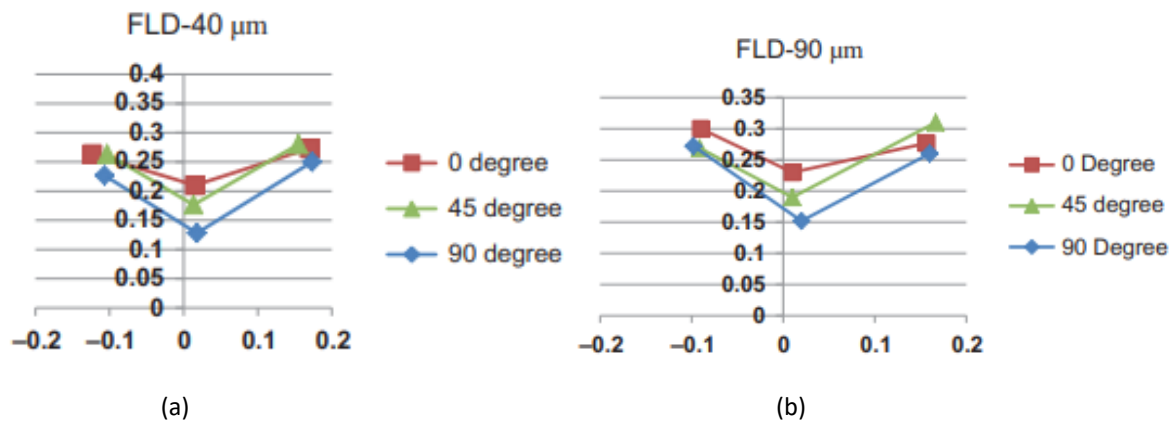


Figure 4.12 represent FLD for different rolling directions (a) 40  $\mu\text{m}$  thickness (b) 90  $\mu\text{m}$  thickness [37]

#### 4.5.2 Effect of foil thickness on forming limit curve

Figure 4.13 shows the comparison of the FLDs for different thickness with the same rolling direction, the results conclude that the safe zone increases with increase in the thickness

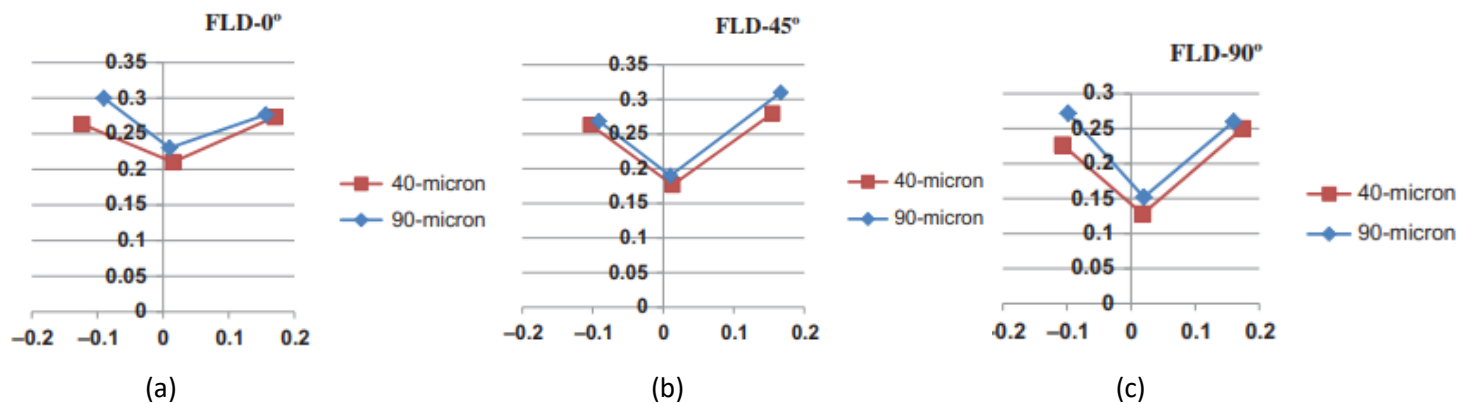


Figure 4.13 Comparison of forming limit curves: 40 and 90  $\mu\text{m}$  thickness for (a) 0-degree rolling direction (b) 45-degree rolling direction (c) 90-degree rolling direction [37]

As a conclusion we can say that

- Uniaxial and biaxial are similar for different rolling direction and for both thicknesses.
- Formability is high for thicker foils and for zero degree rolling direction.

#### 4.5.3 Formability aspects of different steels

In figure 4.14 we can see an overview of FLCs for different families, the mild steels in this graph are colored with blue (DX56D+Z and DX53D+Z), the HSS are in green (HSLA340 and HSLA420), and the DP family that are in yellow orange and red (DP600, DP800 and DP1000) and complex phase the dotted red line (CP800), it can be clearly seen that the FLC decreases with increasing the strength

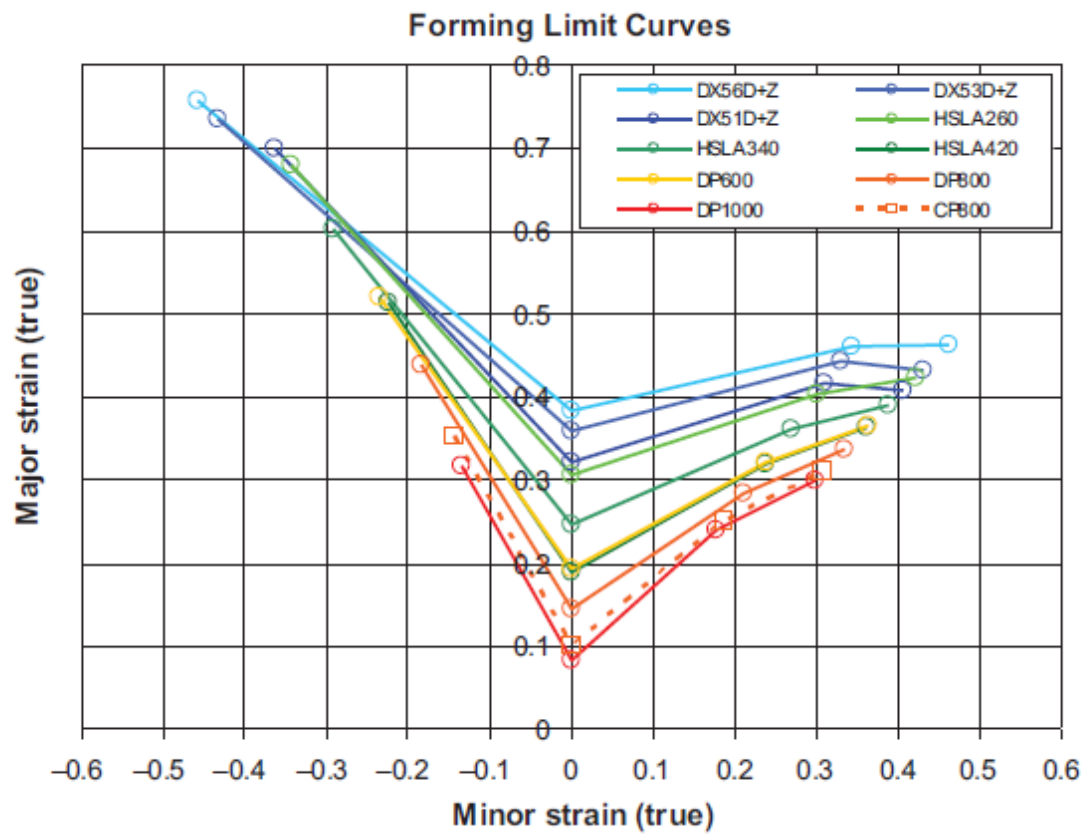


Figure 4.14 Overview of forming limit curves for different steel families [10]

## 5. OEMs needs and regulation

### 5.1 History of steel usage in the vehicle's body and significant events impacting steel application in vehicle design in USA

Since the early 1900s the steel has been considered as an important material for car body construction that was due to its low cost, its ability to be pressed and shaped to complex shapes and easily joined through welding process.

Starting from 1960s there were a regulatory demand for safer, cleaner and more fuel efficient vehicles so the automotive industry faced a significant challenge fundamentally changed the vehicle's structure to meet the regulations, which requires new steel products with improve manufacturability and new higher strength. [10]

A significant growth in automotive industry was clear after the World War 2 in the 1950s and 1960s with this success there was a public pressure to safety and the environmental performance of the automotive industry. The government of U.S. responded to this public pressure through several legislative actions:

- 1- The Federal Clean Air Act 1970. This act was established in order to regulate the framework for monitoring and reducing emissions. The Environmental Protection Agency (**EPA**) was created under this act.
- 2- The Highway Safety Act 1970. Which created the National Highway and traffic Safety Administration (**NHTSA**). Charged with creating safety requirements for both the roads on which they travel and the motor vehicles, thanks to this act for the first time energy absorbing bumpers, three-point restraint systems, and improved structural requirements for frontal and side impact energy absorption.

At the same time, the Arab oil embargo of 1973 resulted that the price of the gasoline increased dramatically and became very unstable, due to these events the demand for smaller and more fuel efficient vehicles are increased as shown in figure 1, these events resulted a public pressure for political solution in order to improve the fuel economy in the vehicles and the result was the implementation of Corporate Average Fuel Economy (**CAFE**) standards by **EPA**, [10] the **CAFE** specified the values of mpg of fuel (Table 1) and the manufactures have to meet these values otherwise they have to pay a fine of 5\$ for each 0.1 mpg (0.04 Km/l) below the standard times the manufacture's total model year production. [29]

**Passenger Car and Light Truck Corporate Average Fuel Economy (CAFE) Standards, 1978–1985**

Model year	Passenger cars (mpg)	Light trucks <sup>a</sup>			Limited product light truck <sup>c</sup> (mpg)
		Two-wheel drive (mpg)	Four-wheel drive (mpg)	Combined <sup>b</sup> (mpg)	
1978	18.0				
1979	19.0	17.2 <sup>d</sup>	15.8 <sup>d</sup>	—	—
1980	20.0	16.0	14.0	—	—
1981	22.0	16.7	15.0	—	14.0
1982	24.0	18.0	16.0	—	14.5
1983	26.0	19.5	17.5	19	—
1984	27.0	20.3	18.5	20	—
1985 <sup>e</sup>	27.5	21.6	19.0	21	—

<sup>a</sup> Less than or equal to 8500 lb.

<sup>b</sup> Optional total fleet CAFE.

<sup>c</sup> Based on International Harvester medium-duty truck engines.

<sup>d</sup> Less than or equal to 6000 lb.

<sup>e</sup> Secretary of the Department of Transportation may amend the fuel economy standard for model year 1985, or for any subsequent model year, to a level which he determines is the maximum feasible average fuel economy level for such model year, except that any amendment which has the effect of increasing an average fuel economy standard to a level in excess of 27.5 mpg, or of decreasing any such standard to a level below 26.0 mpg, should be submitted to the Congress in accordance with Section 551 of the Energy Policy and Conservation Act and shall not take effect if either House of the Congress disapproves such amendment in accordance with the procedures specified in such section.

Source: Kulp *et al.*, ed. (1981).

Table (5.1) the passenger car and light truck average fuel Economy (CAFE) standards, 1978-1985

The key point of meeting the **CAFE** requirements is Downsizing which is defined as decreasing the weight of the vehicle by using lighter materials. [29]

This focus on mass reduction led to improve the structural efficiency when the strength-to-weight ratio of the materials is increased. The high-strength steel products that would become most widely used at this time were the micro alloyed high strength, low alloy (HSLA) steels. [10]

As show in figure 1 the requirements of **CAFE** are steadily increased from 18 mpg (7.65Km/l) to 27.5 mpg(11.7Km/l) (miles per gallon)

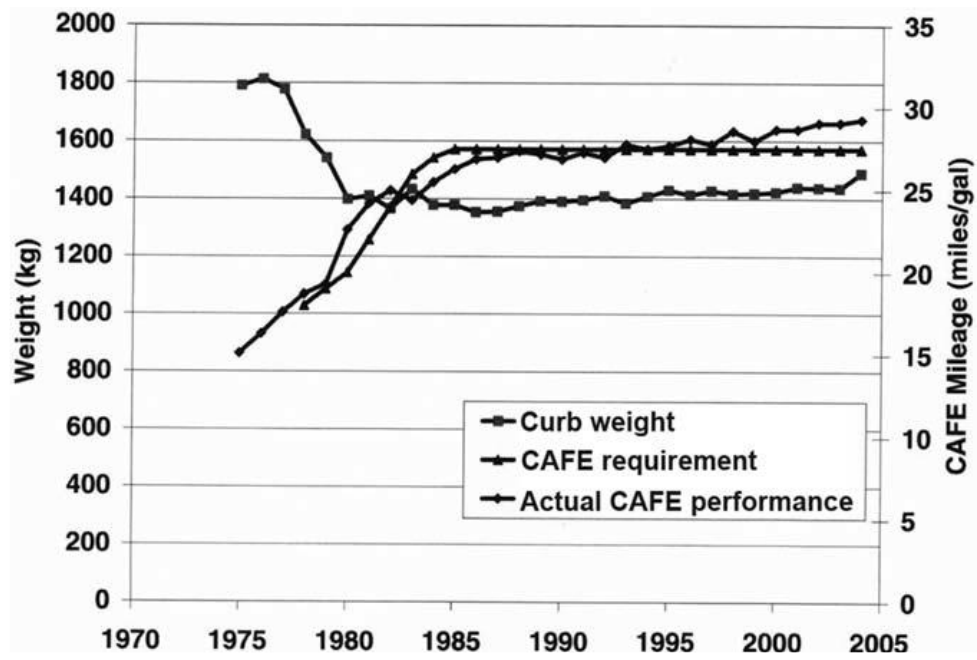


Figure (5.1) History of vehicle curb weight, CAFE mileage requirements and actual CAFE Performance for the U.S. fleet [10]

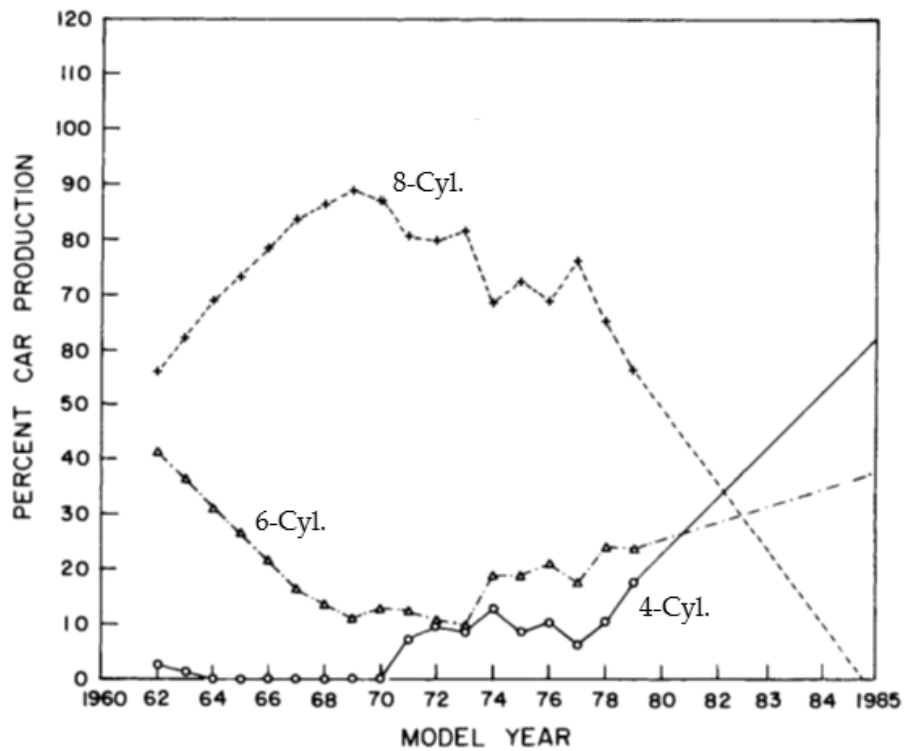


Figure (5.2) USA car production by cylinder type, 1962-1979. : (O) four-cylinder, (Δ) six-cylinder, (+) V-8.[29]



## 5.2 Tradeoff material mass and application in vehicle.

Customer needs the vehicle to be safer, environmentally friendly and more fuel efficient. The material trend generally is driven by regulation and customer desire.

In the following figure (5.3) which represents the average of steel used according to EuroCarBody 2009, 2012 and 2020. The analysis shows a significant change of the material trend, the LC and HSS are reduced while the AHSS, UHSS and PHS are increased:

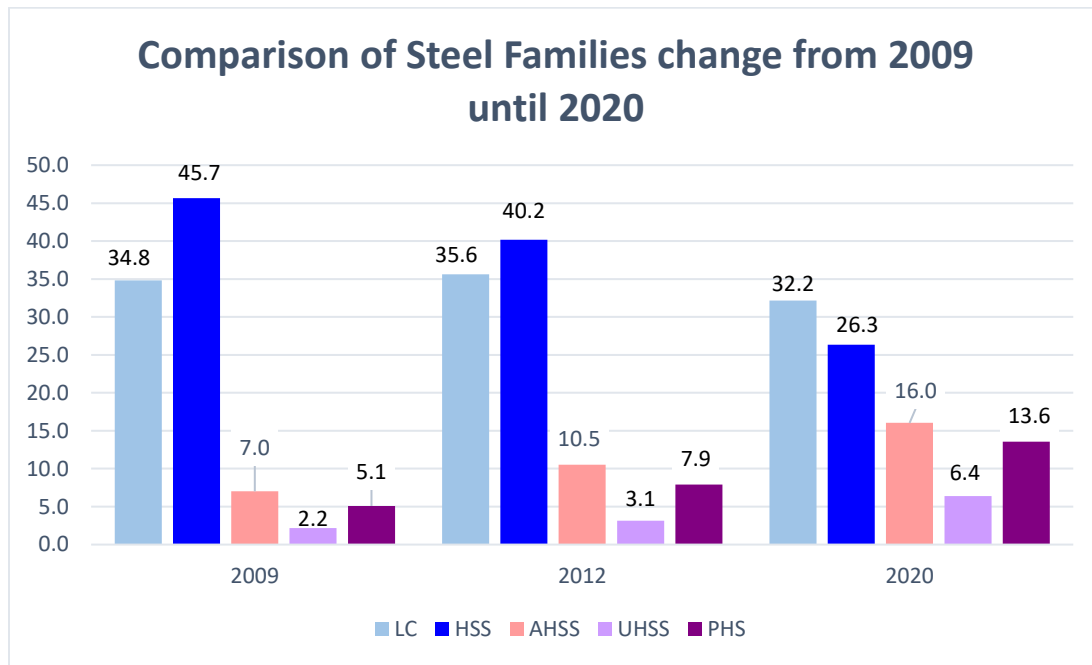


Figure (5.3) steel families that are used in years 2009, 2012 and 2020 according to EuroCarBody Conference.

## 5.3 Safety regulations

Since the customers around the world are demanding safe vehicles and the governments are regulating strictly crashworthiness, this requires choosing proper materials that meets the governmental regulations by passing these crash tests, the most improved areas in the vehicle are the most critical one like front, side, rear and roof impact performance.

There is a strong direction in the automotive supply chain that is the safe vehicle can be designed with reduced weight in order to avoid another issue, which is the emission. So, engineers and designers started working on modifying the used steels in order to be stronger and lighter [31]

## 5.4 Major Car Crash Test Providers

The major providers of car crash test are in the following table

<b>Name</b>	<b>Abbreviation</b>	<b>Founded</b>	<b>Location</b>
United States New Car Assessment Program	US NCAP (U.S. NCAP)	1978	Washington, DC, USA
Insurance Institute for Highway Safety	IIHS	1959, Ratings from 1995	Arlington, VA, USA
Australasian New Car Assessment Program	ANCAP	1993	Canberra, Australia
Japan New Car Assessment Programme	JNCAP	1995	Tokyo, Japan
European New Car Assessment Programme	Euro NCAP	1996	Brussels, Belgium
Korean New Car Assessment Programme	KNCAP	1999	Seoul, South Korea
China – New Car Assessment Programme	C-NCAP	2006	Tianjin, China
Latin New Car Assessment Programme	Latin NCAP	2010	Montevideo, Uruguay
New Car Assessment Program for Southeast Asia	ASEAN NCAP	2011	Kajang, Selangor, Malaysia
Global New Car Assessment Programme	Global NCAP	2011	London, Great Britain

Bharat New Vehicle Safety Assessment Program	BNVSAP	2017	India
Green NCAP (operated by Euro NCAP for emissions)	Green NCAP	2019	Brussels, Belgium

Table (5.2) the major car crash test providers [24]

Let's choose for example **Euro NCAP** in order to see how these crash tests are performed, the score is determined according to frontal impact, lateral impact and whiplash test. From the score we can evaluate the protection of the driver and the passengers that can be showed by the tested vehicle. [25]

### Frontal Impact

#### **Mobile Progressive Deformable Barrier**

the vehicle is propelled by speed of 50 km/h (31 mph) at 50% overlap in to a barrier that mounted on trolley that weights 1400 kg and also travelling at 50 Km/h

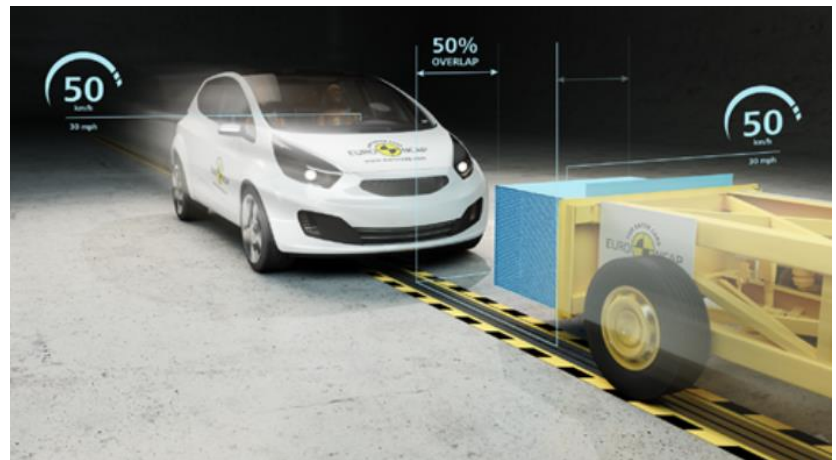


Figure (5.4) front Impact test [25]



**Full Width Rigid Barrier** the car is driven to a rigid barrier at speed of 50 Km/h (31 mph) with full overlap

Figure (5.5) Full Width rigid barrier [25]

## Lateral Impact

**Side Mobile Barrier** the trolley is driven at speed of 60 Km/h with a deformable barrier carried on it into the side of the stationary car



Figure (5.6) lateral Impact [25]



Figure (5.7) side Pole [25]

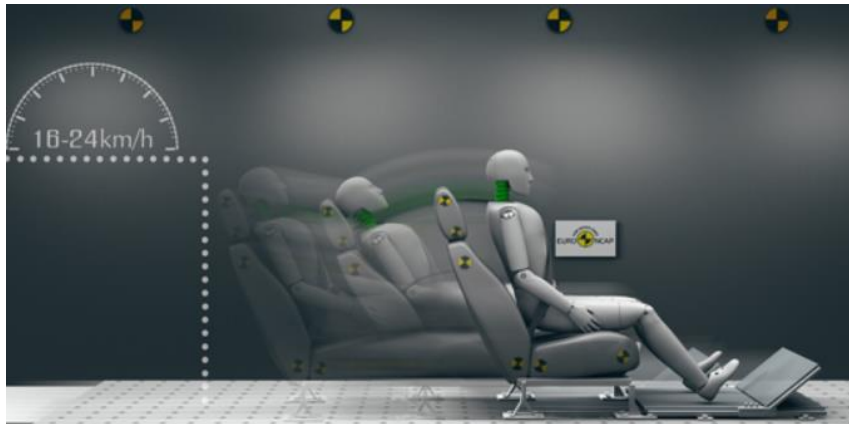
**Side Pole** the car is propelled sideways against a rigid at speed of 32 Km/h (20 mph)

**Far-Side Impact** the white inner body of the vehicle which is attached to a sled, is propelled sideways to provide side acceleration. The far side testing was implemented in 2020



Figure (5.8) Far-side Impact [25]

## Rear Impact



**Whiplash** the seat of the vehicle is propelled to the forward direction rapidly at speed of 16 and 24 Km/h (9.9 and 14.9 mph)

Figure (5.9) Whiplash [25]

## 5.5 Fuel Economy

On the following part we are considering the USA's fuel regulation through different years, CAFE standards were first introduced by Congress in 1975 to help reduce the USA's dependence on foreign oil.

Regulations were not steady during the 1980s for both cars and trucks before reaching a steady target for cars in 1990 through 2010,

The trucks moderately increased during the year of 2005 from **20 to 21 mpg** (8.5 to 8.9Km/l), then it reached **23.5 mpg** (9.9Km/l) by 2010

For further reduction of foreign oil dependence, the Energy Independence and Security Act was signed in 2007 which increased the fuel economy standards by 40%

This regulation set a goal for fuel economy standards to reach **35 mpg** (14.88Km/l) for the fleet average of cars and trucks by 2020.

NHTSA proposed a plan in April 2008 for model year 2011\_2015 vehicles to reach the 2020 goal

In 2009, the Obama administration proposed a change in the program for 2012\_2016 to get the fleet average of cars and trucks to **35.5 mpg** (15Km/l) by 2016.

Then, in 2011, President Obama announced a plan to get **54.5 mpg** (23Km/l) by 2025

In the following figure (5.10), we can see the changes in the fuel economy standards by year for passengers, cars and light trucks. The dotted lines for model year that start from 2017 until 2025 represent the planned increases needed to reach 54.5 mpg equivalent (mpg) fleet-wide average by 2025. [10]

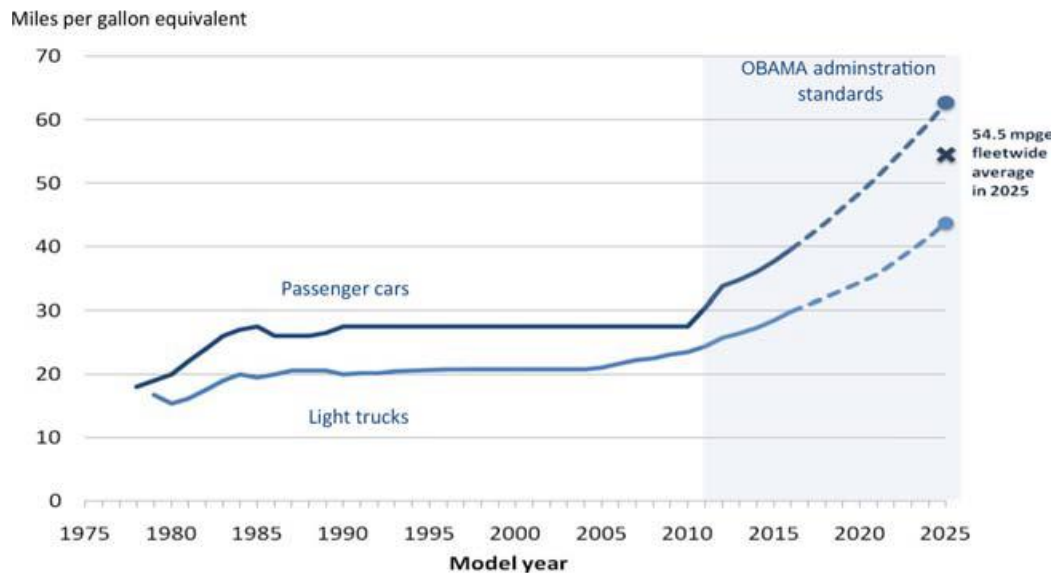


Figure (5.10) Fuel economy plan for year 2025 [10]

The automakers approach and strategy on how to meet fuel economy regulations are different depending on type and mix of vehicles, manufacturing capabilities, and other criteria. However, they all must meet the regulations and make vehicles which are affordable to the consumer.

## 5.6 Concerns of CO<sub>2</sub> emissions

CO<sub>2</sub> is the main greenhouse gas all the countries are putting regulations in order to reduce it, as the chart shows there is a huge reduction in the CO<sub>2</sub> per Km normalized to NEDC test cycle. The lowest value among the represented data belongs to EU with 95 g CO<sub>2</sub>/km so let's focus more on the European regulations and target levels that have been set for 2030. Passenger vehicles and light commercial vehicles are responsible of about 12% and 12.5% respectively of the total EU emissions of CO<sub>2</sub> [27]

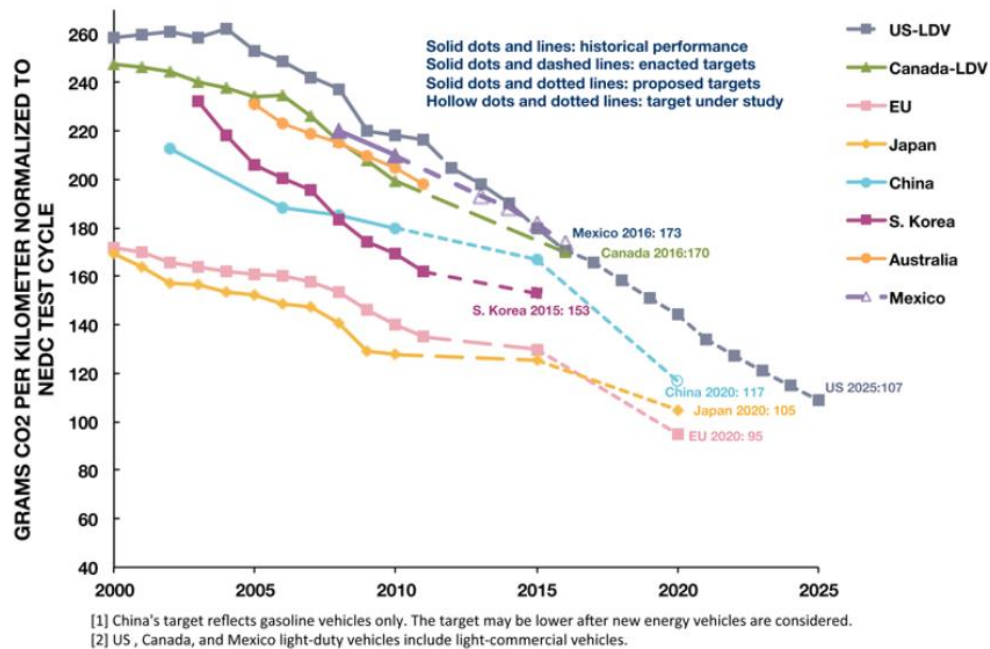


Figure (5.11) the regulations of different countries on the allowable Grams of CO<sub>2</sub> per Kilometer. [26]

The regulation sets CO<sub>2</sub> target emissions for 2 periods the first period is between 2020 and 2024 while the second is between 2025 and 2030.

According to Regulations (EC) No 443/2009 and (EU) No 510/2011 the allowable CO<sub>2</sub> emission for passenger cars is 95 g CO<sub>2</sub>/km while for vans it is 147 g CO<sub>2</sub>/km for the first period 2020-2024, the previously mentioned values based on NEDC emission test procedure but starting from 2021 onwards the emissions targets will be based on WLTP emission test procedure.

Starting from 2025 according to the regulation (EU) 2019/631 that sets stricter EU fleet-wide CO<sub>2</sub> emission targets to be considered as a reduction percentage from the 2021 starting point, for cars and vans the reduction is 15%.

Starting from 2030 it also follows the same thing that happened in 2025 but with increased reduction percentage, for cars the reduction percentage is 37.5% and for vans 31%.

If the average of the CO<sub>2</sub> emission of the manufacture's fleet is more than the specific target in a given year, the manufacture has to pay as a penalty for each CO<sub>2</sub> gram/Km 95 Euros [27]

## 6. Material Evolution

[from 41 to 107] In this chapter we will discuss the material evolution of different types of steel that are used for automotive industry by analyzing and comparing between different car brands, models, segments, and year model.

EuroCarBody is a conference which offers a forum of defining and discussing the state of the art in modern series car body engineering, the presentations are given by OEM engineers that are directly involved in their planning and realisation, in this conference the development, material and production concepts of the car bodies are introduced in details.

All the analyzed data are based on the presentations and benchmark data of different vehicles that were provided by the carmakers who participated in EuroCarBody Conference for years of 2009,2011,2012,2013,2016,2020.

It should be noted that special and high performance vehicles are not included in the following analysis since they are mainly built with Aluminum and plastics which are out of our focus also the trucks are excluded.

First, it is important to clarify which steel grade is used in each family according to EuroCarBody they are introduced in the following table:

Grade	Standard
<b>Low Strength Steels:</b> Mild steels	CR1
	CR2
	CR3 {CR04}
	CR4 {CR05}
	CR5 {CR06}
	HR11
	HR0
	HR2 {HR12}
	HR13
<b>HSS:</b> Interstitial-free, Bake Hardening, High Strength Low Alloy	CR210LA
	CR160IF
	CR180BH
	CR210BH
	CR240BH



	CR270BH
	MCH550Y600T
	MCH600Y650T
	MCH650Y700T
	MCH700Y750T
	PQS340Y410T

<b>AHSS:</b> Dual Phase, Transformation Induced Plasticity	CR290Y490T-DP
	CR330Y590T-DP
	CR440Y780T-DP
	CR590Y980T-DP {550Y}
	CR700Y980T-DP
	DPC820Y1180T
	HR330Y580T-DP
	CR440Y780T-DH
	CR700Y980T-DH
	CR400Y690T-TR
	CR450Y780T-TR
	TBC330Y590T
	TBC420Y780T
	TBC700Y980T
	HR300Y450T-FB
	HR440Y580T-FB {CR}
	HR600Y780T-FB
	FNH680Y780T
	FNH850Y960T

<b>UHSS:</b> Complex Phase, Martensitic	CR570Y780T-CP
	CR780Y980T-CP
	CR900Y1180T-CP
	HR660Y760T-CP
	MPH780Y980T
	MTC700Y900T
	MTC950Y1200T

	MTC900Y1200T
	CR860Y1100T-MS
	CR1030Y1300T-MS
	CR1220Y1700T-MS
	CR1350Y1700T-MS
	HR900Y1180T-MS
	TWC450Y950T
<b>Press Hardened Steels (PHS)</b>	PQS800Y1000T
	PQS370Y550T
	PHS950Y1300T
	PHS950Y1300T

Table (6.1)

## 6.1 Overview on the share of the market and different steels families that has been used in different segments

### 6.1.1 The share of each segment of passenger vehicles in EMEA

First let's see the number of passenger cars that are in Europe, the Middle East and Africa (EMEA) on 2019 according to ACEA

Segments	A-B	C	D	E	Others	Total
<b>Number of passenger vehicles EMEA 2019</b>	4,200,000	5,650,000	3,060,000	400,000	1,100,00	14,410,000

Table (6.2) number of passenger vehicles according to EMEA 2019

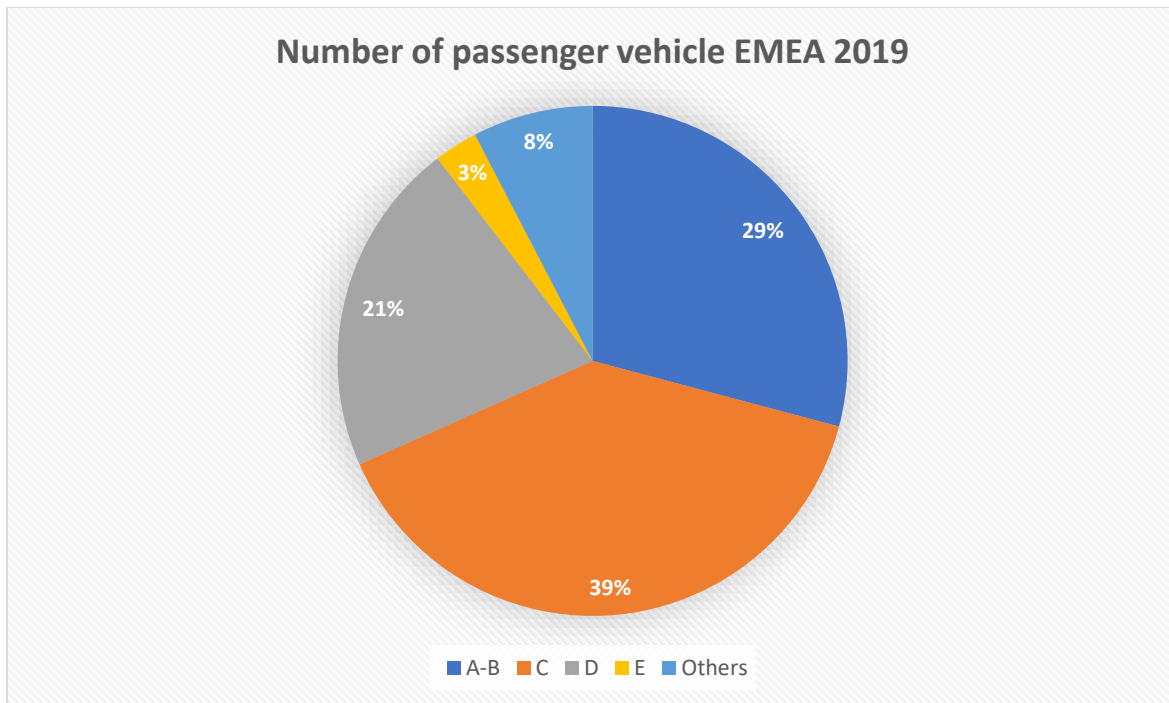


Figure (6.1) the share of each segment from the market according to EMEA 2019

As the pie chart figure (6.1) shows to us that segments A, B and C are about 68% from the total number of passenger vehicles in EMEA

### 6.1.2 Different steel families that are used in passenger vehicles in EMEA 2019 (ACEA source)

the steel families that are used in passenger vehicles in Europe, Middle east and Africa are low carbon steel (LC) 39%, High strength steel (HSS) 34%, Advanced High Strength Steel (AHSS) 15%, Ultra High Strength Steel (UHSS) 4% and Press Hardening Steel (PHS) 9%.

STEEL FAMILY	STEEL TONS	% STEEL
<b>LC</b>	4,953,719.6	39%
<b>HSS</b>	4,301,501.6	34%
<b>AHSS</b>	1,955,245.6	15%
<b>UHSS</b>	533,607.8	4%
<b>PHS</b>	1,096,150.6	9%

Table (6.3)

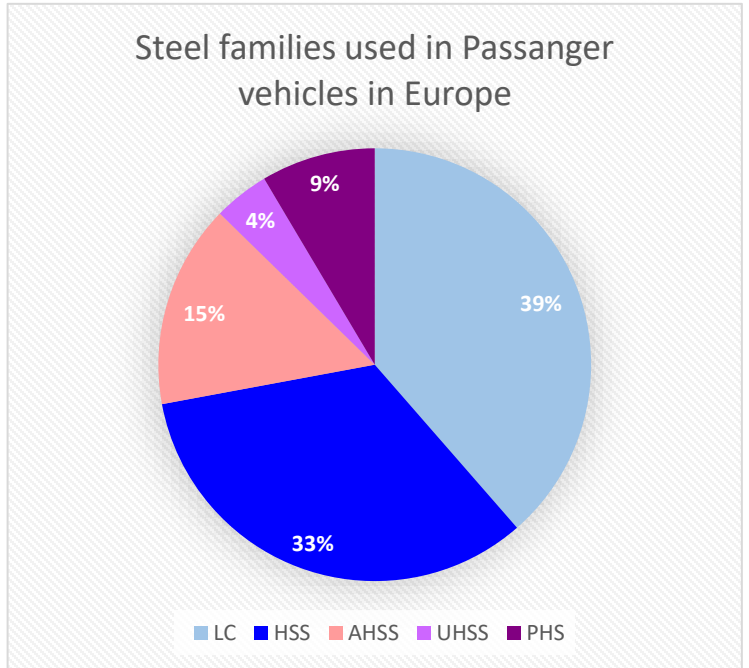
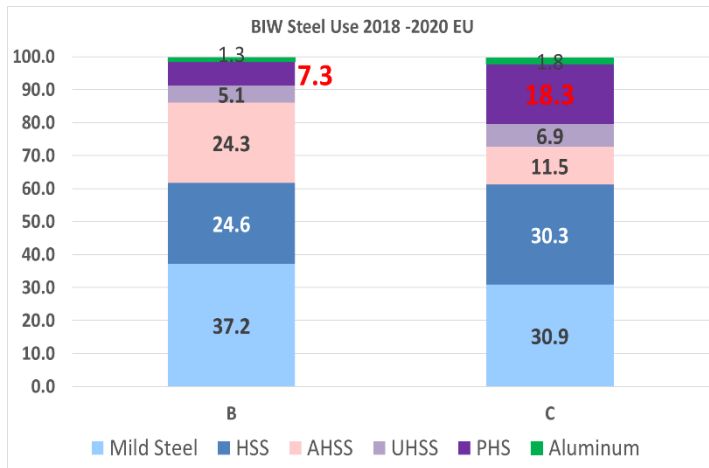
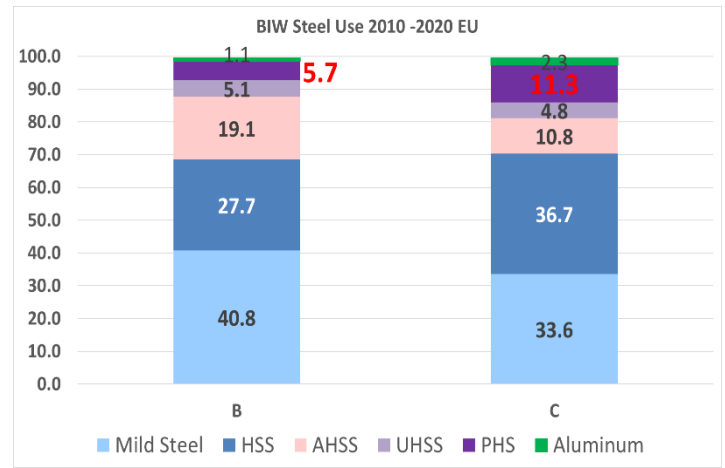


Figure (6.2) Steel families used in passenger vehicles in EU

## BIW Steel used on 2010-2020 and 2018-2020 for segments B and C in Europe



(a)



(b)

Figure (6.3) Steel used in BIW (a) between 2018-2020 (b) between 2010-2020

B-Segment			
	BIW 2010-2020	BIW 2018-2020	
Mild steel	40.8	37.2	↓ 3.6%
HSS	27.7	24.6	↓ 3.1%
AHSS	19.1	24.3	↑ 5.2%
UHSS	5.1	5.1	0 %
PHS	5.7	7.3	↑ 1.6%
Aluminum	1.1	1.3	↑ 0.2%

Table (6.4) Average Steel used in BIW between 2018-2020 and between 2010-2020 for B-segment

C-Segment			
	BIW 2010-2020	BIW 2018-2020	
Mild steel	33.6	30.9	↓ 2.7%
HSS	36.7	30.3	↓ 6.4%

AHSS	10.8	11.5	↑ 0.7%
UHSS	4.8	6.9	↑ 2.1 %
PHS	11.3	18.3	↑ 7%
Aluminum	2.3	1.8	↓ 0.5%

Table (6.5) Table (6.4) Average Steel used in BIW between 2018-2020 and between 2010-2020 for C-segment

As shown in the tables, table (6.4) and table (6.5), The average amount of steel used in 2018-2020 shows a significant increment in PHS by 7% in C-Segment and 1.6% in B-Segment compared to the average steel used in 2010-2020 while the amounts of Mild steels and HSS were reduced in both segments by 3.6% and 3.1% respectively in B-Segment and by 2.7% and 6.4% in C-Segment.

In the following graphs figure (6.4) and figure (6.5) the materials evolution were analyzed based on the information of EuroCarBody starting from 2009 until 2020 considering only B and C segments, as we can see the linear trend “dotted lines” shows that the use of Mild steels and HSS are reduced in both segments while AHSS, UHSS and PHS are significantly increased. Which confirms the results that we discussed previously of BIW of steel used in Europe.

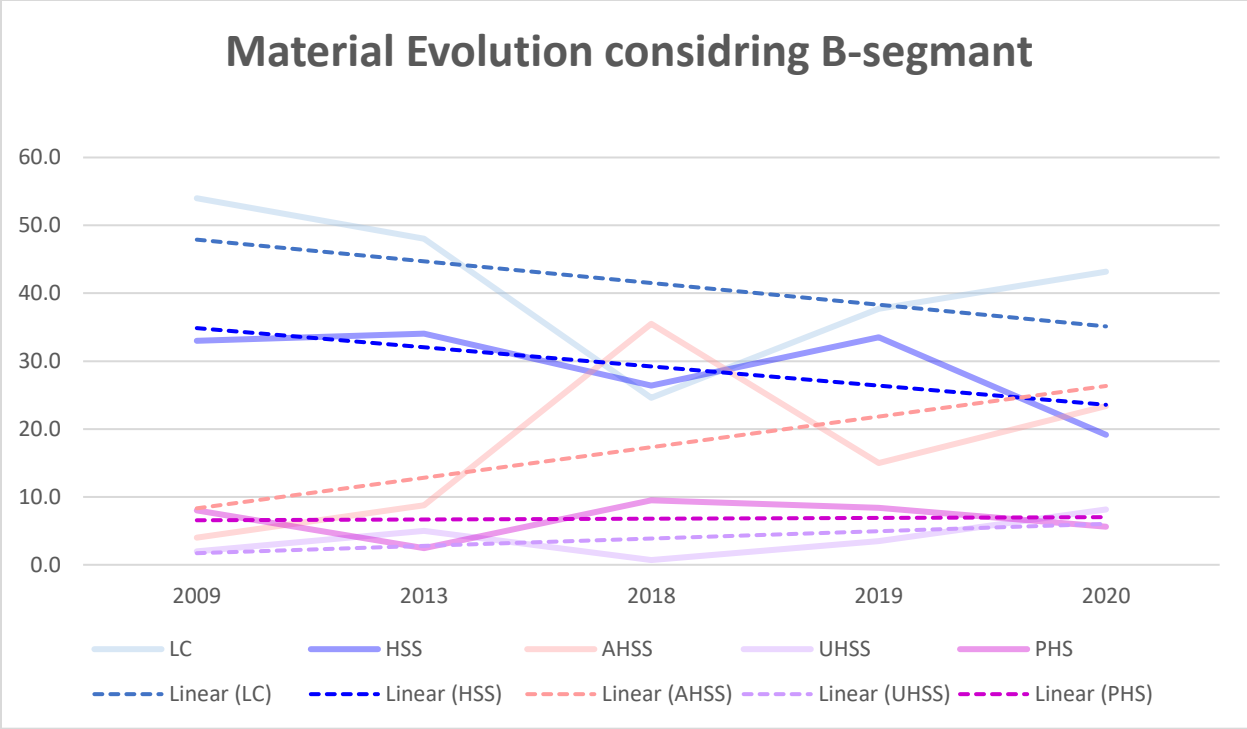


Figure (6.4) material evolution between years 2009-2020 considering only B-segment

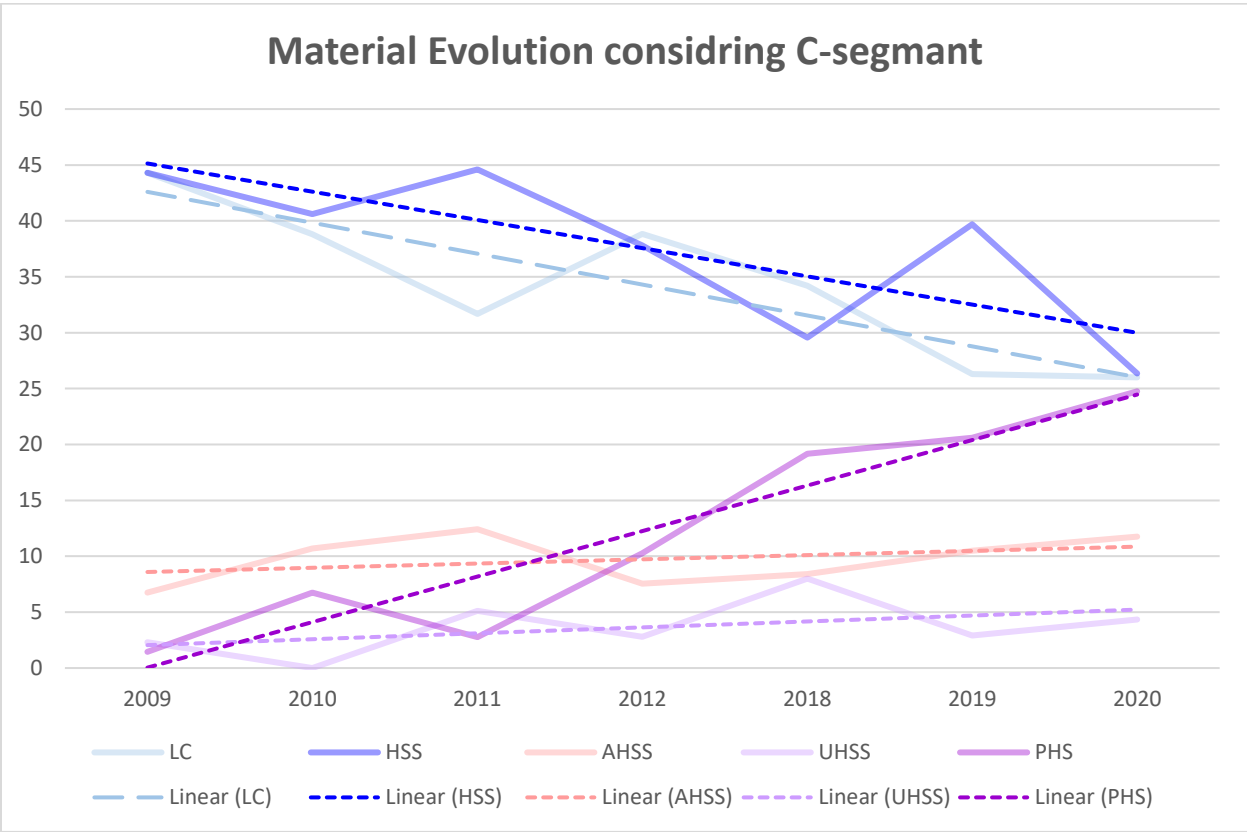


Figure (6.5) material evolution between years 2009-2020 considering only C-segment

### 6.1.3 Material Evolution in Europe and China based on “EuroCarBody from 2012 to 2020” and “8th China Lightweight Car Body Conference -20201129”

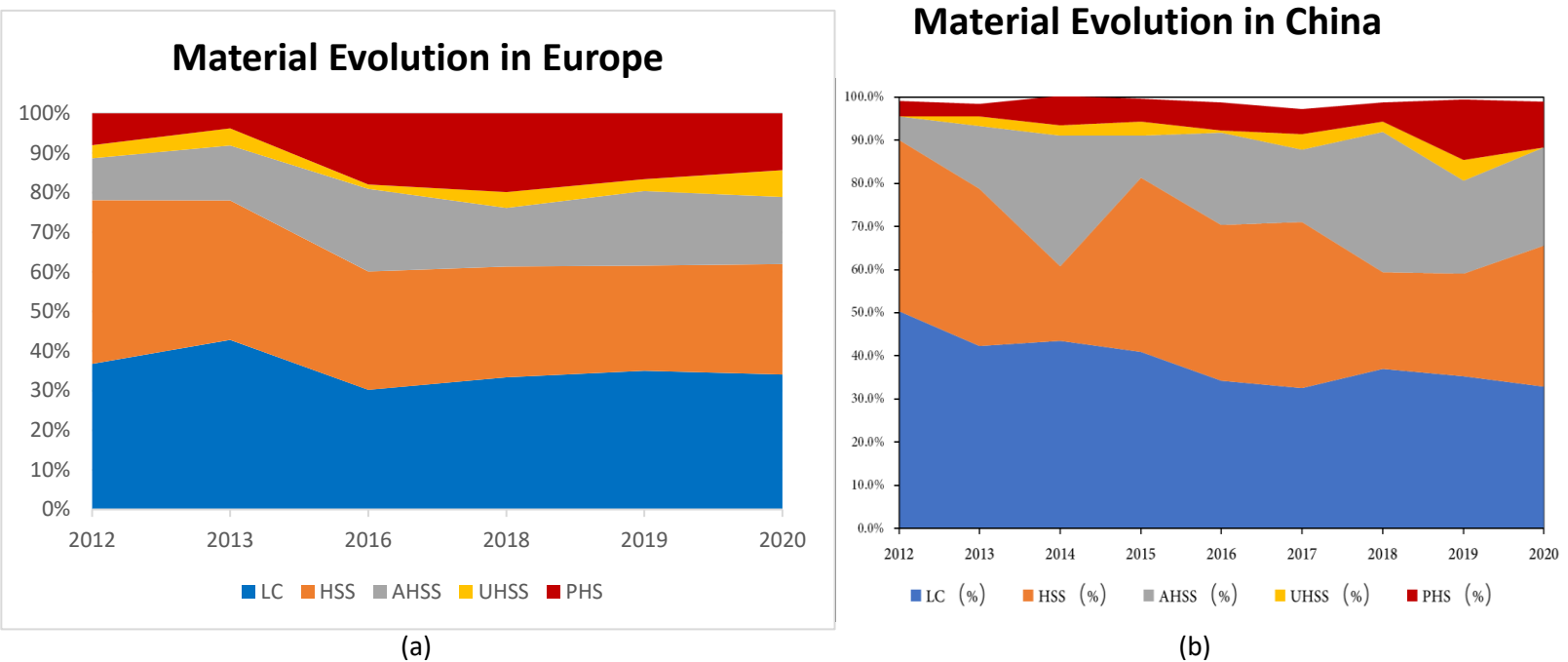


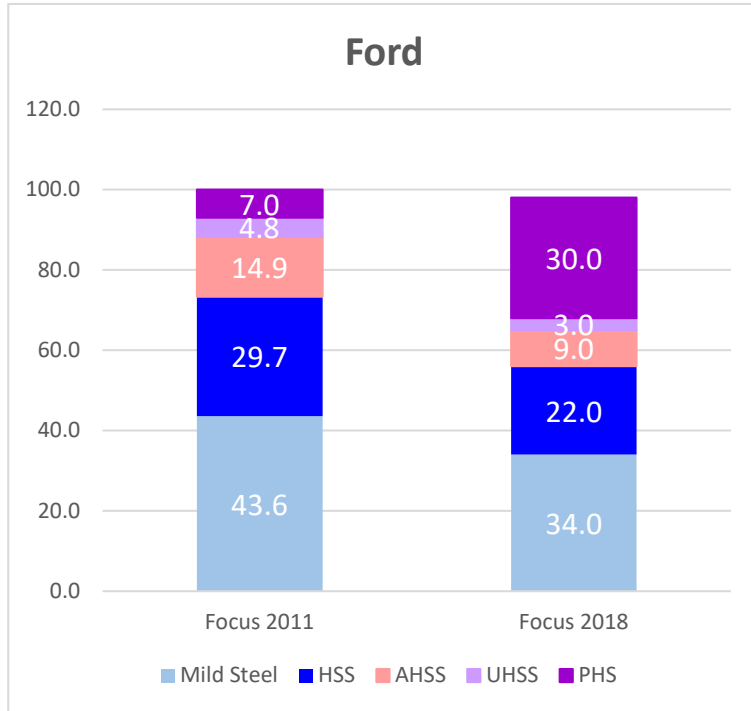
Figure (6.6) material Evolution in (a) Europe (b) China [30]

It could be seen in figure (6.6) that the overall trend of the material evolution in both Europe and China are almost the same which is reducing the usage of LC and HSS while expanding in the use of the other three families which are PHS, AHSS and UHSS.

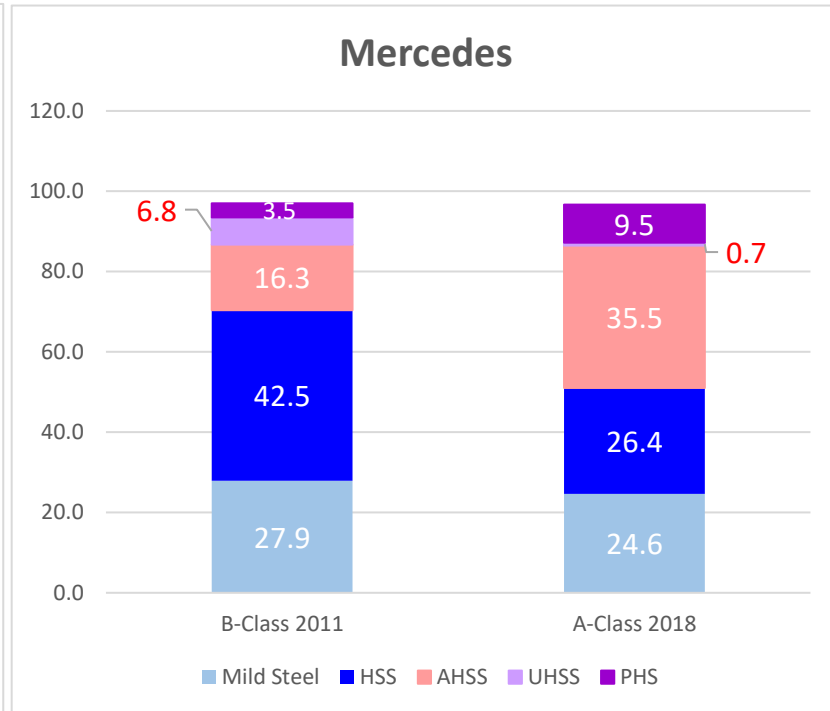
In Europe we can see that there is a dramatic expand in the use of PHS starting from 2013.



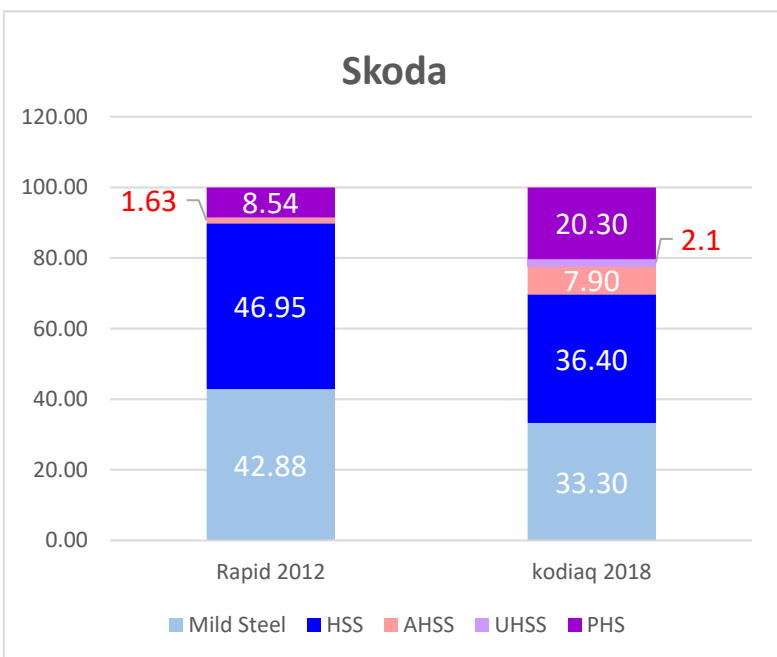
## Steel Use evaluation in different car models for the same carmaker



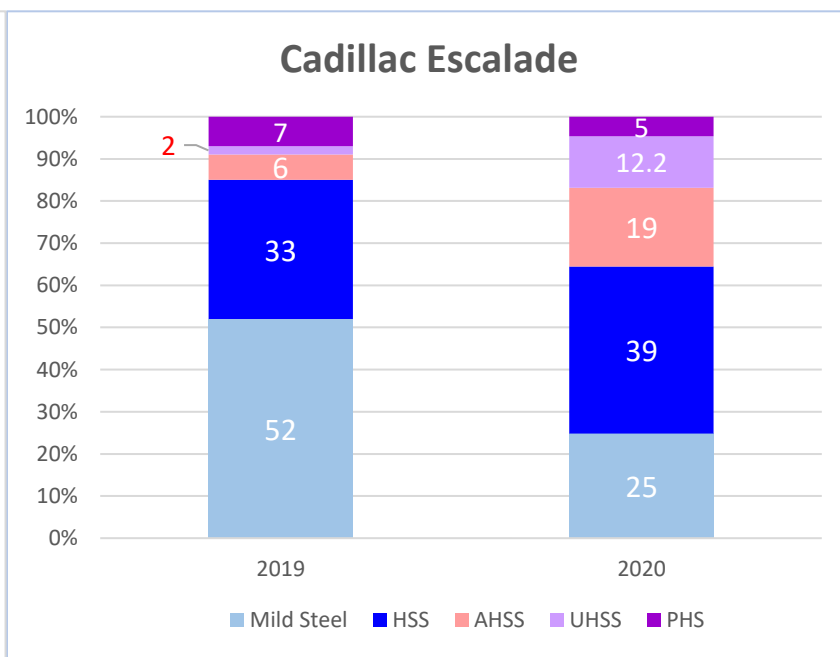
(a)



(b)

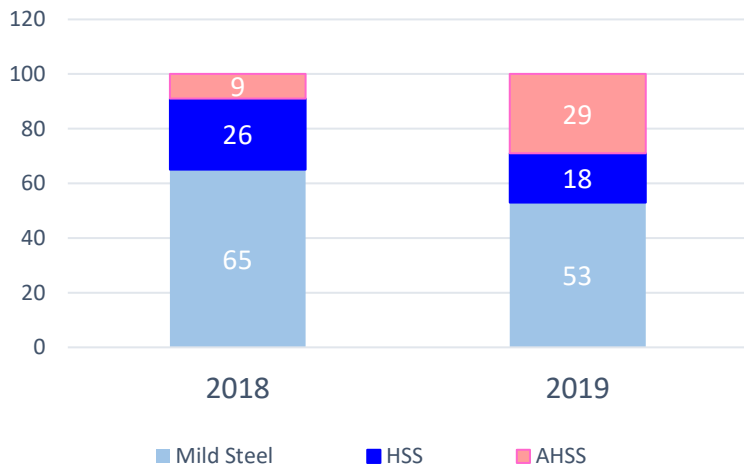


(c)



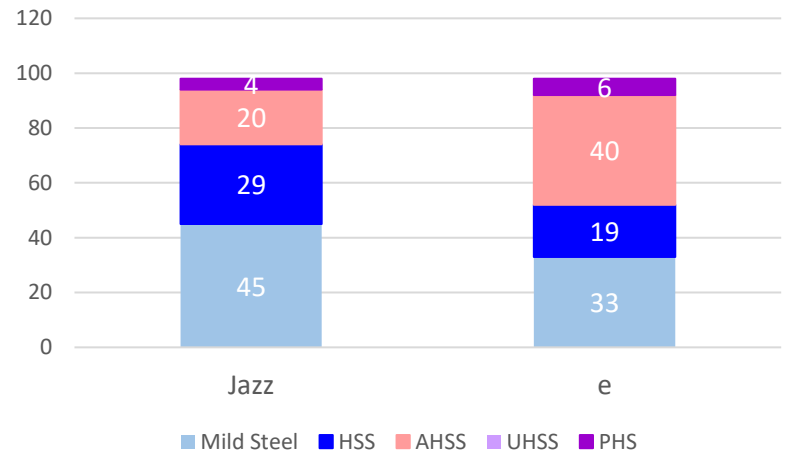
(d)

**Isuzu D-MAX**



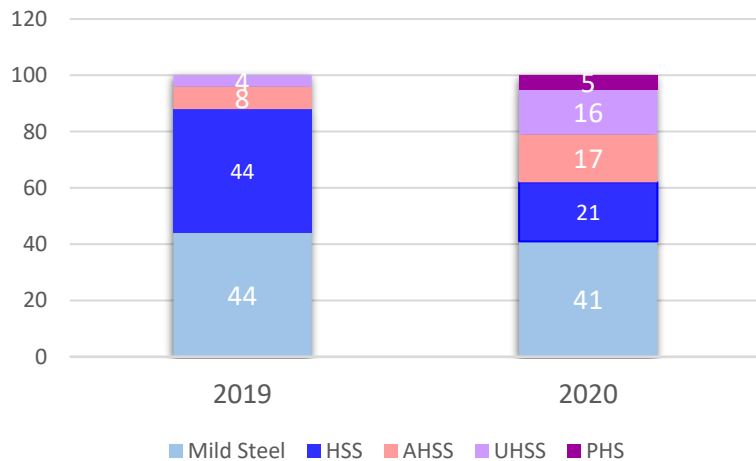
(E)

**Honda**



(F)

**Toyota Yaris**



(G)

Figure (6.7) comparison between the year model and previous year for the same car brand.

In the following table (6.6) we can make a summary that shows the increment and reduction of different steel types used for a vehicle compared to the same car model but previous year

	Toyota Yaris	Honda-e	Isuzu D-MAX	Cadillac Escalade	Ford Focus	Mercedes	Skoda
Mild Steel	3% ↓	12% ↓	12% ↓	27% ↓	10% ↓	3% ↓	10% ↓
HSS	23% ↓	10% ↓	8% ↓	6% ↑	8% ↓	16% ↓	11% ↓
AHSS	9% ↑	20% ↑	20% ↑	13% ↑	6% ↓	19% ↑	6% ↑
UHSS	12% ↑	0%	0%	10% ↑	2% ↓	6% ↓	2% ↑
PHS	5% ↑	2% ↑	0%	2% ↓	23% ↑	6% ↑	12% ↑

Table (6.6) Steel Use evaluation in different car models for the same carmaker

## 6.2 Detailed analysis considering

In this section a detailed analysis will be discussed considering B and C segments only since they are representing about 68% of the totally passenger vehicles in EMEA, these analyses are carried out based on EuroCarBody's data starting from 2009 until 2020.

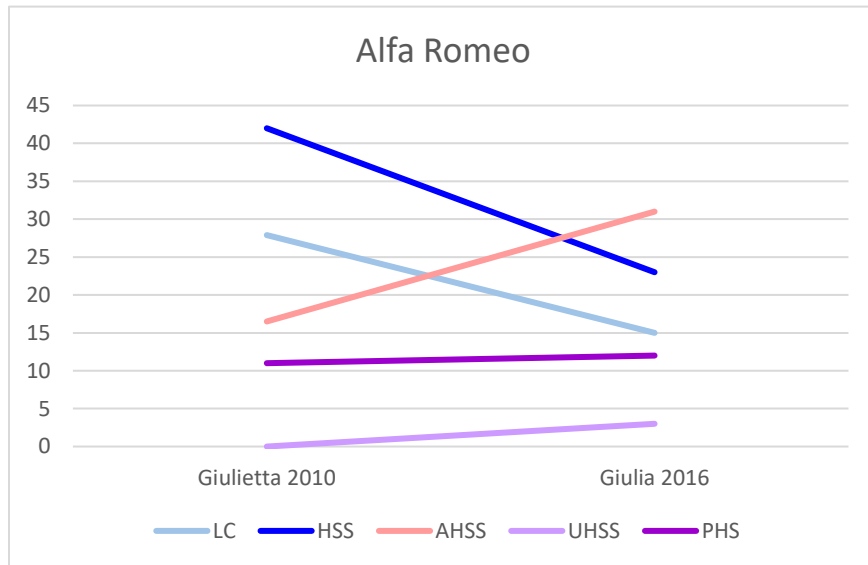
A comparison shall be carried out between deferent vehicles for the same car brand with different segments and also with the same segment in order to distinguish the evolution of the material used, and how deferent car makers are changing their philosophy among years and most of them are following a specific trend.

also we will see in some detailed comparisons some critical parts in the vehicles such as A-pillar, B-pillar Longitudinal Beam, Frontal Beam and the Tunnel, these parts are critical from point of view of safety but on the other hand the weight reduction concerns plays an important role so will see how deferent carmakers dealt with such an issue by making some comparisons showing the material that they used in deferent vehicles models

### 6.2.1 Alfa Romeo (C&D)

	Guilietta 2010	Giulia 2016	
LC	27.9	15.0	12.9%↓
HSS	42.0	23.0	19% ↓
AHSS	16.5	31.0	14.5%↑
UHSS	0.0	3.0	3% ↑
PHS	11.0	12.0	1% ↑
Weight of BIW	280 Kg	322 Kg	42 Kg

TABLE (6.7) percentage of used material in Alfa Romeo **Guilietta 2010** and **Giulia 2016**



Alfa Romeo Giulietta is C-segment, while Giulia is D-segment, as we see from 2010 to 2016 many things are changed, the low Carbon steels and HSS are both reduced by 12.9% and 19 % respectively, While AHSS, UHSS and PHS are increased by 14.5%, 3% and 1% respectively.

Figure (6.8) the trends of the steel families in Alfa Romeo for year model 2010 and 2016.

## Giulia 2016

Car body structure

Body-in-white structure

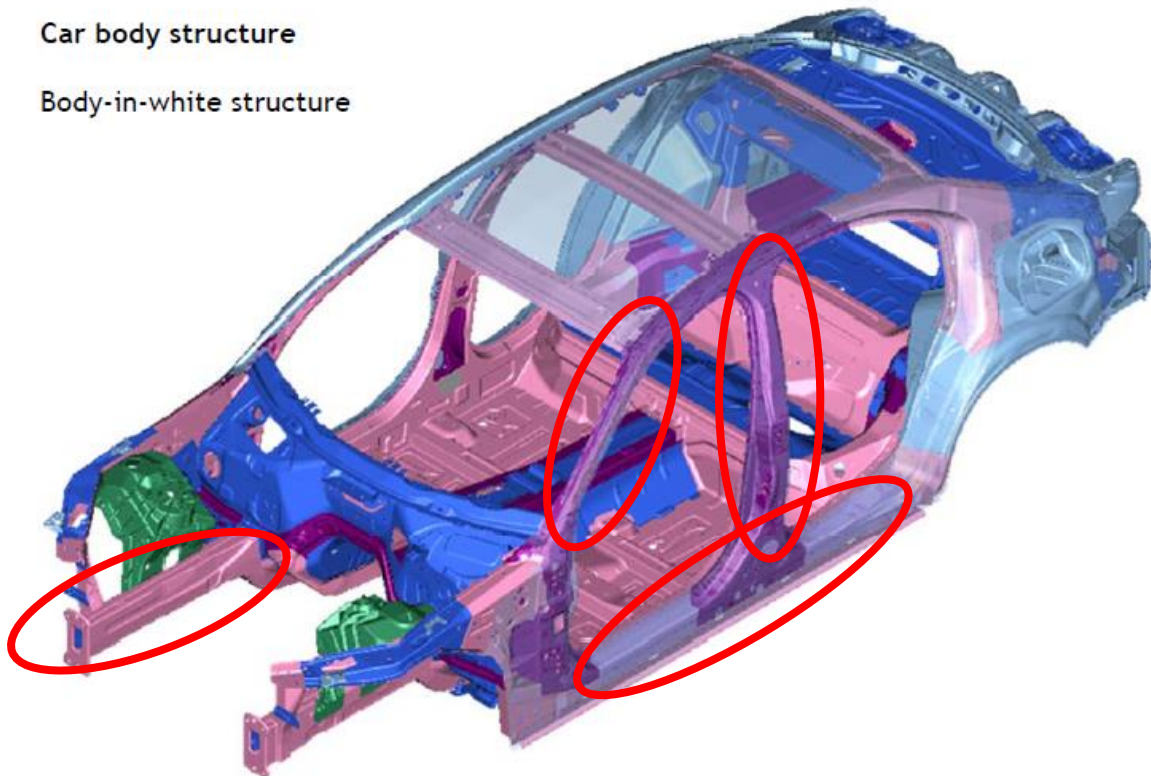


Figure (6.9) BIW of Alfa Romeo Giulia 2016.

## Giulietta 2010

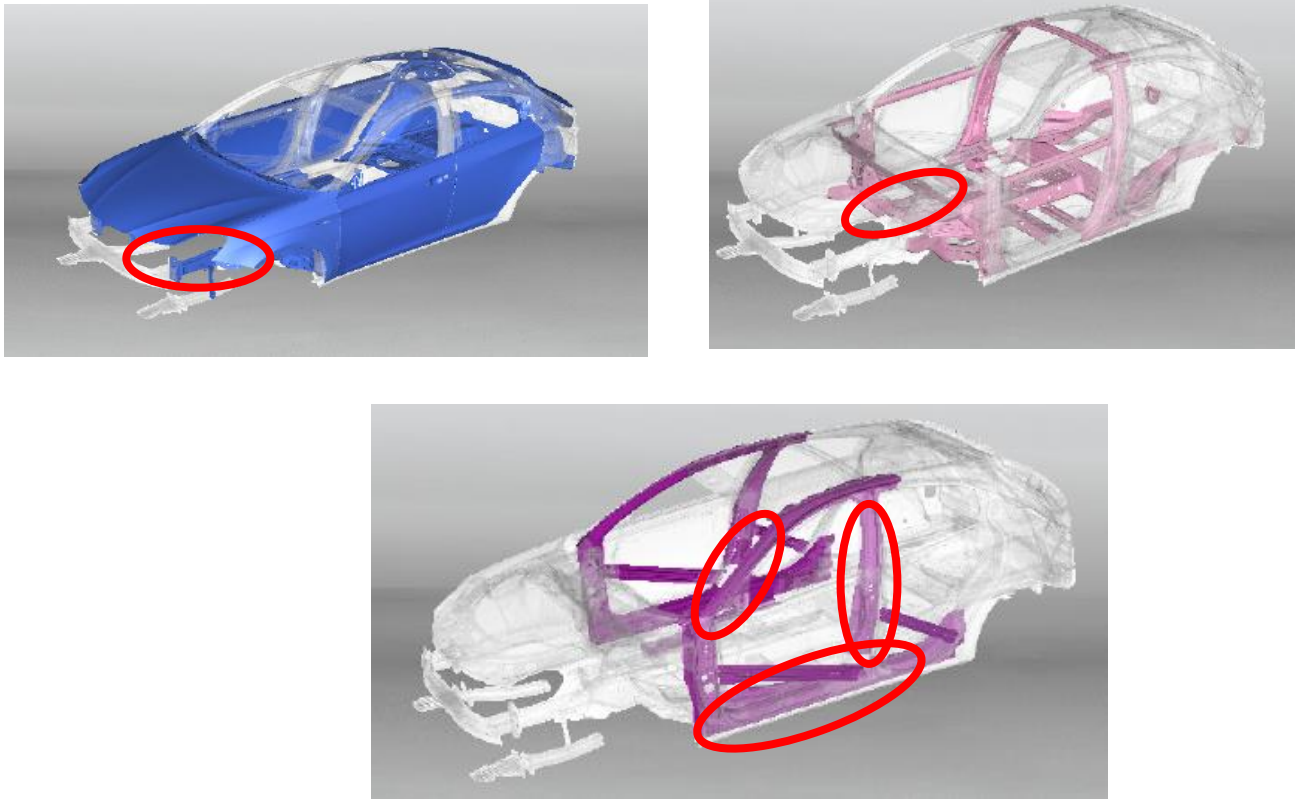


Figure (6.9) BIW of Alfa Romeo Giulietta 2010

	Giulietta 2010	Giulia 2016	
A-pillar	PHS	PHS	
B- Pillar	PHS	PHS	
Longitudinal Beam	PHS	UHSS	
Frontal Beam	HSS	AHSS	
Tunnel	AHSS	PHS	HSS

Table (6.8) comparison of steel families used in specific parts of the vehicle

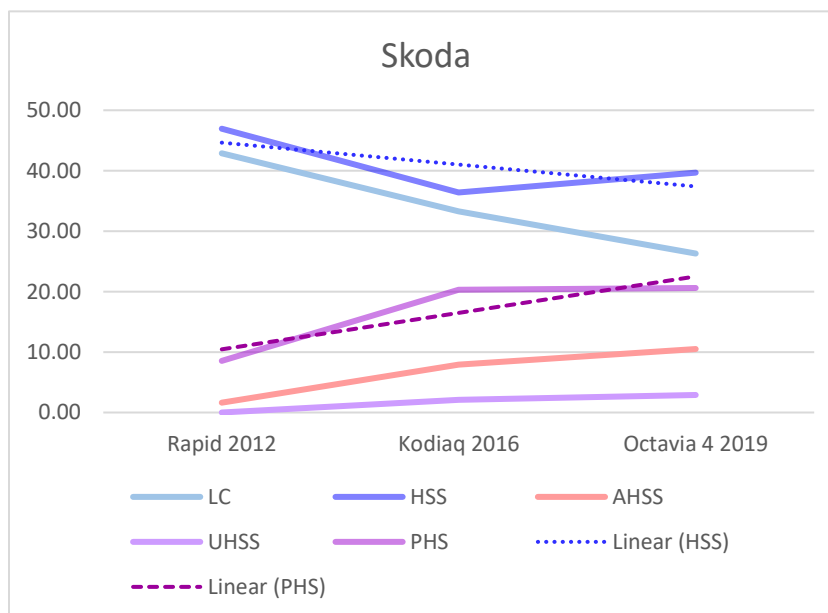
## 6.2.2 SKODA (C)

Here all the represented vehicles are Skoda and C-segment

	Rapid 2012	Kodiaq 2016&2018	Octavia 4 2019	Percentage of reduction/increment of diff. steel families between Rapid & Kodiaq	Percentage of reduction/increment of diff. steel families between Kodiaq & Octavia
<b>LC</b>	<b>42.9</b>	<b>33.3</b>	<b>26.3</b>	<b>9.6 ↓</b>	<b>7.0 ↓</b>
<b>HSS</b>	<b>46.9</b>	<b>36.4</b>	<b>39.7</b>	<b>10.5 ↓</b>	<b>3.3 ↑</b>
<b>AHSS</b>	<b>1.6</b>	<b>7.9</b>	<b>10.5</b>	<b>6.3 ↑</b>	<b>2.6 ↑</b>
<b>UHSS</b>	<b>0.0</b>	<b>2.1</b>	<b>2.9</b>	<b>2.1 ↑</b>	<b>0.80 ↑</b>
<b>PHS</b>	<b>8.5</b>	<b>20.3</b>	<b>20.6</b>	<b>11.8 ↑</b>	<b>0.30 ↑</b>
<b>Weight of the BIW</b>	<b>329 Kg</b>	<b>327 Kg</b>	<b>281 Kg</b>	<b>2 Kg</b>	<b>46 Kg</b>

Table (6.9) steel families used for Skoda between years 2012,2016 and 2019.

The material evolution here too is following the same trend if we looked at rapid 2012



compared to Kodiaq 2016, 2018 and Octavia 4 2019, the LC and HSS are both reduced by a considerable number while the AHSS and UHSS are increased and the PHS is significantly increased too by about 12.1% in 2019.

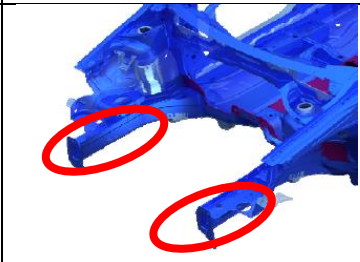
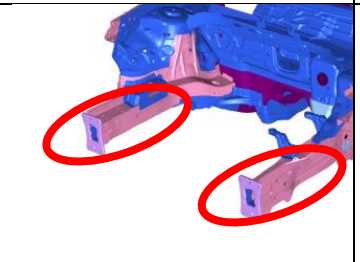
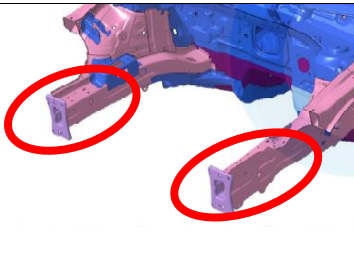
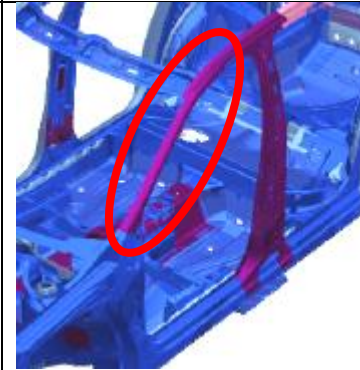
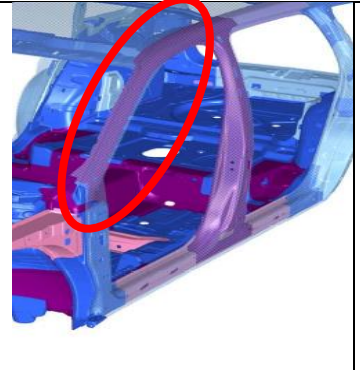
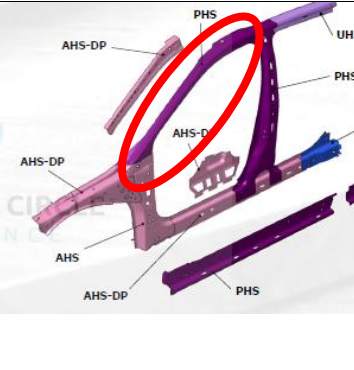
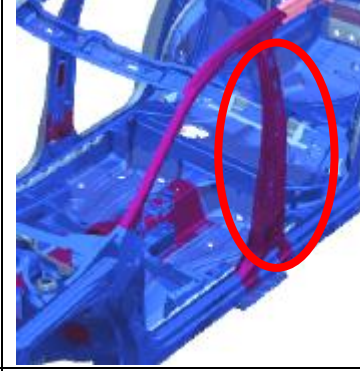
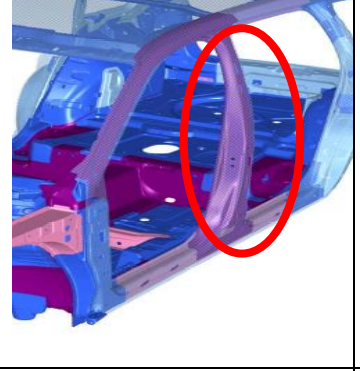
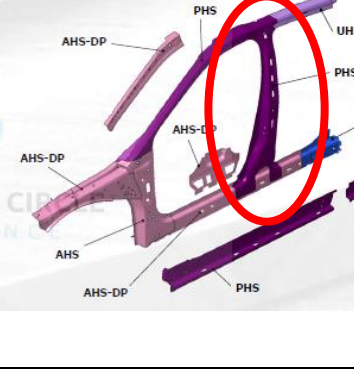
The differences of the amounts of used materials doesn't show a significant change between Kodiaq and Octavia 4 except that they reduced the percentage of low carbon steel by 7%.

Figure (6.10) steel families trend for Skoda between years 2012,2016 and 2019.

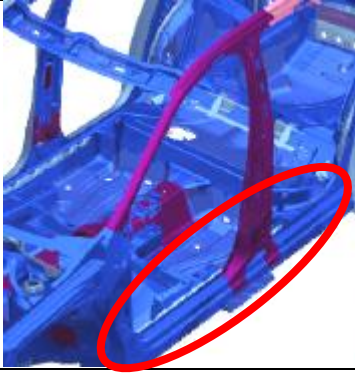

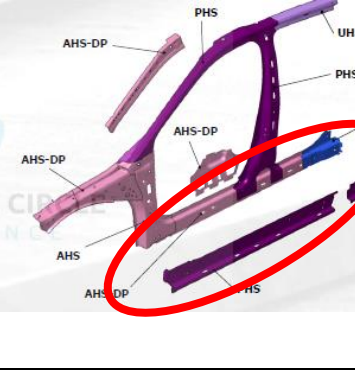
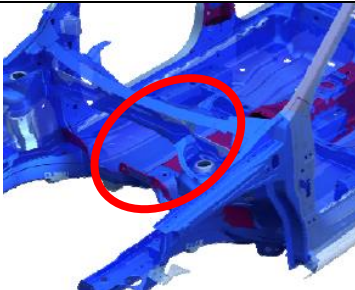


Another important point that needs to be mentioned in this part that all of the previously mentioned vehicles are ICE so we can make a weight comparison between them in order to know how the modifications and replacements of the different materials can affect the vehicle's weight.

We can see that the weight is reduced by about 2 Kg when the weight of Rapid 2012 is compared to Kodiah 2016&2018 while it is reduced by about 46 Kg in Octavia 4 compared by Kodiah

#### Steel evolution in some specific critical parts

	Rapid 2012	Kodiah 2016&2018	Octavia 4 2019
Frontal Beam			
	HSS	AHSS	AHSS
AHSS is used instead of HSS			
A- Pillar			
	UHSS	UHSS	PHS
PHS replaced The UHSS in A-Pillar			
B- Pillar			
	PHS	UHSS	PHS



Longitudi nal Beam			
	HSS	AHSS	PHS+AHSS
Tunnel			
	HSS+PHS	PHS+AHSS	PHS

Safety Results according to Euroncap [42,43,44]

	Adult occupant	Child Occupant	Pedestrian
Rapid 2012	94%	80%	69%
Kodiaq 2016	92%	77%	71%
Octavia 4 2019	92%	88%	73%

Table (6.10)

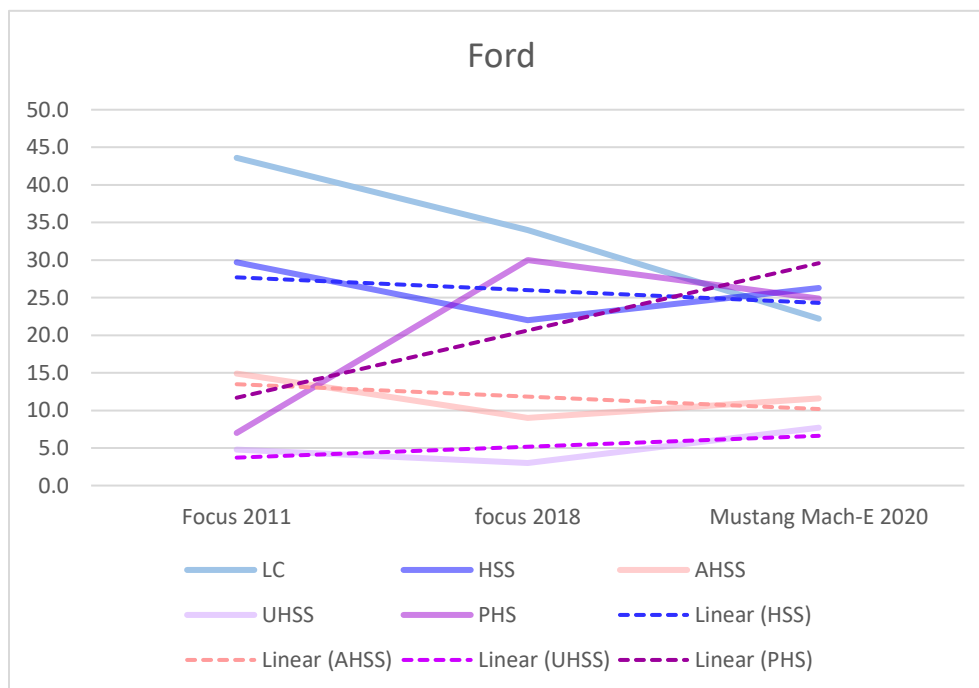


### 6.2.3 FORD (C)

Here also all the vehicles are the same segment which is C and the same brand “Ford”

	Focus 2011	Focus 2018	Mustang Mach-E 2020	Percentage of reduction/increment of diff. steel families between Focus 2011 & focus 2018	Percentage of reduction/increment of diff. steel families between focus 2018 & Mustang Mach-E
LC	43.6	34.0	22.2	9.6 ↓	11.8 ↓
HSS	29.7	22.0	26.3	7.7 ↓	4.3 ↑
AHSS	14.9	9.0	11.6	5.9 ↓	2.6 ↑
UHSS	4.8	3.0	7.7	1.8 ↓	4.7 ↑
PHS	7.0	30.0	24.9	23.0 ↑	5.1 ↓
Weight of the BIW	280 Kg	264 Kg	381 Kg	16 Kg	116 Kg

Table (6.11) Steel families used for Ford between years 2011,2018 and 2020.



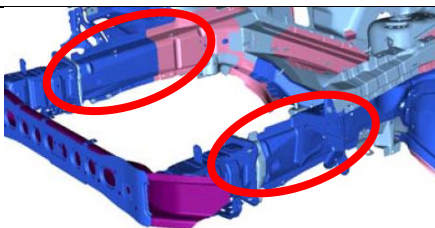
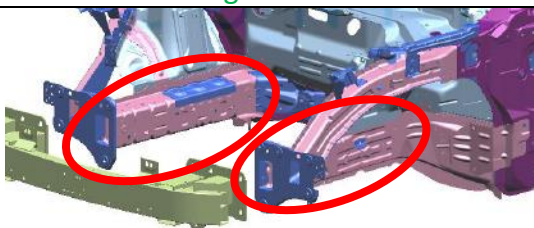
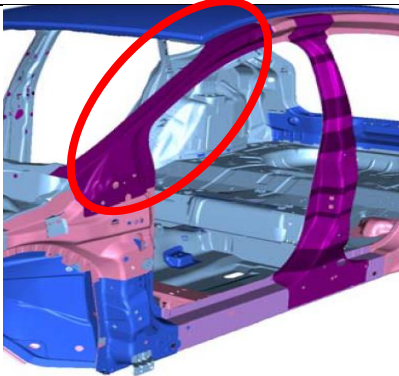
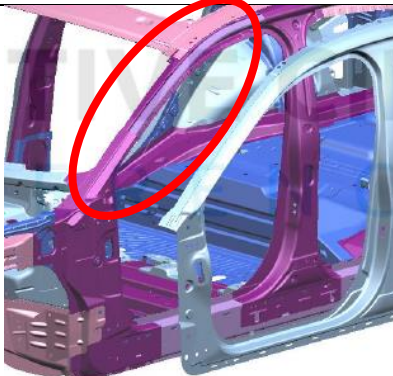
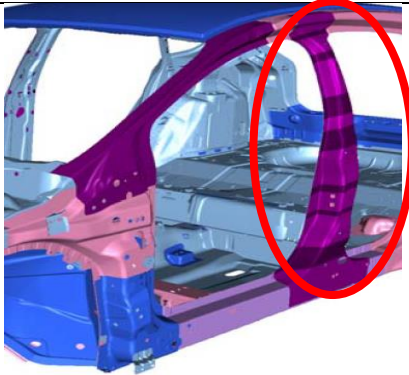
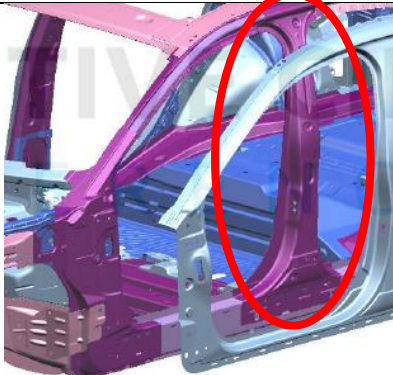
Here the situation is a little bit different from the previous cases since all the steels that are used are reduced including AHSS and UHSS in Ford focus 2018 compared to 2011 while the PHS is increased by 23% which led to reduce the weight of Ford focus by about 16 Kg.

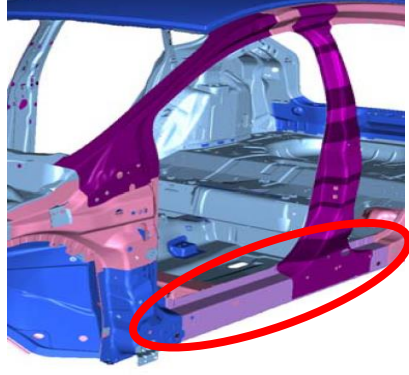
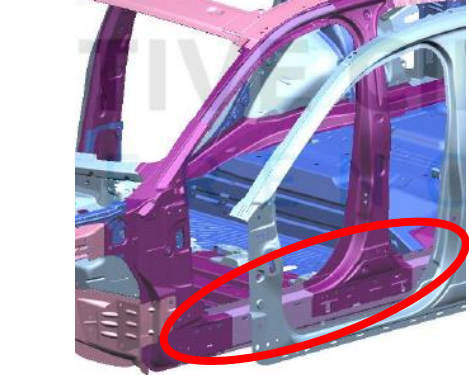
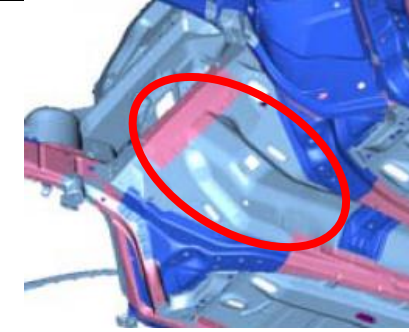

Figure (6.11) Steel families trend for Ford between years 2011,2018 and 2020.

In the case of Mustang Mach 2020 it is a different case since it is an electrical vehicle but it followed the trend of reducing the amount of low carbon steel by 11.8% and the PHD represents about the quarter of the steel used in the vehicle

The weight comparison is not sufficient here since Mustag Mach-E is **BEV**

#### Steel evolution in some specific critical parts

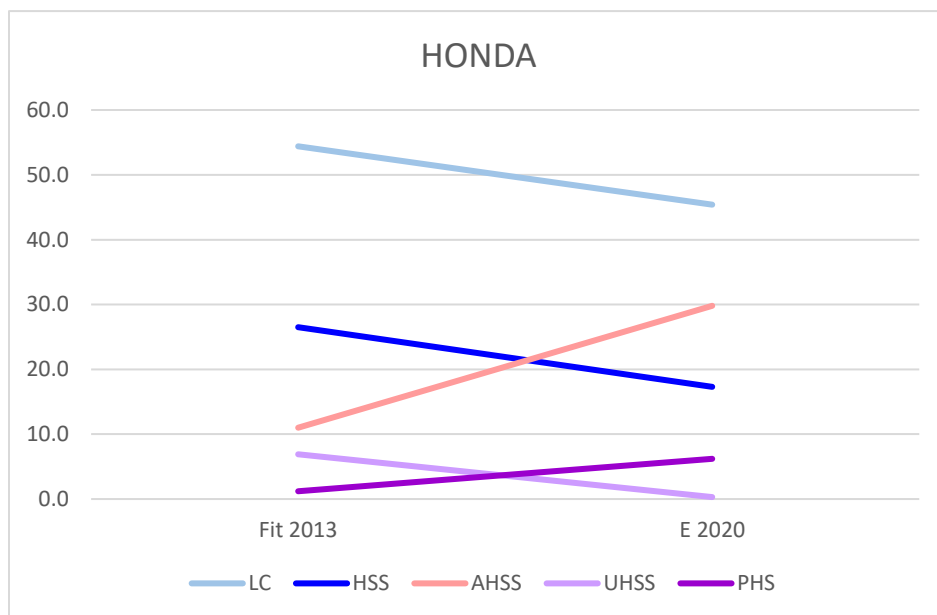
	Focus 2011	Mustang Mach-E 2020
Frontal Beam		
	HSS	AHSS
A- Pillar		
	PHS	UHSS+PHS
B- Pillar		
	PHS	PHS

Longitudinal Beam		
	HSS+UHSS+PHS	UHSS+PHS
Tunnel	 Bottom view	
	LCS+AHSS	HSS+PHS

### 6.2.4 HONDA (B)

	Fit 2013	E 2020	Percentage of reduction/increment of diff. steel families between Fit 2013 & E 2020
LC	54.4	45.4	9.0 ↓
HSS	26.5	17.3	9.2 ↓
AHSS	11.0	29.8	18.8 ↑
UHSS	6.9	0.3	6.6 ↓
PHS	1.2	6.2	5.0 ↑
Weight of the BIW	231 Kg	267 Kg	36 Kg

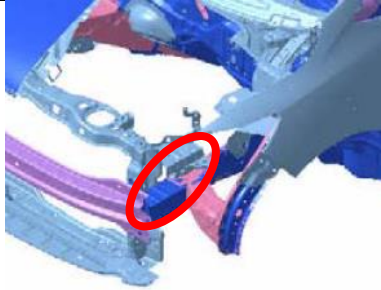
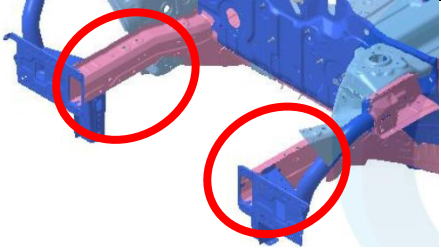
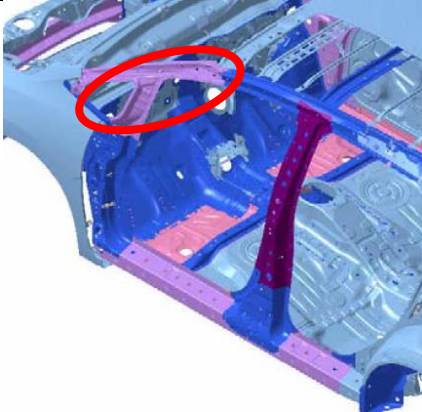
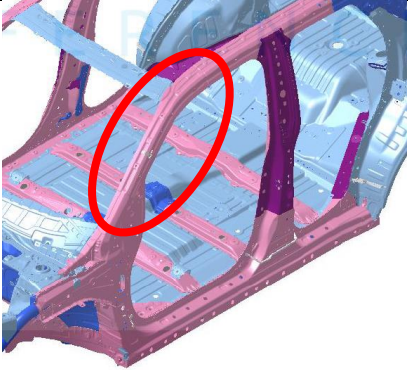
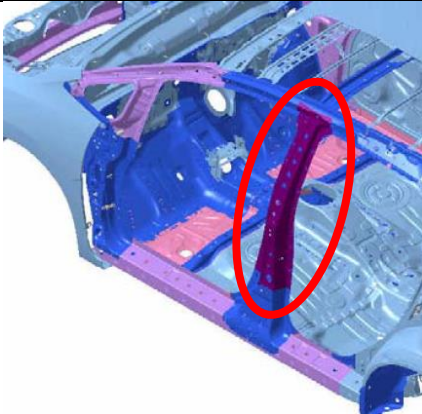
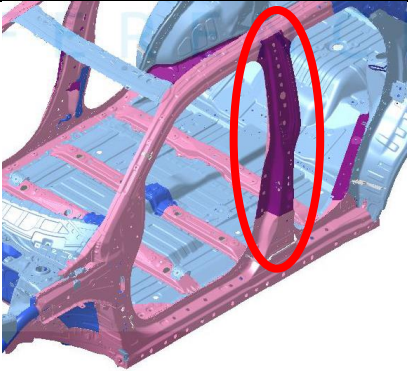
Table (6.12) Steel families used for Honda between years 2013 and 2020.



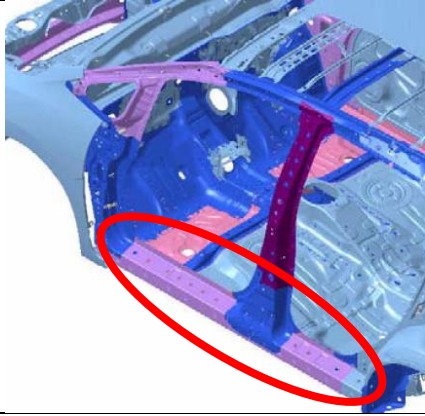
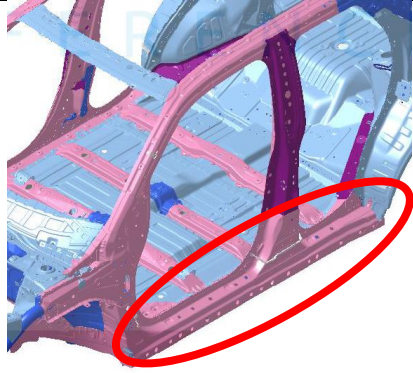
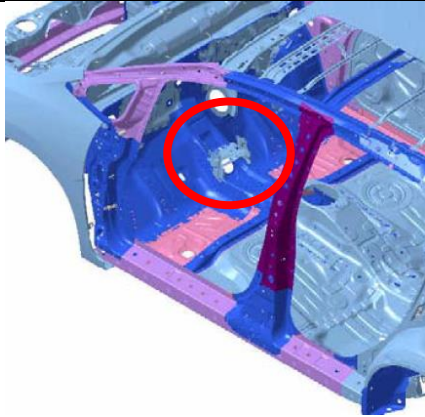
Both the vehicles are B segments but Honda E 2020 is **BEV** so The weight comparison doesn't make sense, but when we compare it to Honda Fit we will see that LC, HSS and UHSS are reduced while PHS and AHSS are increased by 5% and 18.8%

Figure (6.12) Steel families trend for Honda between years 2013 and 2020.

## Steel evolution in some specific critical parts

	<b>Fit 2013</b>	<b>E</b>
Frontal Beam		
	HSS	AHSS
A- Pillar		
	UHSS	AHSS
B- Pillar		
	PHS	PHS



Longitudinal Beam		
	UHSS+LC	AHSS
Tunnel		Doesn't exist
	LC+HSS	

We can conclude that as a final result there is a huge reduction in the use of LC and the HSS while on the other hand there is an increment in the use of AHSS and UHSS and a significant increment in the use of PHS as shown in the following figure. Also in the most critical parts from point of view of safety that we discussed previously we will figure out that these parts are made only using these 3 families of steels which are AHSS, UHSS and PHS

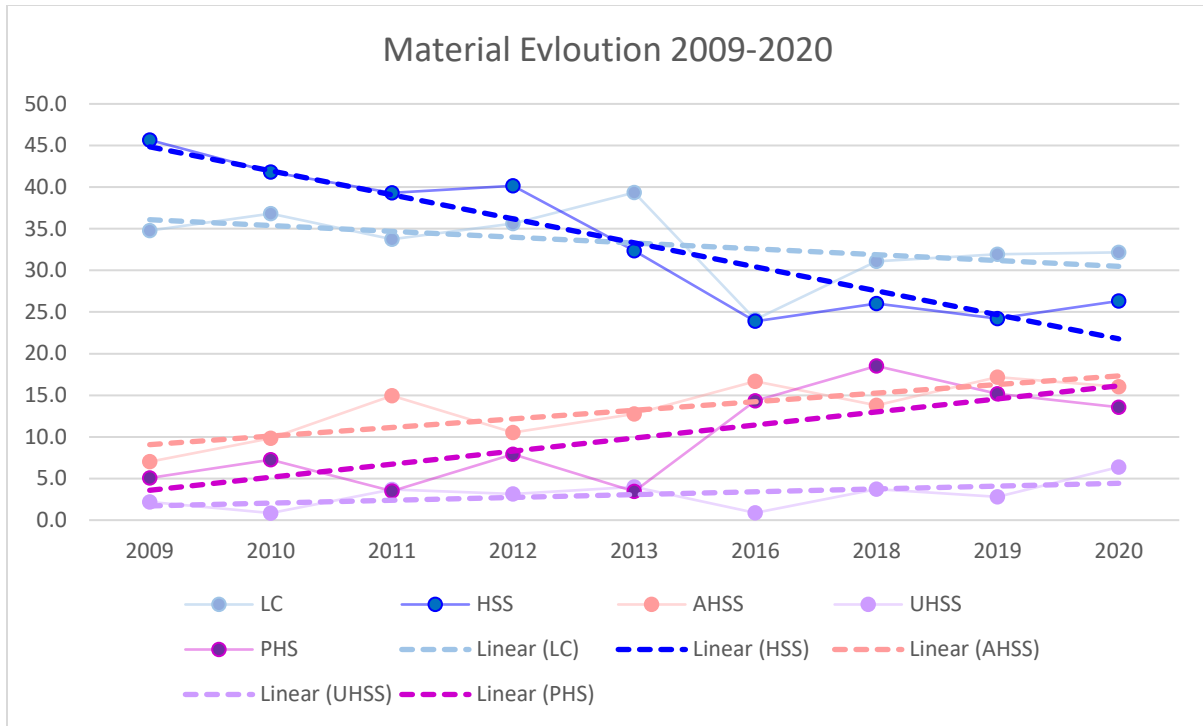


Figure (6.13) overall material evolution from 2009 to 2020

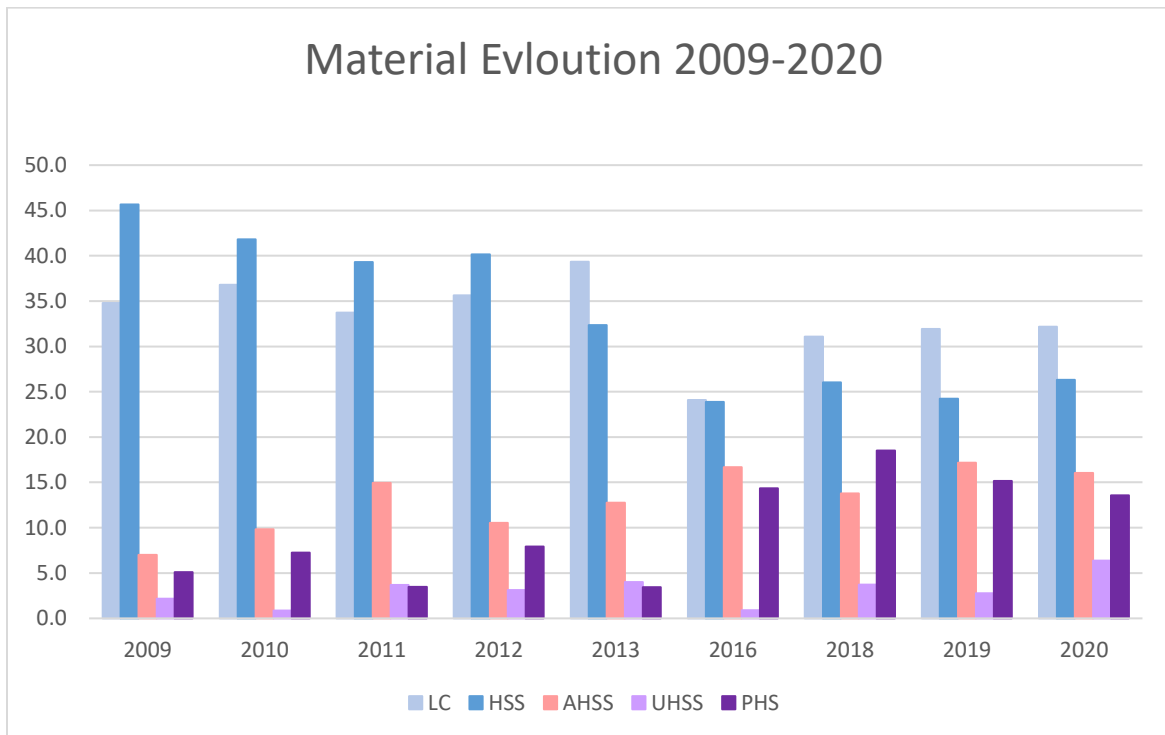


Figure (6.14) the average amount of used Steel families in the years between 2009 and 2020

Note that special and high performance vehicles are not included in the previous charts since they are mainly built with Aluminum and plastics which are out of our focus also the trucks are excluded

### 6.3 Electrical Cars

Here we will analyze the material used for the Electrical cars in the first bar chart we analyzed segments B and C while in the second we analyzed J based on EuroCarBody 2020.

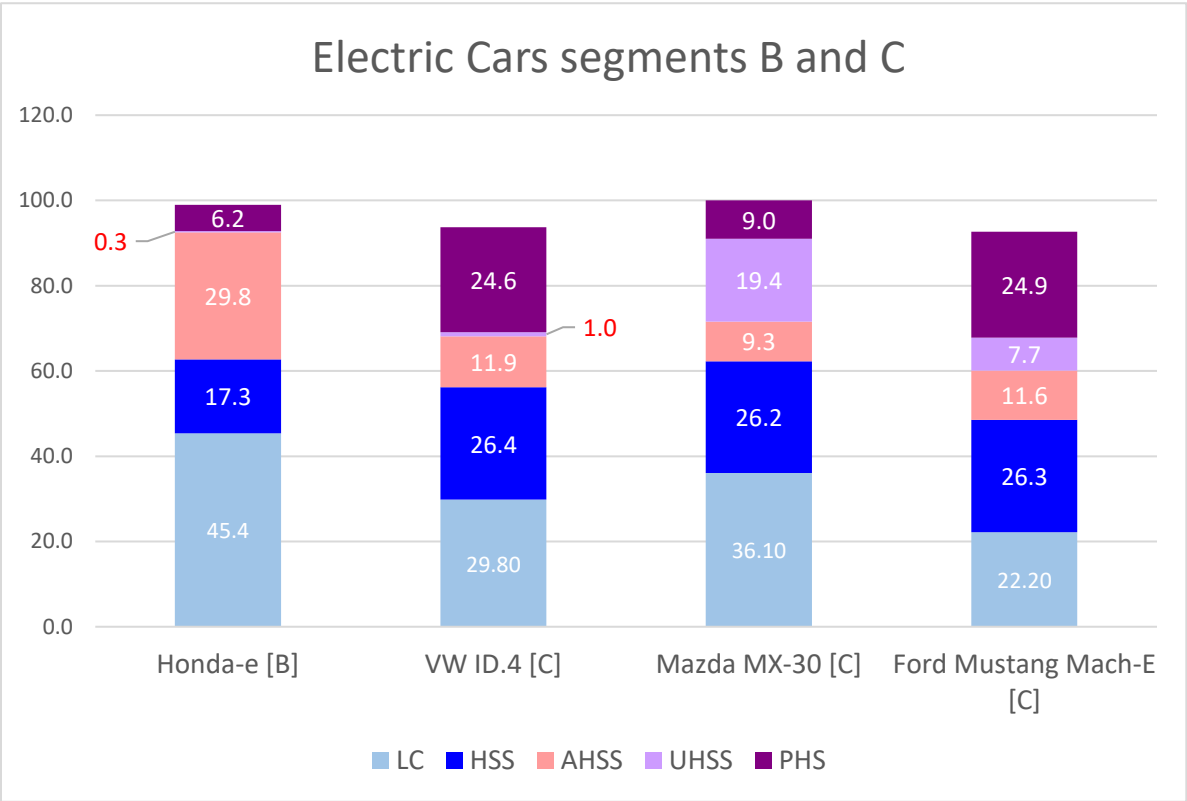


Figure (6.15) Steel families used in electrical vehicles segments B and C

We can see in the previous chart that the B-segment has cheap materials and it has the lowest PHS compared to the others C-segments vehicle and that’s make sense, because generally speaking B-segments vehicles are cheaper than C-segments.



We can see that each region has its own strategy in Europe and North America that are represented by VW and Ford they go more for PHS while in Japan they are using more AHSS and in Korea they are using a mix of all the materials “the best material in the best place”.

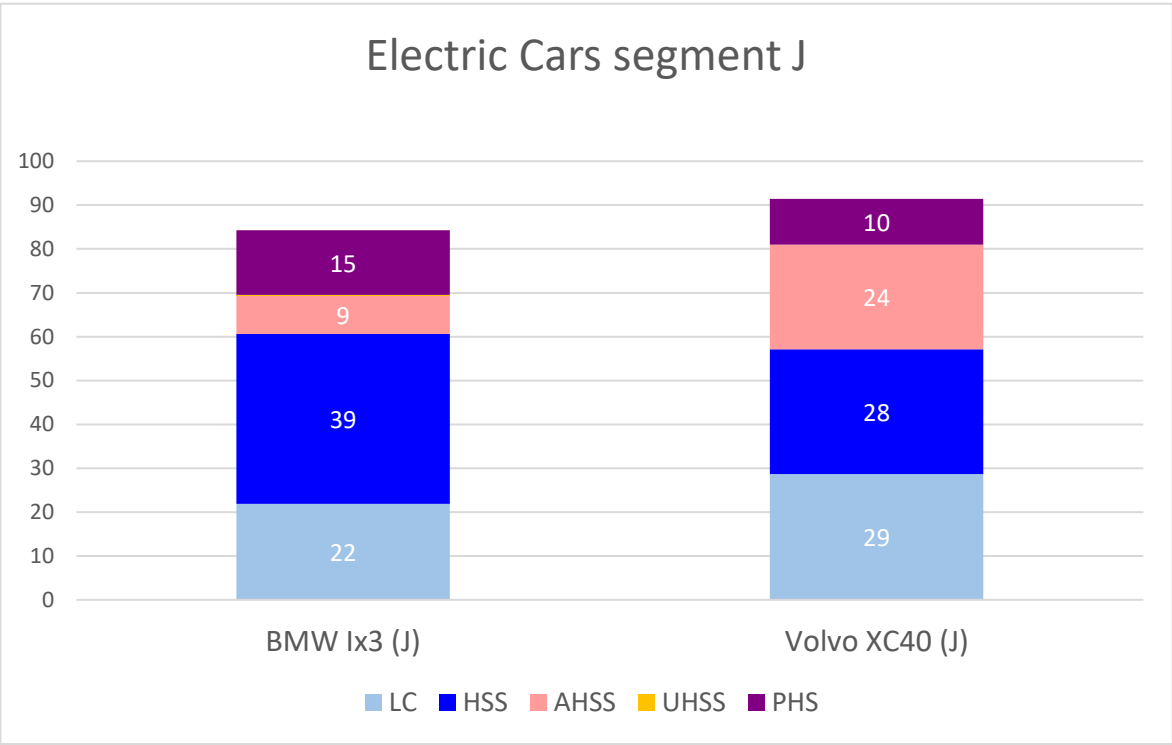
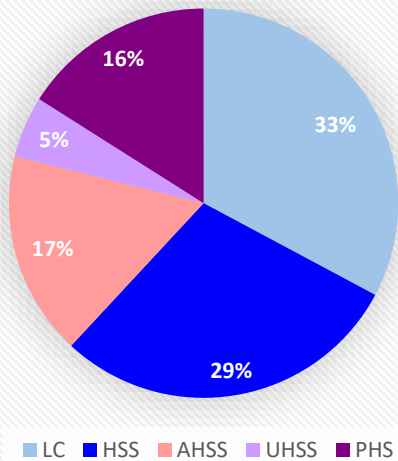


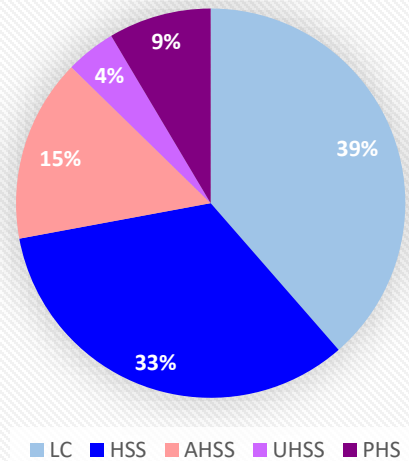
Figure (6.16) Steel families used in electrical vehicles segment J

**Average Amounts of Steel Used  
in BEV 2020**



(a)

**Steel families used in  
Passanger vehicles 2019**



(b)

Figure (6.17) Comparison between steel used in BEV and other passenger vehicles

The Pie Chart on the left represents the average amount of steel used in BEV based on EuroCarBody **2020** that includes Honda-e, VW ID.4, Mazda MX-[30], Ford Mustang Mach-E 2020, BMW Ix3 and Volvo XC40, while on the right the pie chart shows the amount of steel used in passenger cars **2019**.

it is clear that the LC steels and HSS are reduced in the BEV by 6% and 4% respectively while the AHSS, UHSS and PHS are increased by 2%, 1% and 7%.

## Conclusion

From all the previously analyzed data it is clear that all the car makers are targeting the steel that has lightest weight for meeting the OEMs needs and regulations, the highest strength for safety concerns and ductile in order to easily shaped and there is an overall trend in the last 10 years that the Low Carbon steel (LC) and High strength steels (HSS) are decreased in the vehicles while the Advanced High strength steel (AHSS), Ultra High strength Steel (UHSS) and Press hardening steel (PHS) are mostly used specially in parts that are directly exposure to accidents.

# REFERENCES

1. George E. Totten, *Steel Heat Treatment*, Second Edition, Taylor & Francis Group, 2006.
2. Sidney H. Avner, *Introduction to Physical Metallurgy*, Second Edition, City University of New York, 1974.
3. William F. Smith and Javad Hashemi, *Foundation of Material Science and Engineering*, Third Edition, The McGraw-Hill Company, 2004.
4. George Krauss, *Steels, Processing, Structure, and Performance*, Second Edition, ASM International®, 2015.
5. John D. Verhoeven, *Steel Metallurgy for the Non-Metallurgist*, ASM International®, 2007.
6. Richard J. Fruehan, *The Making, Shaping and Treating of Steel (Steel Making and Refining)*, The AISE Steel Foundation Three Gateway Center, 1998.
7. W. R. IRVING, *Continuous Casting of Steel*, The Institute of Materials, 1993.
8. Keith J. Barker, Charles D. Blumenschein, Ben Bowman, Allen H. Chan, Richard J. Choulet, William L. Roberts, *Hot Rolling of Steel (Manufacturing Engineering and Materials Processing)*, The AISE Steel Foundation Three Gateway Center, 1998.
9. William L. Roberts, *Cold Rolling of Steel (Manufacturing Engineering and Materials Processing)*, Marcel Dekker.INC, 1978
10. Radhakanta Rana and Shiv Brat Singh, *Automotive Steels, Design, Metallurgy, Processing, and Applications*, Woodhead Publishing, 2017.
11. J.R. Davis, Davis & Associates, *ALLOYING UNDERSTANDING THE BASICS*, ASM International, The Material Information Society, 2001.
12. Mayank Singh, *Application of Steel in Automotive Industry*, ResearchGate, Article: July 2016.
13. JOHN G. SPEER, E. DE MOOR, K.O. FINDLEY, D.K. MATLOCK, B.C. DE COOMAN, and D.V. EDMONDS, *Analysis of Microstructure Evolution in Quenching and Partitioning Automotive Sheet Steel*, The Minerals, Metals & Materials Society and ASM International 2011.
14. Takehide SENUMA, *Physical Metallurgy of Modern High Strength Steel Sheets*, ISIJ International, Vol. 41 (2001), No. 6, pp. 520–532.
15. Nazim Baluch, Zulkifli Mohamed Udin, C S Abdullah, *Advanced High Strength Steel in Auto Industry*, Technology and Applied Science Research, Researchgate, Article: August 2014.
16. Raid Fekhreddine Meknassi, Miklós Tisza, *RECENT THIRD GENERATIONS OF ADVANCED HIGH STRENGTH SHEET STEELS: PROCESSING ROUTES AND PROPERTIES*, 2021.
17. Tarun Nanda, Vishal Singh, Virender Singh, Arnab Chakraborty and Sandeep Sharma, *Third generation of advanced high-strength steels: Processing routes and properties*, Institution of Mechanical Engineers, IMechE 2016.
18. <https://metallurgydata.files.wordpress.com/2020/01/heat-treatment-of-steel.pdf>
19. <https://metallurgydata.files.wordpress.com/2020/01/alloying-effects-on-heat-treatment.pdf>
20. <https://metallurgydata.files.wordpress.com/2020/01/effect-of-alloying-elements-on-steel.pdf>

21. Xuejun Jin, *Quenching and Partitioning Heat Treatment: High-Strength, Low-Alloy*, Cornell University, 2016.
22. Daniel Krizan, *STEEL – MATERIAL OF CHOICE FOR AUTOMOTIVE LIGHTWEIGHT APPLICATIONS*, Researchgate, Conference Paper, May 2012.
23. Qinglong Liu, Qingjun Zhou, Jeffrey Venezuela, Mingxing Zhang, Jianqiu Wang and Andrej Atrens, *A review of the influence of hydrogen on the mechanical properties of DP, TRIP, and TWIP advanced high-strength steels for auto construction*, 2016.
24. [https://en.wikipedia.org/wiki/Crash\\_test](https://en.wikipedia.org/wiki/Crash_test)
25. <https://www.euroncap.com/en/vehicle-safety/the-ratings-explained/adult-occupant-protection/>
26. *International Council on Clean Transportation* <https://theicct.org/>
27. *European Commission* [https://ec.europa.eu/clima/policies/transport/vehicles/regulation\\_en](https://ec.europa.eu/clima/policies/transport/vehicles/regulation_en)
28. Fabio D’Aiuto, *EFFECT OF MICROALLOYING IN STEELS AND ADVANTAGES OF NIOBIUM FOR MOBILITY*, March 2020.
29. PETER AUER, *Advances in Energy Systems and technologies*, Academic Press, A Subsidiary of Harcourt Brace Jovanovich, Publishers, 1982.
30. Lu, *8th China Lightweight Car Body Conference*, 23rd Nov 2020.
31. <https://www.worldautosteel.org/why-steel/safety/facing-the-challenge-for-crash-safety>.
32. M. Shehryar Khan, M. H. Razmpoosh, E.Biro & Y.Zhou, *Review on the laser welding of coated 22MnB5 press-hardened steel and its impact on the production of tailor-welded blanks*, Science and Technology of Welding and Joining, Taylor and Francis, 2020.  
[www.Tandfonline.com/loi/ystw20](http://www.Tandfonline.com/loi/ystw20)
33. Brandon M. Hance, Robert J. Comstock and Daniel K. Scherrer, *The Influence of Edge Preparation Method on the Hole Expansion Performance of Automotive Sheet Steels*, SAE International 2013.
34. Kyohei KAMIBAYASHI, Yutaka TANABE, Yoshito TAKEMOTO, Ichirou SHIMIZU and Takehide SENUMA, *Influence of Ti and Nb on the Strength–Ductility–Hole Expansion Ratio Balance of Hot-rolled Low-carbon High-strength Steel Sheets*, ISIJ International, Vol. 52 (2012), No. 1, pp. 151–157, September 8, 2011.
35. Surajit Kumar Paul, Monideepa Mukherjee, Saurabh Kundu, Sanjay Chandra, *Prediction of hole expansion ratio for automotive grade steels*, 2014 Elsevier B.V.  
[www.elsevier.com/locate/commatsci](http://www.elsevier.com/locate/commatsci)
36. Xiping Chena, Haoming Jianga, Zhenxiang Cuia, Changwei Liana, Chao Lu, *Hole expansion characteristics of ultra-high strength steels*, Published by Elsevier, 2014.  
<http://www.elsevier.com/locate/procedia>
37. Gyan Patel and Ganesh Kakandikar, *Investigations on effect of thickness and rolling direction of thin metal foil on forming limit curves in microforming process*, Elsevier Ltd, 2020. <https://doi.org/10.1016/B978-0-12-819496-6.00007-5>
38. euroncap-2019-skoda-octavia-datasheet.
39. euroncap-2017-skoda-kodiaq-datasheet.
40. euroncap\_skoda\_rapid\_2012\_datasheet.
41. BMWix, Euro car body conference, Benchmark data, Presentation,2020.
42. Cadillac Escalade, Euro car body conference, Benchmark data, Presentation,2020.
43. Ford Mustang\_Mach-E, Euro car body conference, Benchmark data, Presentation,2020

44. Honda e, Euro car body conference, Benchmark data, Presentation,2020
45. Isuzu\_D-MAX, Euro car body conference, Benchmark data, Presentation,2020
46. Volvo\_XC40 Recharge, Euro car body conference, Benchmark data, Presentation,2020
47. Lexus\_LC Convertible, Euro car body conference, Benchmark data, Presentation,2020
48. Mazda MX-30, Euro car body conference, Benchmark data, Presentation,2020
49. Skoda Octavia, Euro car body conference, Benchmark data, Presentation,2020
50. Subaru Outback (North America spec.), Euro car body conference, Benchmark data, Presentation,2020
51. Toyota Yaris, Euro car body conference, Benchmark data, Presentation,2020
52. Land Rover Defender, Euro car body conference, Benchmark data, Presentation,2020
53. VW ID.4, Euro car body conference, Benchmark data, Presentation,2020.
54. Aston Martin DB1, Euro car body conference, Benchmark data,2016.
55. Land Rover Discovery, Euro car body conference, Benchmark data, Presentation,2016.
56. Skoda\_Kodiaq, Euro car body conference, Benchmark data, Presentation,2016.
57. Volvo\_V90, Euro car body conference, Benchmark data, Presentation,2016.
58. Acura\_NSX, Euro car body conference, Benchmark data, Presentation,2016.
59. Audi\_A5, Euro car body conference, Benchmark data, Presentation,2016.
60. Peugeot\_3008, Euro car body conference, Benchmark data, Presentation,2016.
61. Bentley\_Bentayga, Euro car body conference, Benchmark data, Presentation,2016.
62. Alfa\_Romeo\_Giulia, Euro car body conference, Benchmark data, Presentation,2016.
63. Alfa\_Romeo\_4C\_fertig\_NEU, Euro car body conference, Benchmark data, Presentation,2013.
64. BMW\_i3\_Druckfreigabe, Euro car body conference, Benchmark data, Presentation,2013.
65. Ford\_Transit\_Custom\_fertig\_NEU, Euro car body conference, Benchmark data, Presentation,2013.
66. Honda\_FIT\_fertig\_NEU, Euro car body conference, Benchmark data, Presentation,2013.
67. Infiniti\_Q50\_fertig\_NEU, Euro car body conference, Benchmark data, Presentation,2013.
68. Lamborghini\_Aventador\_NEU, Euro car body conference, Benchmark data, Presentation,2013.
69. Lexus\_IS\_fertig\_NEU, Euro car body conference, Benchmark data, Presentation,2013.
70. Mercedes-Benz\_S-Class\_fertig\_NEU, Euro car body conference, Benchmark data, Presentation,2013.
71. Opel\_Cascada\_fertig\_NEU, Euro car body conference, Benchmark data, Presentation,2013.
72. Range\_Rover\_Sport\_fertig zum Druck, Euro car body conference, Benchmark data, Presentation,2013.
73. Renault\_Captur\_fertig\_NEU, Euro car body conference, Benchmark data, Presentation,2013.
74. Audi\_A3, Euro car body conference, Benchmark data, Presentation,2012.
75. BMW\_3Series, Euro car body conference, Benchmark data, Presentation,2012.
76. Cadillac\_ATS, Euro car body conference, Benchmark data, Presentation,2012.
77. Ford\_Mondeo, Euro car body conference, Benchmark data, Presentation,2012.
78. Honda\_CIVIC, Euro car body conference, Benchmark data, Presentation,2012.
79. Mercedes-Benz\_SL, Euro car body conference, Benchmark data, Presentation,2012.
80. Range\_Rover, Euro car body conference, Benchmark data, Presentation,2012.

81. Skoda\_Rapid, Euro car body conference, Benchmark data, Presentation,2012.
82. Audi\_A6, Euro car body conference, Benchmark data, Presentation,2011.
83. Mercedes-Benz\_B-Class, Euro car body conference, Benchmark data, Presentation,2011.
84. VW\_golf\_cabriolet, Euro car body conference, Benchmark data, Presentation,2011.
85. Mazda\_cx-5, Euro car body conference, Benchmark data, Presentation,2011.
86. Range\_rover\_evoque, Euro car body conference, Benchmark data, Presentation,2011.
87. Opel\_zafira, Euro car body conference, Benchmark data, Presentation,2011.
88. Nissan\_leaf, Euro car body conference, Benchmark data, Presentation,2011.
89. BMW\_1series, Euro car body conference, Benchmark data, Presentation,2011.
90. Ford\_Focus, Euro car body conference, Benchmark data, Presentation,2011.
91. Hyundai\_i40, Euro car body conference, Benchmark data, Presentation,2011.
92. ECB\_agenda\_e, Euro car body conference, Benchmark data, Presentation,2011.
93. Honda\_CR\_Z, Euro car body conference, Benchmark data, Presentation,2010.
94. Citroen\_C4, Euro car body conference, Benchmark data, Presentation,2010.
95. Alfa\_Romeo\_Giulietta, Euro car body conference, Benchmark data, Presentation,2010.
96. Volvo\_S60, Euro car body conference, Benchmark data, Presentation,2010.
97. Latitude Renault\_SM5, Euro car body conference, Benchmark data, Presentation,2010.
98. Euro car body conference, Benchmark data, Presentation,2010.
99. Saab\_9\_5, Euro car body conference, Benchmark data, Presentation,2010.
100. BMW\_5\_series, Euro car body conference, Benchmark data, Presentation,2010.
101. Audi\_A8, Euro car body conference, Benchmark data, Presentation,2010.
102. Aston\_Martin\_Rapide, Euro car body conference, Benchmark data, Presentation,2010.
103. Ferrari\_458\_Italia, Euro car body conference, Benchmark data, Presentation,2010.
104. Ford\_C\_MAX, Euro car body conference, Benchmark data, Presentation,2010.
105. Opel\_Meriva, Euro car body conference, Benchmark data, Presentation,2010.
106. VW\_Sharan, Euro car body conference, Benchmark data, Presentation,2010.
107. Lexus\_LFA, Euro car body conference, Benchmark data, Presentation,2010.